Utilization of char from biomass gasification in catalytic applications

Naomi Klinghoffer

Submitted in partial fulfillment of the
requirements for the degree
of Doctor of Philosophy
in the Graduate School of Arts and Sciences

COLUMBIA UNIVERSITY

2013

ABSTRACT

Utilization of char from biomass gasification in catalytic applications

Naomi Klinghoffer

Utilization of biomass as an energy source is likely to increase in the near future. One way to recover energy from biomass is via gasification, which enables the production of electricity, heat, chemicals, or fuels such as synthetic natural gas or gasoline. The desired product from gasification is synthesis gas, which is a mixture of CO and H_2; however by-products such as tar and char are formed. The tars must be decomposed or removed, as they can cause clogging in downstream equipment. Tars are most commonly decomposed catalytically or thermally. However, thermal decomposition requires high temperatures, and catalyst deactivation takes place during catalytic decomposition. This thesis focuses on the utilization of char as a catalyst for tar decomposition. Char has a surface area that is higher than many typical catalysts, and contains catalytic minerals and metals which are well dispersed on the surface. Using char in this application would eliminate the need for purchasing expensive catalysts, and deactivation would not be a concern since deactivated char could be easily replaced by fresh char which is produced inside the gasifier. In addition, it provides a useful application for the char, which would otherwise be considered to be a low value product.

In this work, poplar wood was gasified in a fluidized bed reactor under steam and CO_2 at 550, 750, and 920^{o}C for different periods of time. The char was recovered from the fluidized bed, and its properties were studied. The BET surface area of the char ranged from 429-687 m^2 g^{-1} and increased with increasing gasification temperature or time. In addition, micropores were observed in char that was made in CO_2, but not in char that was made in steam. Gasification was also done in an ESEM under air, steam, and CO_2. ESEM results showed sintering of the metals and minerals on the char surface during gasification

in air and steam, but sintering was not observed during gasification with CO_2. This showed that the properties of char depend on the gasification conditions.

Catalytic activity of the char was demonstrated for decomposition of methane, propane, and toluene, which is a major component of gasification tar. The light off temperature for methane decomposition using a char catalyst was 100^oC lower than the light off temperature when a commercial Pt/Al_2O_3 catalyst was used. Higher surface area char had higher catalytic activity. However, microporous char had lower catalytic activity than non-microporous char with a similar surface area, indicating that diffusion limitations occur in the micropores, reducing access to these catalytic sites. Deactivation was observed during catalytic cracking of CH_4. A 20% reduction in surface area and 33% reduction in mesopore volume were observed when comparing the used char catalyst to the fresh sample. This indicates that deactivation occurs via pore blocking. Kinetic analysis of the data showed a steeper deactivation function for mesoporous char that was made in H_2O compared to microporous char that was made in CO_2. A steeper deactivation function is indicative of a higher number of catalyst sites per pore, since once a pore becomes blocked all of the catalytic sites within the pore will become inaccessible. Therefore, char made in steam, which is mesoporous, has more accessible catalyst sites per pore. The char morphology influences its catalytic activity, which increases with increasing *accessible* surface area. The accessible surface area of the char depends on both the surface area and the porosity of the char.

Carbon based materials such as chars have been used in low temperature catalytic applications. In these applications, the catalytic activity is attributed to the presence of oxygen groups on the surface. Therefore, in this thesis the role of oxygen groups in the catalytic activity of the char for high temperature applications was investigated. Temperature programmed desorption (TPD) was used to identify the types of oxygen groups on the char surface and both acidic (lactone, carboxylic) and basic (pyrone, quinone) groups were identified. There were no significant differences in the concentration and type of surface oxygen groups amongst the different char samples. In order to understand the role that these compounds play in the catalytic activity of the char, oxygen was added to the surface of a char sample via nitric acid treatment and its catalytic performance was

compared to the raw char. However, when the sample was heated in nitrogen to the reaction temperature (850^{o}C) prior to utilization for methane decomposition, the oxygen groups desorbed, and the catalytic activity of the oxygenated char was the same as the raw char. Therefore, the char has catalytic activity even when the acidic surface oxygen groups have been removed.

The role of metals in the catalytic activity of the char was studied. Metals were removed via acid washing, and the catalytic activity of the acid washed char was compared to the untreated char. The catalytic activity of the acid washed char was 19% lower than the untreated char, which demonstrated that the presence of metals increases the catalytic activity of the char. The metals were found to be dispersed on the surface of the char. When the char was heated to 1000^{o}C, and was then used to catalyze the decomposition of CH_4, the catalytic activity of the char was lower than the untreated sample. Therefore, the gasification process preserves the high dispersion of inorganic elements in the char, which improves the catalytic performance of the char.

Char is often considered to be a by-product of gasification processes. However, this work has shown that char is a valuable product that has the potential to be used in catalytic applications. It has a surface area which is higher than many commercial catalysts, and contains metals and minerals which are catalytically active and are well dispersed on the char surface.

Table of Contents

List of Figures

List of Tables

Acknowledgments

There are many people who have provided me with support and guidance throughout my PhD. I am very grateful to my advisors, Professor Marco Castaldi and Professor Ange Nzihou, for the opportunities and mentorship that they have provided me with throughout my graduate studies.

I am very grateful to the technicians at the Ecole des Mines d'Albi, Céline Boachon, Sylive Delconfetto, Sévérine Patry, Jean Marie Sabathier, Jean Claude Poussin, and Bernard Auduc for their support during my PhD in helping me to run experiments and sharing with me their knowledge of analytical techniques. The contributions of Christine Rolland, who helped with all ESEM experiments and imaging, were extremely valuable and I am grateful for her expertise, interest, and commitment to helping me complete many hours of testing with the ESEM. I am thankful to Alexsandra Guerra, who worked with me in the lab for 2 years during her undergraduate degree. Her capabilities in setting up and running experiments, as well as her enthusiasm and motivation were a great help in completing the work for this PhD.

I could not have completed the PhD program without the inspiration, friendship and support of my colleagues and friends, Eilhann Kwon, Scott Kaufman, Federico Barrai, Tim Rappold, Forrest Zhou, Amanda Simson, McKenzie Kohn, Garrett Fitzgerald, Tim Sharobem, Heather Lanman, Eric Dahlgren, Tom Ferguson, Marcella Lusardi, and Melis Duyar. I am very grateful to the research group that I worked with at the Ecole des Mines - Doan Pham Minh, Elsa Weiss-Hortala, Nathalie Lyczko, Jocelyn Ramaroson, Moussa Dia, Haroun Sebei, Marion Ducousso, Nayane Macedo Portela, Suenia de Paiva Lacerda, Francois Veynandt, Martha Galera,and Antoinette Magadi - for welcoming me into their group and for providing me with the resources and help that I needed during each of my visits to France, for having the patience to help me learn French, as well as for making each

stay in France an enjoyable experience. Finally, I am thankful to my family for their love and support, without which I would not have reached this point.

Part I

Introduction

Chapter 1

Introduction

1.1 Energy distribution systems

There is currently growing interest in utilization of distributed and renewable energy sources. This will reduce the need for transportation of either fuels or electricity across large distances and will allow regions of the world that are not rich in fossil fuels to approach energy independence. In addition, with concerns of climate change becoming increasingly prevalent, many countries are working on increasing utilization of fuels that release less CO_2 into the atmosphere. However, the introduction of new types of fuels presents logistical challenges, as many parts of the world currently have well developed infrastructure for their existing energy distribution systems. Therefore, one way to bridge the gap between utilization of 'new' energy resources without major overhauls of current energy systems is to convert non-conventional fuels into those which can be easily integrated into existing infrastructure.

1.1.1 Renewable fuels

The most common types of renewable fuels that are currently being considered for future development are biofuels, solar , wind, and geothermal energy. The European Environment Agency predicts that by 2030 the world's renewable energy consumption will increase by ~400% and the world's biofuel consumption will increase by ~50% [1]. Solar and wind power are distributed energy sources that could be used on large or small scales, and

produce very little greenhouse gas emissions. The main issue associated with utilization of solar and wind power is energy storage, since the availability of these energy sources is intermittent. Geothermal energy is continuously available, but requires large amounts of land and would generally require a centralized power plant [2]. Biological sources of energy in their natural state have very low energy densities due to their high concentrations of moisture and oxygen. Therefore, in order to be utilized on a large scale, biofuels must be processed to produce fuels with high energy densities. There are many different methods for producing biofuels. One method for recovering energy from biomass is anaerobic digestion. Anaerobic digestion is a biochemical conversion process where bacteria decompose organic matter in oxygen-lean environments to produce biogas, which is composed of CH_4 (40-70%), with the balance being primarily CO_2. This is done actively in some treatment facilities but also takes place naturally, for example in landfills, soils, and animal intestines [3]. Biogas is often processed to remove the CO_2, and the remaining CH_4 is integrated into the natural gas distribution system. Physicochemcial conversion mechanisms are used to directly extract bio oils from feed stocks such as oilseed, rapeseed, or groundnuts. This process produces glycerin as a by-product. It is not widely used due to the high cost of raw materials [3]. Bioethanol can be produced from fermentation of biomass; this process is appropriate for crops with a high sugar content, which are primarily food crops such as sugar cane, corn, and lignocellulosic crops.

1.1.2 Energy recovery from waste

Energy from waste technologies are currently being implemented and developed for future use. These processes address the issue of finding distributed energy sources, since waste is produced wherever there are people. In addition, it can offset the use of fossil fuels, and a significant portion of municipal solid waste is from biological sources, which means there are very low CO_2 emissions. This also reduces the need for landfills, which use land and emit CH_4 from the anaerobic decomposition of waste. The most common methods for energy recovery from waste are grate combustion or anaerobic digestion (which takes place naturally in landfills). There are many countries which combust municipal solid waste and use the heat to produce steam which is used for district heating or electricity production

via a steam turbine. For example, Sweden sends only 4% of its waste to landfills; the rest is either recycled or incinerated for energy recovery. In addition, they import waste from Norway, as the capacity of their plants is greater than the waste produced in Sweden. The electricity provided by these facilities powers a quarter of a million homes, and 20% of Sweden's district heating is derived from waste to energy [4]. Other countries that process a significant portion of their waste via waste to energy are the Netherlands, Germany, Austria, and Denmark. This technology is well developed and is much more prevalent in European countries and Japan compared to North America.

Another method for energy recovery from waste or biomass is gasification, a thermochemical conversion process, which is the subject of this research.

1.2 Gasification

Gasification is a well known process for converting solid fuels into synthesis gas, which can be used to produce liquid fuels, synthetic natural gas, or electricity and heat. Gasification of coal has been used as far back as the 1800's, where gasification products, known as coal gas, were used as a source of fuel [5]. However, as natural gas became widely available in the 1900's, the use of coal gas was reduced, as it was replaced with natural gas [6]. With the development of Fischer-Tropsch synthesis in the 1920's, which enables the production of liquid fuels from gasification products, the objective of gasification became more focused on production of liquid fuels. Since the 1950's, interest in gasification for production of fuels and chemicals has increased.

A schematic of the gasification process is shown in Figure 1.1. This process involves reacting a solid fuel with an oxidant in sub-stoichiometric concentrations in order to partially oxidize the fuel to produce synthesis gas (syngas), which is composed primarily of CO and H_2. The oxidants that are most commonly used in gasification processes are air (in sub-stoichiometric quantities), steam, or CO_2. Syngas also contains gaseous products such as CO_2, CH_4, and other light hydrocarbons. The composition of the syngas depends on the feedstock, the type and amount of co-reactant used (air, H_2O, or CO_2), and the reaction conditions (temperature, heating rate, etc.). For example, gasification with steam

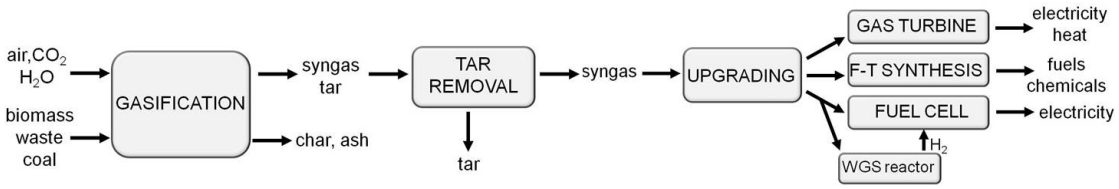

Figure 1.1: Schematic of gasification process.

will produce syngas with a high H_2 to CO ratio whereas this ratio will be lower when gasification is done with CO_2.

The desired syngas composition depends on the way the syngas will be used. If it is to be used in a PEM fuel cell, which can only accept pure H_2, a high H_2 to CO ratio from the gasifier is desired. The syngas would then pass through a water gas shift reactor in order to increase the H_2 production and decrease the CO concentration, according to Equation 1.1. Solid oxide fuel cells (SOFCs) can oxidize both CO and H_2, which eliminates the need to remove all of the CO from syngas. A SOFC can accept a wide range of H_2/CO ratios, however electrochemical oxidation kinetics are faster for H_2 than for CO (1.9-2.3 times higher at 750^{o}C and 2.3-3.1 times higher at 1000^{o}C [7]), so higher H_2 concentrations are still desirable for syngas that will be used in a fuel cell. The syngas can be combusted directly in a gas turbine to produce electricity and heat. Finally, the Fischer-Tropsch synthesis process can be used to produce liquid fuels from syngas. The H_2 to CO ratio for this process will influence the types of products that will be formed; a higher H_2 fraction will produce smaller molecules, such as liquid hydrocarbons, methane or ethane, since hydrogen can terminate chain growth. Lower H_2 to CO ratios will result in higher yields of heavier hydrocarbons [8].

$$H_2O + CO \leftrightarrow H_2 + CO_2 \tag{1.1}$$

The first commercial gasification plant was developed by Sasol, a company based in South Africa. This plant has been in operation since the 1950's, when it produced automotive fuels from coal. There are a few other systems that are currently in operation. The PROLER Syngas system has a demonstration unit (48 tpd) in Houston, TX, USA. This facility uses auto-shredder residue as feedstock for gasification. Natural gas and oxygen

are used to maintain a temperature of 850^{o}C in the gasifier. Plasma-assisted gasification is another technology which is being developed. This process uses plasma, which is generated by electricity, to provide the heat required for gasification. Some companies that are currently using or developing plasma-assisted gasification technologies are Westinghouse Plasma (owned by AlterNRG), Plasco Energy Group, Europlasma and InEnTec (owned by Waste Management Inc.). Enerkem is a Canadian company which produces ethanol and methanol from gasification of solid waste. Enerkem has one commercial facility in Quebec, Canada, which processes treated wood waste and is developing two more in Alberta, Canada and Mississippi, USA. Other companies which are developing or have developed gasification processes are Ebara, Entech, OE Gasification, Mitsui R21, INEOS Bio, Nippon Steel DMS, Taylor Biomass Energy, Energos, Chinook Energy, and Ze-Gen.

While there are many companies that are developing, or have developed gasification systems for processing waste and biomass, this technology has yet to be commercialized on a large scale. Some of the main reasons for this are the heterogeneity of the fuel and the problem of tar handling. Tars are heavy organic hydrocarbons that are produced from incomplete conversion of the solid fuel. They are produced in gasification processes because of the low temperatures and low concentration of oxidant. As a comparison, combustion processes operate at higher temperatures and with excess oxygen so tars are almost always oxidized to combustion products. Tars are problematic because they can deposit on the walls of tubing, or cause clogging in downstream equipment. They can also crack to deposit carbon on surface of pipes and equipment, and they can be hazardous. In addition, the production of tars results in a lower overall conversion of reactants to gas phase products, which lowers the overall process efficiency. Section 1.3 discusses the current methods for handling tars in gasification processes. Another by-product of gasification is char or ash, which is discussed in Section 1.4.

1.2.1 Comparison of gasification and combustion

Combustion is a process that is central to our current energy distribution systems and is the most well known method for recovering energy from solid, liquid, or gaseous fuels. Processes have been developed for recovering energy from solid waste via combustion,

where the heat is captured and used to generate steam which is fed to a steam turbine for electricity generation. This process allows for the production of electricity from unconventional and highly heterogeneous fuels. Gasification provides another mechanism to recover energy from unconventional or heterogeneous fuels, such as biomass and waste. The parameter which defines a process as gasification or combustion is the air to fuel ratio, commonly described with the *equivalence ratio*, which is defined in Equation 1.2. Figure 1.2 shows the adiabatic flame temperature for the reaction of municipal solid waste (MSW) with air at different equivalence ratios [9].

$$equivalence\ ratio\ (\phi) = \frac{\left(\frac{oxidant}{fuel}\right)_{stoichiometric}}{\left(\frac{oxidant}{fuel}\right)_{actual}} \tag{1.2}$$

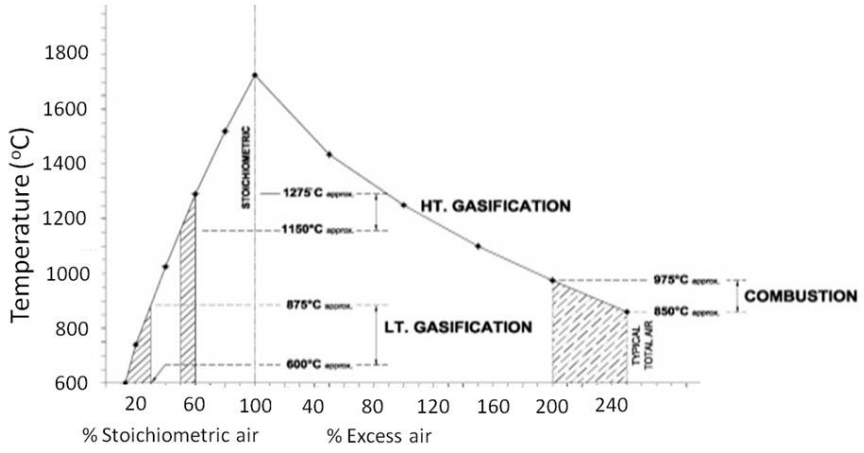

Figure 1.2: Adiabatic temperature of gasification and combustion reactions of municipal solid waste (MSW) reacted with air. The highest temperature is achieved at an equivalence ratio of 1. Image modified from [9].

Processes operating at sub stoichiometric conditions are defined as gasification whereas processes operating with stoichiometric, or excess air are combustion processes. The benefits of combustion are that it is a well developed process and generally achieves

approximately 100% conversion of the solid fuel (carbon) to gas products, thus releasing essentially all of the chemical energy stored in the fuel. In addition, there are fewer by-products in combustion processes compared to gasification. However, gasification is beneficial because it enables the production of synthesis gas, which can be used in a variety of applications. For example, synthesis gas can be used to produce liquid fuels which are energy dense and easier to transport than solid or gaseous fuels.

1.3 Tars

1.3.1 Tars: What they are and why they form

Tar handling is one of the major barriers to commercialization of gasification technologies. Tars are formed from incomplete combustion of fuel and are particularly prevalent in gasification systems due to the low temperatures and low concentration of oxidants. Tars are typically single or multi ring aromatics, since they derive from lignin or cellulose which are ringed carbon structures. The composition of tar is quite variable, but efforts have been made to characterize tar. As an example, Mun et al. characterized tar generated from air gasification of woody biomass in a two stage gasifier which consisted of a fluidized zone and a tar cracking zone. They measured the presence of single ring aromatics, including toluene, benzene, and styrene, 2-ring aromatics, including naphthalene, indene, and methylated naphthalene, 3 and 4 ring aromatics, including phenanthrene and acenaphthylene, and oxygenated compounds such as dibenzofuran and phenol [10].

1.3.2 Tar handling methods

There have been a number of methods developed for tar handling, and Table 1.1 lists each method, along with its pros and cons. This table illustrates that each method has significant drawbacks and there is still a need for an effective and economic solution for how to handle tars that are produced in gasifiers.

Tar Handling Method	**Pros**	**Cons**
Thermal destruction [11]	• Does not require catalysts, which are expensive	• Requires high temperatures (700-1250 ^{o}C) [12]
Catalytic decomposition [13–17]	• Tars can be reformed at low temperatures (550-900 ^{o}C [12]) • Selective catalysts can be used to produce desired reaction products (ex. syngas)	• Tars cause rapid catalyst deactivation, so catalysts need to be replaced or regenerated frequently; this can be expensive. (ex. Bridgwater et al. estimate a requirement of 0.68t of dolomite per oven dry ton of biomass gasified in order to fully crack the tars; the cost of dolomite cited is 30 €/t. [18])
Tar recycle and combustion for process heat	• Tar combustion is a cheap and simple process that does not require thermal input or catalysts	• Heating value of tar + char is greater than process heat required for gasifiers operating <1000^{o}C; therefore thermal energy is wasted by burning all of the tar + char

Other uses (for example, separating single ring aromatics for use in making aromatic polymers, such as plastics and fibers) [19,20]	• Produces a valuable product (ex. The price of toluene for benzene production was estimated at $0.648/kg. [21])	• Requires a high level of processing to separate the tar into its components since gasification tars can contain hundreds of different components • Since gasification destroys many of the aromatic rings in the biomass, it is not a good procedure if the final goal is to produce chemicals; pyrolysis or liquefaction should be used instead
Operate at process conditions that avoid tar formation (i.e. tars are destroyed inside the gasifier, for example by high temperature gasification) [22–24]	• Tar formation is avoided	• High temperatures are required (ex. Temperature increase from 600^{o}C to 1000 ^{o}C required to achieve 95% reduction in tar for air gasification of palm biomass.) [22]

Table 1.1: Methods for handling tars from gasification systems

Of the methods listed in Table 1.1, one of the most common ones is catalytic tar cracking or reforming. Catalysts are typically composed of minerals such as olivine or dolomite, or

base metals such as nickel, and have been shown to achieve conversions of up to 99% with tar surrogate molecules. However, as mentioned above, one of the main concerns with this process is catalyst deactivation. The most common methods of deactivation are coking, attrition, or sulfur poisoning [25]. For example, Yamaguchi et al. observed that the gas yield decreased by 50% over 50 hours on stream when using an alumina supported nickel catalyst for treatment of gas produced from steam gasification of wood [26]. Bain et al. measured deactivation experimentally, and developed a deactivation model, using a NiO based catalyst on an alumina support for the reforming of tars produced from gasification of mixed wood [27]. Coking is particularly prevalent with nickel catalysts [14]. In order to reduce coking, others have looked at combining nickel with other alkali or alkaline earth metals. For example, using a guard bed of calcined dolomite or addition of magnesium to the nickel catalyst has been shown to reduce coke formation [14,15]. Di Felice et al. found that combining iron with CaO and MgO catalysts for decomposition of benzene produced similar conversion values to that of dolomite [28]. Using catalysts such as dolomite and olivine without the addition of base metals, is less effective for conversion of tars than using metal catalysts. For example, Swierczynski et al. found that the same conversion was achieved with a Ni/olivine catalyst operating at 560^{o}C and an olivine catalyst operating at 850^{o}C [29]. El-Rub et al. report that nickel based catalysts are 8-10 times more active than dolomite [13].

Catalytic destruction of tars can be done in a secondary catalytic reactor or by introducing the catalyst into the gasifier (pre-mixed with the solid fuel) [16,17]. However, both pre-mixing catalysts and placing them in a secondary reactor present a problem of catalyst recovery. The challenge of catalyst recovery and the rapid catalyst deactivation during tar decomposition necessitates use of a catalyst that is inexpensive and easily replaceable.

1.4 Char and Ash

Another by-product of gasification is char or ash. Ash is the solid residue that is composed of inorganic elements that are inherently present in the raw fuel source. Char is a solid residue that is composed primarily of carbon and also contains ash. Processes that operate

at higher temperatures, or with more oxidant are more likely to form ash whereas operating at lower temperatures or with less oxidant will result in more residual carbon, so char is formed. Currently, there are limited uses for ash or char from gasification systems, aside from use in construction applications or as alternate daily cover for landfills [30]. There is active research in the use of char for soil amendment but this has yet to be deployed on a large scale [31,32].

Meyer et al. studied the use of char for soil amendment and compared the cost of producing char from biomass via various different methods, such as fluidized bed fast pyrolysis, slow pyrolysis, gasification, and flash carbonization. Flash carbonization is a process where a flash fire is ignited at pressures of 1-2MPa at the bottom of a packed bed of biomass which moves up the bed as air flows down (temperature range is 300-600^{o}C) [31]. For gasification, which is an endothermic process, it is only beneficial to sell the char if the selling price is higher than the cost of raw wood with the same total heating value. In other words, since process heat is needed, the char could be burned to provide this heat. If the char is sold, raw biomass would be burned to provide process heat, so the selling price for the char must be higher than what it would cost to replace the char with raw biomass. They calculated this price to be $380 US per tonne of char (value has been inflation-adjusted to the year 2010). As a comparison, they reported costs of $51 and $373 per tonne of charcoal for production via slow pyrolysis (depending on the process conditions), and $560 per tonne of char for fast pyrolysis. Therefore, there is a market for char and its value must be determined in order to make the best use of this product. In Chapter 5 a comparative analysis is done to understand the benefits and drawbacks of different uses for char from gasification processes.

Part II

Process description and demonstration of feasibility through experimentation and modeling

Chapter 2

Motivation

This chapter introduces the process that is studied in this thesis. Chapter 1 discussed why gasification is a promising option for conversion of non-conventional fuels into conventional fuels. It also discussed some of the major issues with gasification, such as production of tars, and the need to find useful applications for char and ash. In this section, a solution to this problem is proposed, and our method for testing and understanding this process is discussed.

This thesis is based on a process which is shown in Figure 2.1. Here, residual char that is produced from gasification is used as a catalyst for tar reforming. This process is beneficial because it addresses 2 problems: the issue of tar destruction, and the issue of char disposal or utilization. One of the main challenges with catalytic methods for tar destruction is that catalyst deactivation is very rapid, as discussed in Chapter 1. Char, however, is produced on site and is therefore a practical option for catalytic tar decomposition. Since it is produced during the gasification process, it can be replaced with fresh char as it deactivates. The properties of char suggest it will be a good catalyst as well. It is a very high surface area material, with surface areas ranging from 450 - 687 m^2 g^{-1} [33]. It is very porous and can contain both micropores and mesopores. In addition, char contains metals and minerals that are present in the raw material. Catalysts are typically made of a high surface area support with the catalyst material dispersed finely on the support [34]. Similar to conventional catalysts, the metals and minerals in the char are dispersed [35].

Carbon has been used extensively in catalytic applications, both as a catalyst and as a

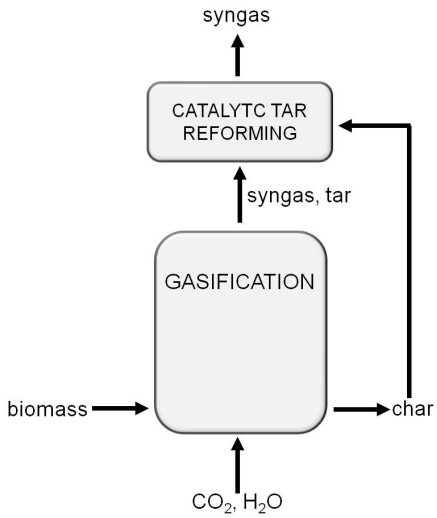

Figure 2.1: Schematic of process where char is recyled for use as a catalyst for tar reforming.

support. In general, the carbons used in catalytic applications have a graphitic structure, such as activated carbon, or carbon black. Carbons have been used as catalysts in many different types of reactions such as oxidative dehydrogenation of hydrocarbons, dehydration and dehydrogenation of alcohols, NO_x reduction, SO_x reduction, and H_2S oxidation, among others [36]. The catalytic activity of these carbons has been attributed to the oxygen functional groups on the surface of the material (the type and concentration) as well as the morphology, which influences the accessibility of these sites. Activated carbon has also been used in some applications as a catalyst support. Prasad et al. used activated carbon as a support for NiO to catalyze the decomposition of methane to C and H_2 [37].

In the past 3 years, there have been a few papers which have reported the use of char or similar materials as a catalyst or catalyst support for reforming tar [10, 38–43]. Mun et al. gasified woody waste with air and used activated carbon in a secondary reactor for tar removal [10]. They measured the concentration of tars in the producer gas to be 3.4 mg Nm^{-3} in the absence of the activated carbon and 1.9mg Nm^{-3} with the activated carbon. In addition, the concentrations of hydrogen and carbon monoxide were higher with the activated carbon, indicating that it catalyzed the reforming of tars. Striugas et al. also used activated carbon, which was obtained from fast pyrolysis of tire wastes, to catalyze the decomposition of real tars produced from gasification of softwood pellets, and

also observed higher production of syngas with the activated carbon catalyst [39]. Abu El-Rub et al. compared the catalytic performance of commercial biomass char (produced from the pyrolysis of pine wood) to that of conventional tar reforming catalysts, such as nickel, dolomite, and olivine, for reforming of naphthalene and phenol, which are tar surrogates [41]. With the char catalyst, the conversion of phenol at 700^{o}C was almost twice as much as that which was obtained with the olivine catalyst. The conversion with dolomite and nickel catalysts was ~90% and the conversion with char was 81.6% . With naphthalene, almost 100% conversion was obtained with the char catalyst at 900^{o}C. At these conditions, 100% conversion was obtained with the nickel catalyst, and conversion was 55% and 61% with olivine and dolomite respectively. Wang et al. showed that char can be an effective catalyst support for synthesis gas cleanup. Using benzene as a tar surrogate, they achieved 30% conversion with char at 900^{o}C. After mixing NiO with char at a nickel loading of 20 wt%, over 80% benzene removal was achieved at the same temperature [40]. Xiao et al. used brown coal char as a support for a Ni catalyst for syngas cleanup and obtained good dispersion of the Ni catalyst and effective tar removal. Min et al. used char and char supported iron catalysts for steam reforming of biomass tars [42]. Chaiwat et al. also used char as a catalyst in a secondary reactor to reform tars from gasification of Japanese cedar wood [43]. These publications demonstrate that biomass char has catalytic performance for tar destruction. However, there is currently a limited understanding of why the char has catalytic activity, and which char properties will improve its performance.

2.1 Approach

This section discusses the approach used to investigate the feasibility of the process presented here, and outlines the general structure of this thesis. First, gasification experiments were performed in a laboratory bench scale reactor and in an Environmental Scanning Electron Microscope. The goal of these experiments, which are discussed in Chapter 3, was to generate char and to understand its properties. Gasification was done in steam, CO_2, and air at different reaction conditions. The chars from bench scale gasification experiments were collected and their properties were studied. The specific properties investigated were

surface area, porosity, surface functional groups, and composition, which are presented in Chapter 3. Some trends were observed which relate gasification conditions to char properties, however the focus of this work is to understand how char properties influence its catalytic performance. A more detailed study on how process conditions can be modified to create char with specific physical and chemical properties is a subject for future research. The catalytic activities of the different char samples were tested for methane, propane, and toluene cracking reactions. The results of these experiments, and a discussion of why these fuels were selected are presented in Chapter 4. Once the catalytic activity of the char was demonstrated, it was important to understand how the properties of the char influence its catalytic activity. The catalytic activities of different char samples were compared. In addition, the catalytic performance of char was compared to a commercial catalyst. The catalyst deactivation was measured over 3 hours; in this time frame significant deactivation was observed, which is explained in detail in Chapter 5. The kinetics of the char catalyst were then used in a reactor model in order to understand if the performance of the char can meet the needs of an existing gasification system. In addition, this process is compared to an alternate process where char is combusted in order to generate process heat. The energy benefits of these two processes are compared in Chapter 5.

Part III investigates which char properties influence its catalytic performance. The properties that are most commonly attributed to catalytic performance of carbon based materials, such as char and activated carbon, are morphology, functional groups on the surface, and inorganic elements. Chapter 6 discusses how the surface area and porosity of the char influence its catalytic activity. In addition, a kinetic analysis is done in order to understand the type of deactivation taking place. In Chapter 7 the oxygen functional groups on the surface of the char are determined by temperature programmed desorption. The char is modified by oxygenating the surface, and the catalytic performance of the char is tested in order to understand how the oxygen groups influence its catalytic performance. The influence of the inorganic elements is analyzed in Chapter 8. In this chapter, the metals and minerals in the char are analyzed with EDS. These elements were removed by acid treatment and the catalytic performance of the de-ashed char was compared to that of the raw char. The dispersion of metals was modified by thermal treatment of the char and the

catalytic performance of the modified char was tested in order to understand the influence of dispersion on catalytic performance. In addition, the carbon was removed via oxidation of the char, and the catalytic performance was tested in order to understand the role of carbon in the catalytic activity of the char. Chapter 9 concludes this thesis by summarizing the major findings of this work and proposing directions for future research on this topic.

Chapter 3

Char Properties

3.1 Experimental procedure for generation of char

3.1.1 Biomass

Poplar wood chips were used for all experiments presented in this thesis. The raw poplar wood was ground into chips that were ~4mm x 4mm x 1mm. Poplar wood was used for all experiments in order to have a homogeneous starting material. While ultimately gasification could be done with mixed waste, such as agricultural residue, a more homogeneous starting material allows for better comparison of different reaction conditions. Poplar wood was chosen because poplar trees grow quickly (compared to other temperate trees), and can be grown in North America on land that is not considered to be prime crop land [44]. Compared to other commonly used biomass feedstocks such as corn stover or switchgrass, poplar wood has a relatively high heating value (19 MJ/kg dry) and a low sulfur content (0.01 % of dry wt.) [44]. The ash from poplar contains metals which are typically used as catalysts, such as iron and copper. Poplar wood generally has a composition of ~50% carbon, ~43% oxygen, ~6.5% hydrogen, and ~0.5% nitrogen, by weight [44]. The poplar wood chips that were used in all experiments in this thesis are shown in Figure 3.1 .

Figure 3.1: Poplar wood chips used in gasification experiments.

3.1.2 Gasification experiments

Gasification experiments were done in both a fluidized bed reactor and in an Environmental Scanning Electron Microscope (ESEM).

3.1.2.1 Fluidized bed reactor

Char was generated in a fluidized bed reactor where gases at controlled flow rates were introduced into the reactor at 400 SLPM kg^{-1} biomass. The reactor is shown in Figure 3.2. The stainless steel reactor was 23.6 inches high with an internal diameter of 2.4 inches. It was equipped with a frit on the bottom to hold the biomass and 10 thermocouples were placed throughout the reactor in the vertical direction to measure the temperature profile. A thermocouple placed close to the middle of the reactor was connected to a temperature controller (Eurotherm 2216e). A frit was secured on top of the reactor to ensure that all char remained in the reactor for collection. The system was heated at $20^oC\ min^{-1}$ to a pre-determined maximum temperature where it was held there for 30 minutes or 1 hour. Experiments were done with 10% CO_2 in N_2 balance at the following conditions: (i) 550^oC for 30 minutes (ii) 750^oC for 30 minutes (iii) 920^oC for 30 minutes. Gasification was also done in 90% H_2O in N_2 balance at the following conditions: (i) 550^oC for 30 minutes (ii) 750^oC for 30 minutes (iii) 750^oC for 1 hour. After each experiment the char was collected and weighed.

The names used to describe the char samples throughout the rest of this report are described in Table E.1.

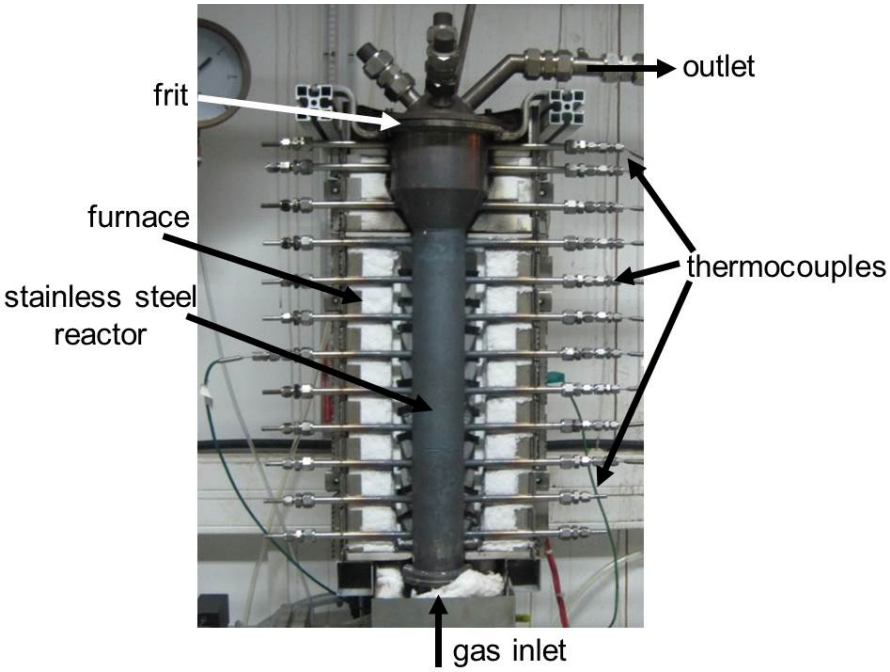

Figure 3.2: Fluidized bed reactor used in gasification experiments.

The surface area for the different char samples is shown in Table 3.2. We were not able to obtain high quality measurements for samples made at 550^{o}C. This is likely due to residual organics that were stuck in the pores, and difficult to remove at low temperatures. The char made in a CO_2 atmosphere shows that increasing the temperature results in higher surface area material. The char made at 750^{o}C has a surface area of 435 m^2 g^{-1} and the char made at 920^{o}C has a surface area of 687 m^2 g^{-1}. The char made under steam at 750^{o}C shows that increasing gasification time (at this temperature) increases surface area. However, the mass loss between the two samples is very similar (95.05% and 94.40%). This demonstrates that the surface area and porosity of the char can change even when there are not significant changes in the mass loss of the char. In addition, the micropore volume of the char was measured for three samples. The cumulative pore volume for pores with a diameter below 0.8 nm was 0.18 cm^3 g^{-1} for char sample *CO_2-750-30*, 0.30 cm^3 g^{-1} for char sample *CO_2-720-30*, and 0.0 for sample *H_2O-750-30*.

Table 3.1: Sample names for different chars created in the fluidized bed reactor

Sample Name	Reactive Gas	Temperature	Time at Temperature
H_2O-550-30	90% H_2O/ 10% N_2	550 ^oC	30 min
H_2O-750-30	90% H_2O/ 10% N_2	750 ^oC	30 min
H_2O-750-60	90% H_2O/ 10% N_2	750 ^oC	60 min
CO_2-550-30	10% CO_2/ 90% N_2	550 ^oC	30 min
CO_2-750-30	10% CO_2/ 90% N_2	750 ^oC	30 min
CO_2-920-30	10% CO_2/ 90% N_2	920 ^oC	30 min

Table 3.2: Mass recovered and surface area of chars (–* indicates quality of measurements was unacceptable)

Sample Name	Mass Recovered (% of initial mass)	Surface Area (m^2g^{-1})
H_2O-550-30	14.1	–*
H_2O-750-30	5.60	429
H_2O-750-60	4.95	621
CO_2-550-30	16.2	–*
CO_2-750-30	15.4	435
CO_2-920-30	11.8	687

The results of these experiments show the following trends with respect to char properties:

(i) Higher temperature or longer reaction time gives a lower char yield.

(ii) Surface area increases with temperature in the temperature range presented here (550-920^{o}C).

(iii) Micropores are present in char made with CO_2 but not with char made under steam, and higher temperature for CO_2 gasification results in higher micro pore volume.

3.1.3 Environmental Scanning Electron Microscope

3.1.3.1 Gasification in ESEM

Gasification experiments were done in an Environmental Scanning Electron Microscope (ESEM, FEI XL30) under air, steam, and CO_2. An ESEM is similar to a conventional SEM, but the ESEM contains a diaphragm in between the sample chamber and the electron source, which allows for higher pressures (up to 10 Torr) to be achieved. This enables the sample to be viewed without being coated in a conductive material, which is often necessary when using conventional SEMs. In addition, the sample can be heated, so physical changes in the sample can be observed as the reaction takes place. A detailed explanation of the ESEM principle of operation can be found in Appendix D.1. In this work, a piece of poplar wood was placed inside the ESEM and was heated under each gas to 1000^{o}C at 20^{o}C min^{-1}. The pressure was typically between 0.7-1.4 Torr. Images were taken throughout the gasification process.

The goal of this experiment was to understand how the structure of the biomass changed as it was gasified since surface area and pore size distribution are important properties of a catalyst. The impact of each of the different co-reactants was studied, with an awareness of the possibility of sintering, which is known to happen with some catalysts at high temperatures. Sintering of the char should be avoided in order to maintain a high surface area char for catalytic applications. These experiments were done by exposing each sample to the same reaction conditions (temperature and time) with different co-reactants. This means that the conversion was different in each case (due to different reaction kinetics), but the same reaction conditions allowed for a direct comparison of the changes in surface structure for each of the co-reactants.

During CO_2 gasification, the small pores in the biomass expanded and sintering was not observed at any point during the process, as shown in Figure 3.3. When air was used as a co-reactant, reactions proceeded rapidly starting at low temperatures, and sintering was observed at high temperatures, as shown in Figure 3.4. Steam gasification showed no significant changes in the structure at low temperatures but at high temperatures (1000^oC) the reaction proceeded rapidly and sintering was observed (Figure 3.5).

When quantifying sintering, the specific surface area is one of the most reliable indicators of sintering. The kinetics of area reduction are linked to the mechanism of the sintering and surface area is easily and reliably measured. Sintering causes both the specific surface area and the porosity to decrease and the density to increase. Sintering occurs in three stages. In the initial stage, the areas of contact between adjacent particles form and grow. In the intermediate stage, growing necks merge and the large number of small particles are replaced by a smaller number of large particles. This stage produces inter-particle porosity whose surface may be inaccessible both to reactant gas during the reaction and to the nitrogen used to measure the specific surface area. In the final stage of sintering, the pore spaces become broken up with isolated closed pores remaining which shrink in size as densification proceeds [45–47].

Earlier in this chapter, we showed that the char made under steam did not contain micropores. The absence of micropores in the char made under steam could be attributed to either a lack of micropore formation, or the sintering of the micropores. While the pores that we can physically observe in the ESEM are on a micron scale (rather than a nano-scale), we can attempt to use the observed sintering behavior to explain the porosity measurements. In the ESEM, sintering is only observed at 1000^oC. Since the fluidized bed experiments were conducted at 750^oC, it is likely that during gasification, micropores were not formed since temperatures were too low for sintering. The density and surface area of char samples produced in the fluidized bed also suggests that sintering takes place at 1000^oC. The density of char samples that were made under steam at 550^oC and 750^oC (for 30 min) were 1.42 and 1.46 g cm^{-3}, respectively. However, char that was made under steam at 1000^oC (not reported in Table 3.2) had a density of 1.76 g cm^{-3} and its surface area was 435 m^2 g^{-1}. Therefore, char produced under steam in a fluidized bed reactor at 1000^oC

had a higher density and lower surface area than char produced at lower temperatures, suggesting that sintering of the char had taken place.

Reactions with CO_2 proceed more slowly than with steam or air, which may influence the porosity of the char. With slower reaction kinetics, the CO_2 can diffuse into the pores of the biomass and modify the pore structure whereas the rapid decomposition under steam (at 1000^{o}C) or with air leads to a collapse in the pore structure of the char. These results show that the co-reactant used for gasification is important in preventing sintering to maintain high surface area char.

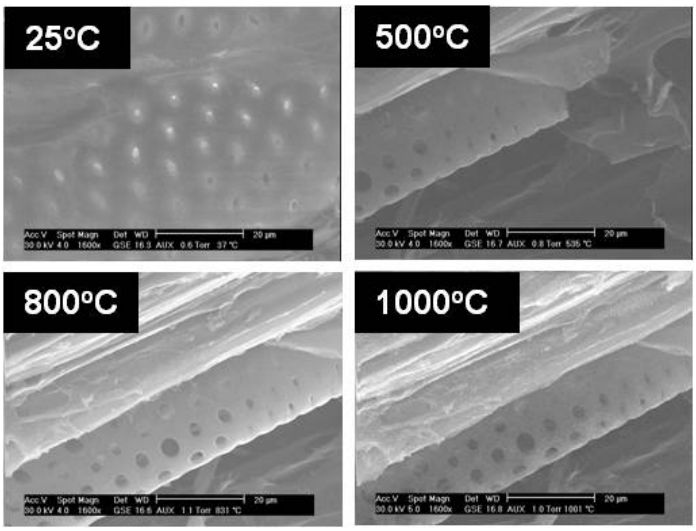

Figure 3.3: Biomass gasification in ESEM under CO_2. Heating rate was 20^{o}C min^{-1}. Pores expand at low temperature and are maintained.

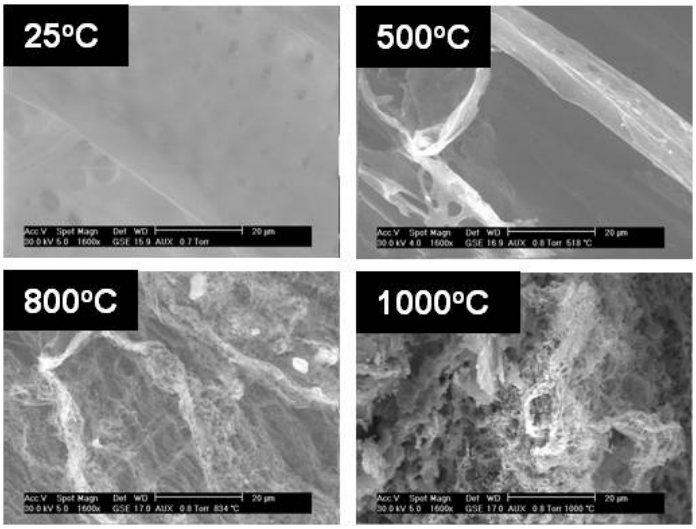

Figure 3.4: Biomass gasification in ESEM under air. Heating rate was 20^{o}C min^{-1}. Structure decomposes rapidly, beginning at low temperatures.

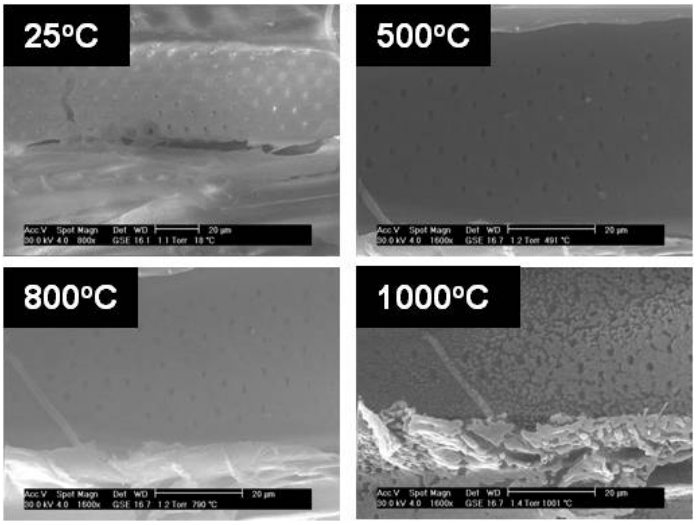

Figure 3.5: Biomass gasification in ESEM under steam. Heating rate was 20^{o}C min^{-1}. No changes at low temperature; rapid sintering at 1000^{o}C.

3.2 Char composition

The concentrations of carbon, nitrogen, sulfur, and hydrogen in the char were measured in a ThermoQuest CHNS elemental analyzer. This instrument works by combusting the

sample with oxygen, and measuring the gases produced. There are catalysts downstream of the combustion chamber in order to ensure complete oxidation of the sample (even with excess air, homogeneous combustion will produce some CO). Nitrous oxide is catalytically reduced to N_2, and the other components (C, H, S) are left in their oxidized forms, which are CO_2, H_2O, and SO_2. The gases are then separated by chromatography and measured with a thermal conductivity detector. The concentrations of C, N, H, and S are shown in Figure 3.6 for all 6 char samples. The concentration of carbon was approximately 85% for all samples, and did not vary significantly among samples. The nitrogen concentration increased with gasification temperature (i.e. decreased with mass loss), indicating that the nitrogen is less volatile than the other species, and is therefore more likely to be retained in the char. For the samples made under CO_2, the hydrogen concentration decreased as temperature increased. This suggests that the hydrogen is more easily removed from the biomass structure and at higher temperatures is more likely to be released as H_2. For the samples made in steam, there is no significant change in hydrogen concentration among the samples. This may be due to the fact that there is a high concentration of hydrogen in the reactor from the reaction of H_2O with the biomass, which reduces the driving force for hydrogen to be released from the biomass as H_2. The sulfur concentrations do not change significantly amongst the samples.

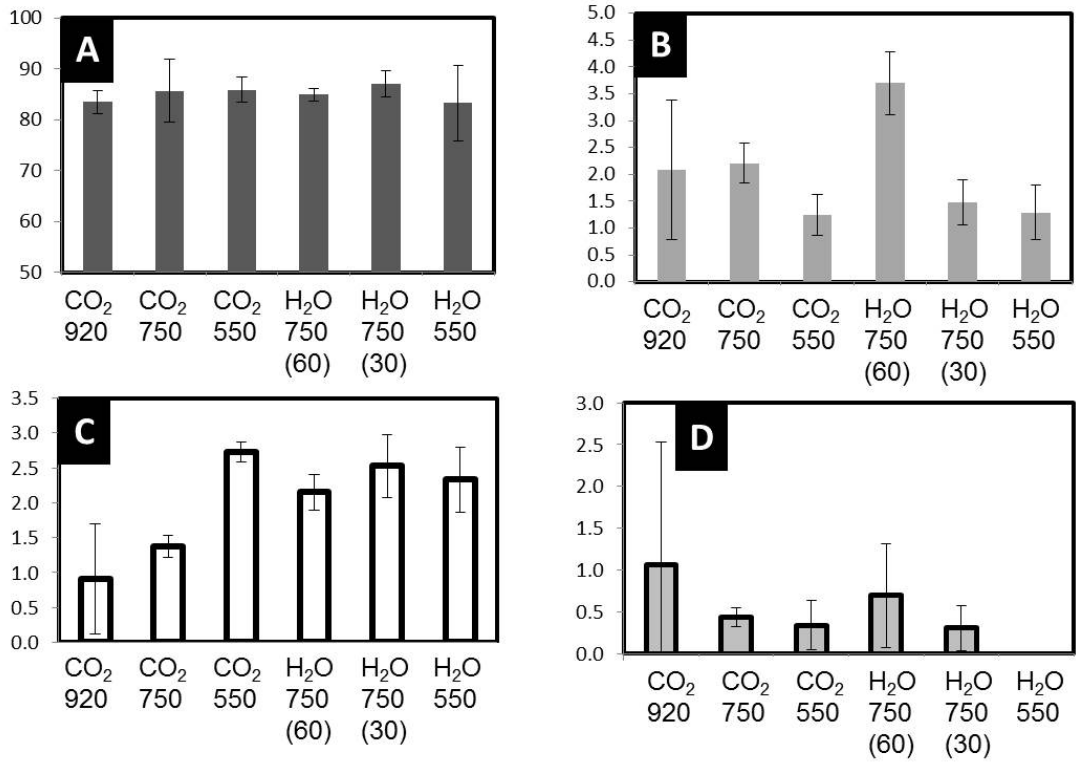

Figure 3.6: Concentrations of (a) carbon (b) nitrogen (c) hydrogen and (d) sulfur in char samples. Units for all graphs are atomic percent.

3.3 Summary

This chapter discussed the properties of char that was generated from gasification of poplar wood in a fluidized bed reactor and ESEM. The surface areas of the char samples ranged from 429-687 m^2 g^{-1}. In the temperature range from 550-920^{o}C the surface area of the char increased with temperature. However, at high temperatures (1000^{o}C), sintering was observed when char was made via gasification in steam or air. Gasification in CO_2 created a char which maintained its porous structure and contained micro pores. The carbon concentration in the char did not vary significantly amongst samples, whereas the nitrogen concentration was higher for chars made in higher temperatures and the hydrogen concentration decreased with temperature for char made in CO_2.

Chapter 4

Catalytic Performance of Char

4.1 Catalytic cracking of light hydrocarbons

The catalytic activity of the char that was described in Chapter 3 was tested by using it to catalyze the decomposition of light hydrocarbons (CH_4 and C_3H_8). These experiments were done in a Netzsch STA409 thermo gravimetric analyzer (TGA) where a char sample was placed in the instrument and a hydrocarbon gas was passed over the sample. The samples were heated to 900^oC at $5^oC\ min^{-1}$. The decomposition of these hydrocarbons results in the formation of coke on the surface of the char, which is measured as a mass gain in the TGA. The use of a TGA for these experiments enables nearly continuous mass measurement, and the TGA can detect very small changes, with good control over the temperature of the system. For example, the light off temperature, which is the lowest temperature where the reaction can take place, can be detected very accurately with a TGA, which will be discussed later in this chapter.

The results from tests with propane, methane, and nitrogen (to show thermal effects) are shown in Figure 4.1 for sample *H_2O-550-30*. Under nitrogen some mass loss is observed, indicating that at high temperatures the char decomposes to some extent. This is expected, especially when the char is heated above the temperature at which it was created (550^oC). In addition, heating the char in an environment that does not contain CO or CO_2 can result in the loss of oxygen functional groups on the surface of the char, which will desorb as CO or CO_2. This is discussed in Chapter 7. Additionally, volatiles are probably present in

the char, since it was created below the temperature where tars can thermally decompose. Water loss also takes place, since the char was stored at atmospheric conditions which can lead to adsorption of water in the pores.

In the presence of methane, mass gain is observed starting at 700°C, which represents the deposition of carbon on the surface of the char, according to Equation 4.1. Propane shows a higher mass gain. These results demonstrate the ability of char to catalyze the decomposition of hydrocarbons via the cleavage of C-C and C-H bonds. The C-H bond in methane is one of the strongest aliphatic bonds, with a bond dissociation energy of 439 kJ mol^{-1} [48]. Toluene, which is a major component of tar, has a bond dissociation energy of 374 kJ mol^{-1} for the cleavage of H from the methyl group and 426.8 kJ mol^{-1} for cleavage of the methyl group from the carbon ring, both of which are lower than the bond dissociation energy for methane [48]. Char's ability to catalyze the decomposition of the hydrocarbons tested here suggests that it may also be a good catalyst for tar decomposition.

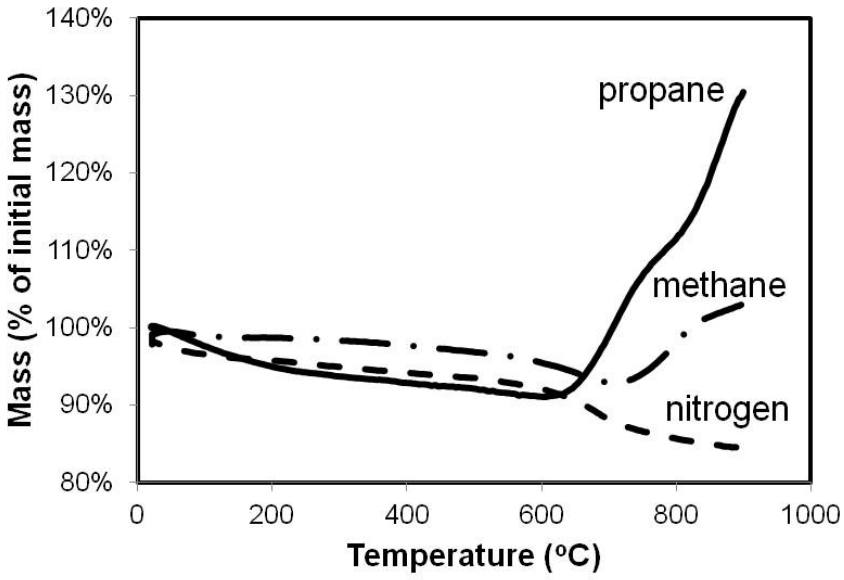

Figure 4.1: Catalytic performance of char for CH_4 and C_3H_8 cracking. Char sample *H_2O-550-30* was heated in a TGA at 5°C min^{-1}.

$$CH_4 \rightarrow C + 2H_2 \tag{4.1}$$

4.1.1 Post-test analysis of char

Post-test characterization of the char was done in the ESEM/EDS in order to understand its structural and chemical properties. Metals appear as bright spots in the ESEM images and compounds such as iron and calcium were detected in the char. An example of this is shown in Figure 4.2, where an iron cluster (measured with EDS) was observed on the surface of the char. Some metals were present in clusters, while others were more evenly dispersed. Iron was present in few locations on the surface, with local concentrations ranging from 2-21 atomic percent whereas potassium was measured in almost all locations with concentrations typically < 1 atomic percent. Calcium was generally present in low concentrations (< 1 atomic percent) throughout the char but clusters of Ca were also observed. Girods et al. observed similar properties in char from wood particleboard waste [49]. They found that Na, K, Mg and Mn were distributed throughout the sample whereas Ca and Fe were localized. The distribution of metals is important in catalytic applications since metals or metal-carbon complexes are likely to be catalytic sites.

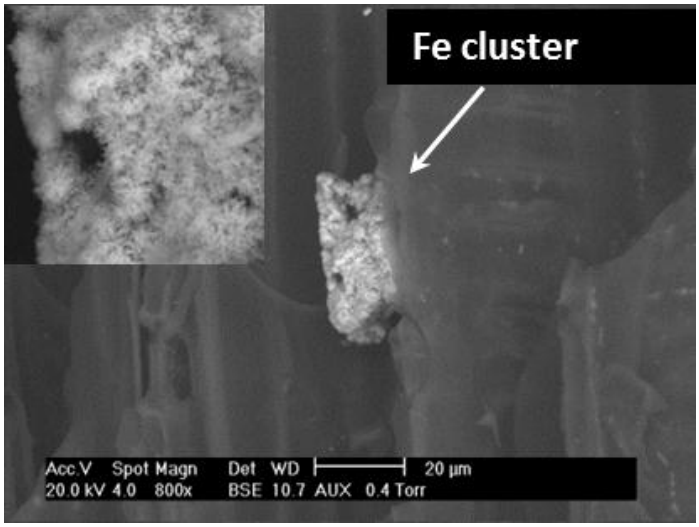

Figure 4.2: Iron cluster on char.

Following propane decomposition reactions, carbon deposition was easily observed as small clusters of carbon on an otherwise smooth char surface (Figure 4.3). Carbon deposition was also observed on the metal sites, as shown in Figure 4.4. Measuring carbon deposition on iron clusters was not straightforward since the iron is not smooth and is

on a carbon support, therefore the EDS measured the deposition of carbon on carbon-iron complexes. It was important to distinguish if the carbon measured by the EDS was deposited from hydrocarbon cracking or the carbon of the char. The C/O ratio was used as an indicator. The C/O ratio measured with EDS was typically between 5 and 15. At the location of the iron cluster, the C/O ratio was 100, which is much higher than that of the char, and is likely a result of carbon deposition from propane cracking. This high carbon concentration could also be a result of the char itself having lower oxygen concentrations at the iron sites. However, EDS measurements of pre-test char showed that this was not the case; the C/O ratio was the same throughout the char sample, including at the iron sites. Therefore, the high carbon concentration at the iron in the post-test char is due to carbon deposition. This suggests that during thermal treatment of poplar wood, the iron in the wood migrates to the surface in clusters, which then acts as an active site for catalytic reactions. The mobility of inorganic elements on the char surface is discussed in detail in Chapter 8. Iron has been used to catalyze tar decomposition in biomass gasification systems. Uddin et al. gasified cedar wood with steam in a two-stage reactor using an iron oxide catalyst supported on alumina [50]. The catalytic tar decomposition took place at 600^{o}C. With the iron catalyst, a higher yield of syngas was obtained, indicating that the iron was catalyzing tar reforming reactions.

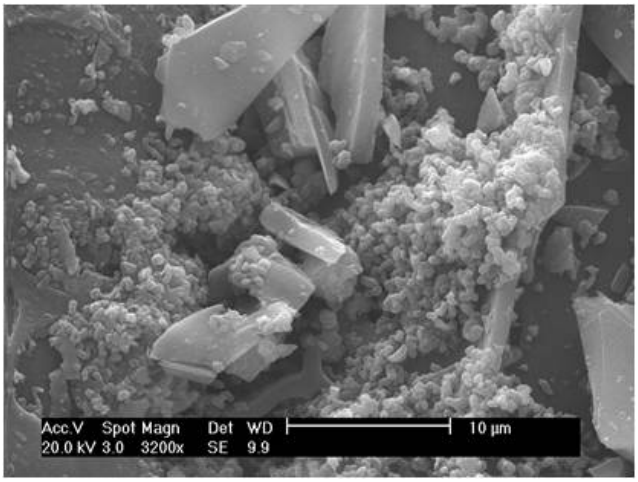

Figure 4.3: Carbon deposition on char sample *H_2O-550-30* after being used to catalyze propane decomposition.

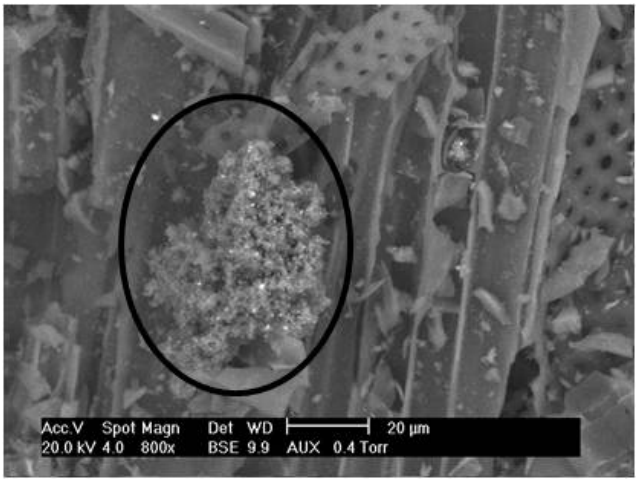

Figure 4.4: Char sample *H_2O-550-30* after being used to catalyze propane decomposition. Iron cluster with carbon deposition, showing that iron is potentially a catalytic site.

During catalytic decomposition of methane with char, carbon deposition was observed around the pores of the char, as shown in Figure 4.5. Figure 4.5A shows char which had not been used as a catalyst, and Figure 4.5B is an image of the char after catalyzing methane decomposition. Carbon deposition is observed around the pores of the char, and some pores are almost completely blocked. This shows that the porosity plays a role in the overall activity of the char. This will be discussed in detail in Chapter 6.

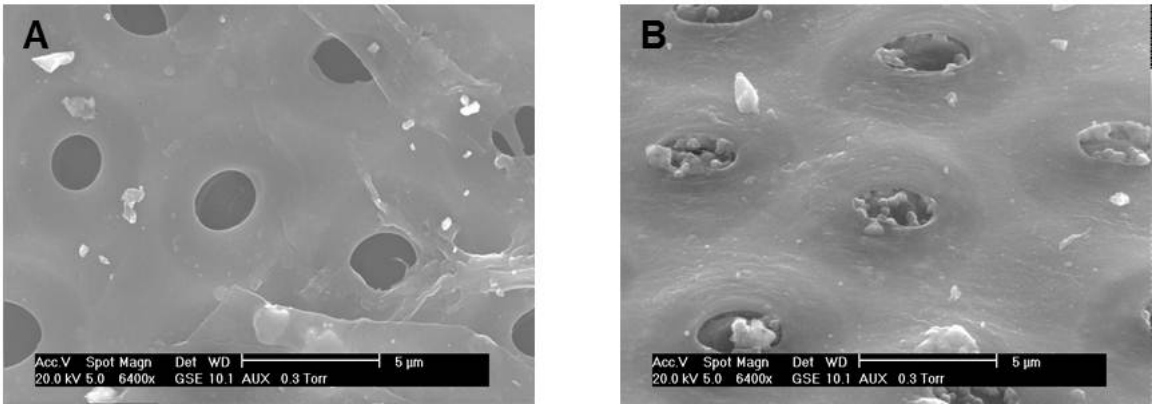

Figure 4.5: Char from CO_2 gasification (sample *CO_2-750-30*) A. Char B. Char after being used to catalyze CH_4 decomposition; carbon deposition is observed on the pores of the char.

4.2 Catalytic cracking of tar surrogate

The experiments presented in Section 4.1 demonstrate that char can catalyze cracking reactions for light hydrocarbons. However, tars are composed of much more complex molecules, as discussed in Section 1.3. Toluene is a major component of tars and is often used in experimental research on tar decomposition [11,51,52]. Therefore, in this work the char's ability to catalyze the decomposition of toluene is tested.

4.2.1 Experimental

A process flow diagram of the reactor used for these experiments is shown in Figure 4.6. The toluene was introduced by flowing nitrogen through a column of toluene at room temperature. The thermodynamic equilibrium for toluene in nitrogen at room temperature is 3%, which is calculated according to the Antoine equation, shown in Equation 4.2. The coefficients used are taken from [53] and are shown in Table 4.1. The flow rate of nitrogen was 100 mL min^{-1}, which enabled the system to reach equilibrium. This was confirmed with micro gas chromatograph (Inficon 3000) measurements of the nitrogen concentration, which stabilized at 97% . The night before each experiment, the nitrogen flow through the toluene column was started in order to allow the system to reach equilibrium. Each experiment used 0.12g of char, which was deposited in a uniform bed across the middle of the quartz reactor. The reactor was first heated in nitrogen to 800 ^{o}C and once a stable temperature was reached the toluene was introduced via a three way valve.

The exhaust of the reactor passed through a condenser which collected the liquid products. The gas was passed through a filter and then to a micro gas chromatograph (Inficon 3000A), which measured the production of light gases (H_2, CO, CO_2, CH_4, C2's, and C3's). The liquid products were measured with an Agilent gas chromatograph (model # 6890) coupled to a mass spectrometer (model # 5973). The experiments lasted for 3 hours from the time of toluene introduction. In order to verify that the reactions were catalytic and not thermal, the same test was done with no char inside the reactor. In addition, since off-gassing of the char is possible, the char was heated to the reaction temperature and

effluent gasses measured in order to verify that the gas products measured were a result of toluene cracking and not simply the off-gassing of the char.

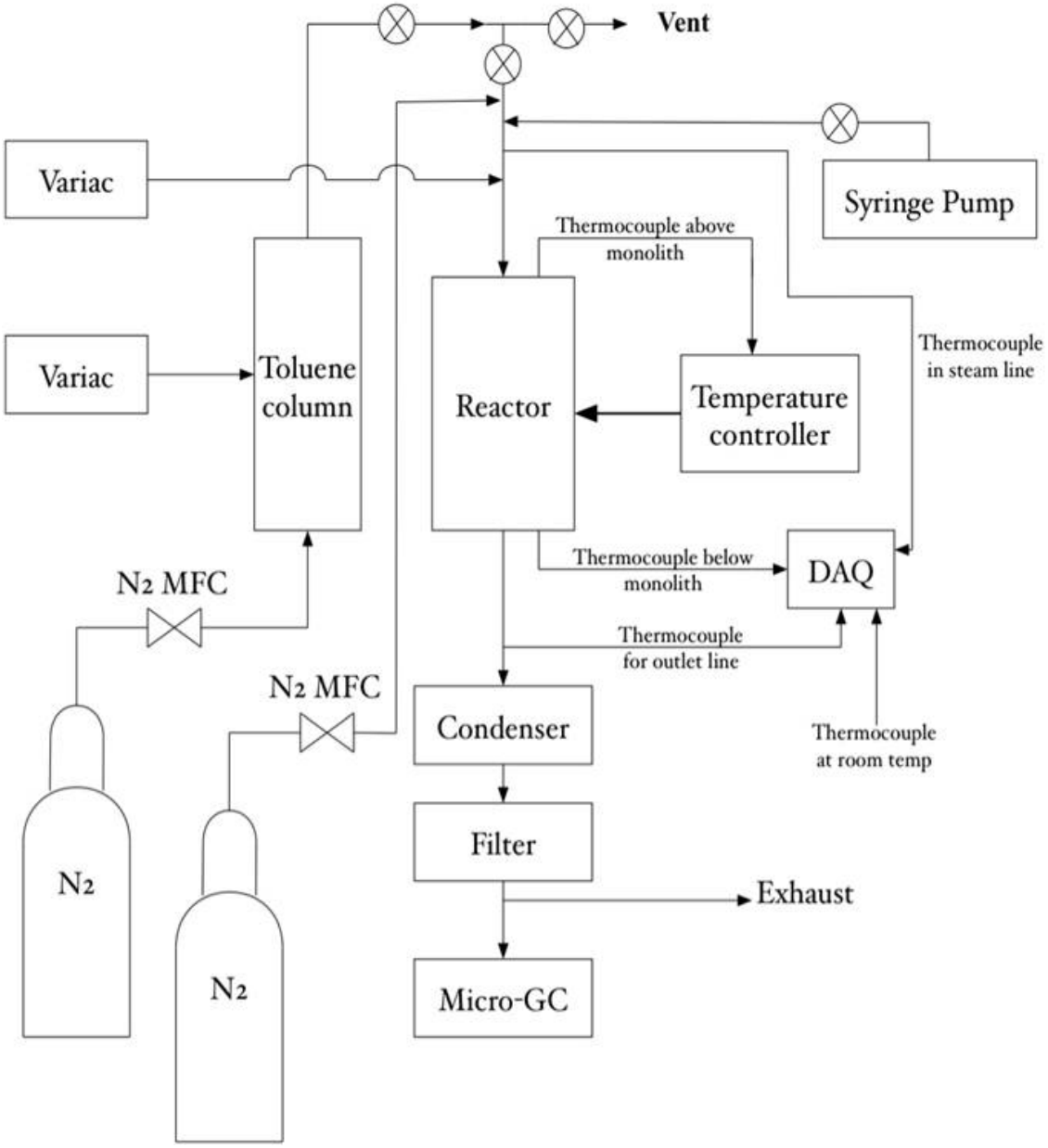

Figure 4.6: Diagram of reactor used for toluene cracking experiments.

$$lnP = A - \frac{B}{T + C} \tag{4.2}$$

Table 4.1: Coefficients used in the Antoine equation for calculation of equilibrium concentration of toluene in nitrogen.

Chemical	A	B	C
Toluene	14.2515	3242.3800	-47.1806
Nitrogen	13.4477	658.2200	-2.854

4.2.2 Char catalyst performance for toluene cracking

Figure 4.7, shows the hydrogen production from catalytic cracking of toluene. The results show a rapid decrease in hydrogen production during the first hour, after which the activity is relatively stable for the next 4 hours. As a point of reference, the molar flow rate of toluene into the system was 12.7 μmol min^{-1}, and the flow rate of H_2 out of the system was 12.1μmol min^{-1}. With this information, it is difficult to know if the reaction proceeded such that each toluene molecule partially decomposed to produce one mole of hydrogen and other reaction products (for example, according to Equation 4.3), or if part of the toluene decomposed to a greater extent, for example, according to Equation 4.4. Of course, there are many other reactions that may have taken place involving partial decomposition of the toluene. The liquid recovered was measured in the GC/MS and the chromatogram is shown in Figure 4.8. It clearly shows that there are many different species present. Many of the peaks were identified as carbon rings with 2 methyl groups (such as o-xylene, 1,3-dimethyl-xylene, and p-xylene), and ethylbenzene was also detected. In the gas phase, CH_4 was detected, in addition to H_2. This demonstrates that the char has catalytic activity for decomposition of aromatic compounds. However, the reactions are complex and there are likely many different reactions taking place. This would make it difficult to quantify reaction products and understand in detail what is taking place on the surface. For example, one char catalyst may be more selective to a certain type of product than another. Reactions that produce only one product, and in particular, a product that is easily quantified, will allow for comparison of different catalysts. Since the focus of this work is to understand the impact of the catalyst's properties on its performance, the methane decomposition reaction was used for most of the tests described throughout this

thesis. A detailed analysis of the reaction mechanism for catalytic decomposition of toluene with char is a subject for future work. However, this test with toluene demonstrates that char has the ability to catalyze the cracking of toluene, which is a major component of tar.

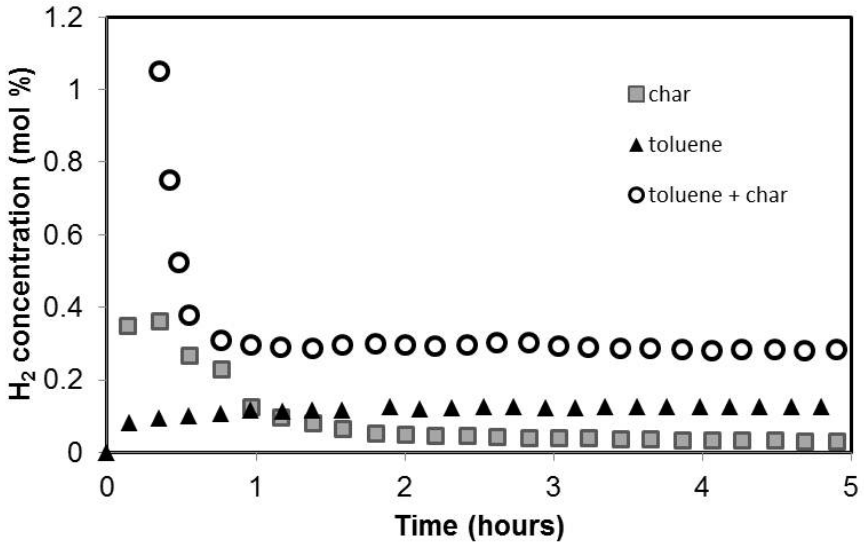

Figure 4.7: Hydrogen production from decomposition of toluene using char catalyst. "Char" indicates the off-gassing of the char, which was heated in N_2. "Toluene" indicates the thermal decomposition of toluene from heating it in N_2. "Toluene + char" indicates the catalytic decomposition from heating toluene (in N_2) in the presence of the char catalyst.

$$C_7H_8 \rightarrow H_2 + C + C_6H_6 \tag{4.3}$$

$$C_7H_8 \rightarrow 4H_2 + 7C \tag{4.4}$$

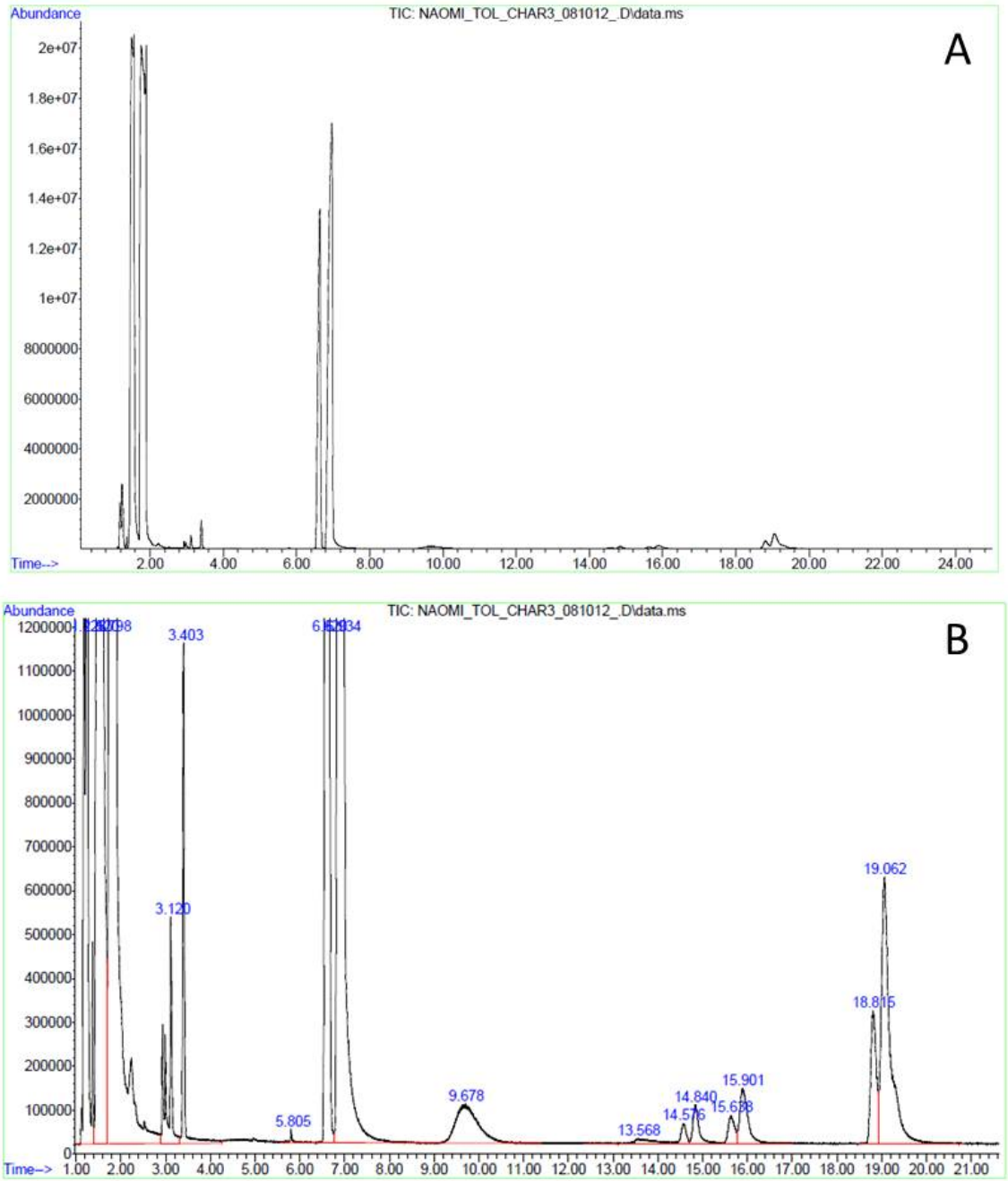

Figure 4.8: GC/MS spectrum of liquids produced from catalytic cracking of toluene. A. Spectrum B. Magnification of spectrum to show smaller peaks.

4.3 Comparison of catalytic performance of char with commercial precious metal catalyst

In order to understand if the catalytic activity of the char is in a practical range, the char was compared to a commercial precious metal catalyst (Pt/γ-Al_2O_3), and to a commercial catalyst carrier (γ-Al_2O_3). Char samples were heated in a TGA to 900^{o}C at 5^{o}C min^{-1} under 30% CH_4 in N_2. The reaction taking place was the decomposition of methane to carbon and H_2, as shown in Equation 4.1. The BET surface area of each material tested is shown in Table 4.2. Mass gain with the different materials is shown in Figure 4.9. H_2 was produced in each experiment, and measured with a gas chromatograph. An example of the hydrogen production from a representative experiment is shown in Figure 4.10. The H_2 production starts at the same time as the mass gain which confirms the relation of mass gain to CH_4 decomposition.

Table 4.2: Surface area of different catalysts tested

Catalyst	Surface area (m^2g^{-1})
Alumina catalyst carrier: γ-Al_2O_3	101
Commercial catalyst: 0.5% Pt on γ-Al_2O_3	130
Char sample *H_2O-750-30*	429
Char sample *H_2O-750-60*	621
Char sample *CO_2-750-30*	435
Char sample *CO_2-920-30*	687

The mass gain for each char sample starts between 2.3-2.4 hours, when the temperature is between 675-700^{o}C. Mass gain for the Pt catalyst starts at 2.7 hours when the temperature is 775^{o}C, and for alumina mass gain starts at 3.0 hours when the temperature is 850^{o}C. Therefore, the onset of reaction is at a lower temperature for char samples, which presents an advantage. Towards the end of the experiment, the slope of the mass gain curve decreases for char samples, indicating saturation of catalytic sites, or pore blocking. The Pt and γ-Al_2O_3 do not demonstrate this which may be because the reaction starts later, so

saturation or pore blocking has not yet been reached. When using char as a catalyst, its long term activity should be considered, and the process designed accordingly.

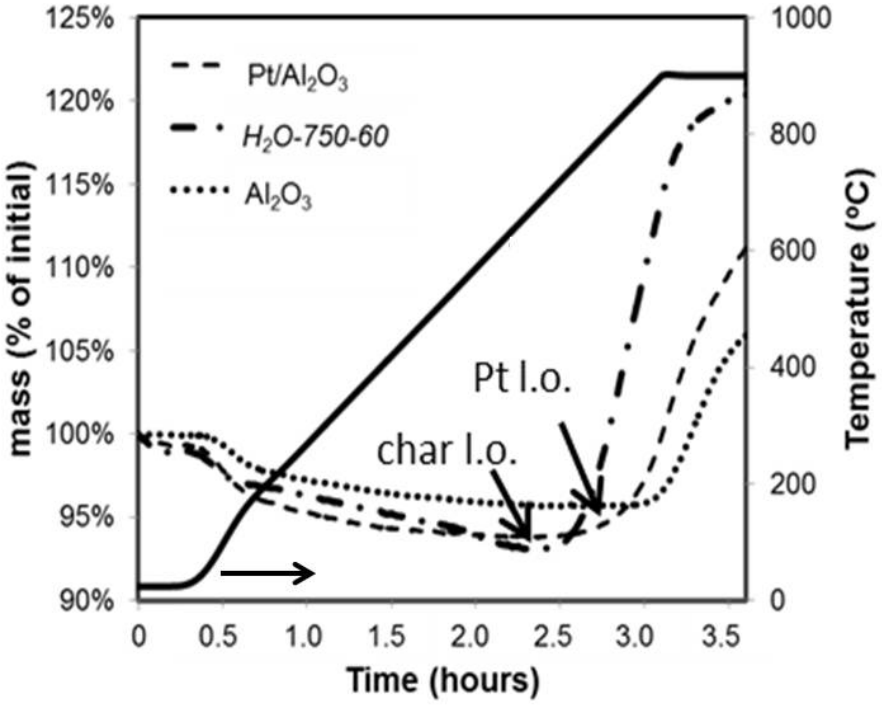

Figure 4.9: Catalytic performance of char compared to commercial Pt/Al_2O_3 catalyst and Al_2O_3 support. Light off temperature is lowest with the char catalyst.

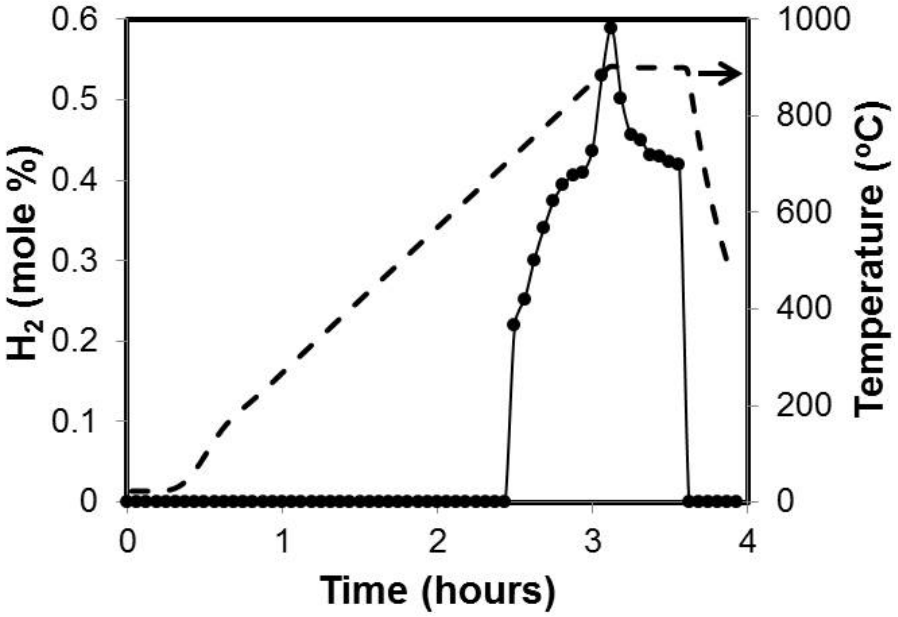

Figure 4.10: Hydrogen produced from catalytic cracking of CH_4.

4.4 Summary

In this chapter, the catalytic activity of char for decomposition of methane, propane, and toluene has been demonstrated. This confirms that the char could be a good catalyst for reforming of tars, since it can decompose C-C bonds and C-H bonds in hydrocarbons. After being used as a catalyst, the char was analyzed in the ESEM. Carbon deposition was observed on the char, specifically on the pores and on the iron cluster. This indicates that the porosity of the char plays a role in its catalytic activity. In addition, the presence of inorganic elements, such as iron, contributes to its catalytic activity. The catalytic performance of the char was compared to that of a precious metal catalyst (Pt-γAl_2O_3) and the light off temperature of the char was 675^{o}C, compared to 775^{o}C for the precious metal catalyst. This presents an energetic advantage for the use of char to catalyze cracking reactions. Since the char has catalytic performance, the next part of this thesis will further investigate which properties give rise to this catalytic performance.

Chapter 5

Process Analyses

5.1 Catalytic performance of char in gasification systems

One of the main benefits to using char instead of commercial catalysts is that the char catalyst can be replaced by ”fresh” char after it has deactivated. The goal of this is to create an integrated system where external catalysts are not needed. However, a gasifier will produce a set amount of tar, char, and syngas depending on the operating conditions of the gasifier and the feedstock. It is therefore important to understand if the catalytic performance of the char produced from a gasifier is high enough to reform all of the tars that would be produced from a gasifier. If the catalytic performance is too low, then additional catalysts would be required, or the char would have to be modified to enhance its catalytic performance. If the catalytic performance of the char exceeds the requirements, then other applications for the char should be considered in addition to catalysis. Therefore, in this section an analysis was done in order to determine if the catalytic performance of the char meets the demand of the tars produced from a gasifier.

The kinetics of the catalytic performance of the char were determined for the methane decomposition reaction (Equation 4.1). Catalyst deactivation should be considered in determining the overall kinetics of the reactions, since deactivation is likely to take place during tar decomposition. The deactivation rate of the char catalyst was measured in a TGA. The char was heated to 750^{o}C in the presence of methane and the char catalyzed the decomposition of methane. The reaction rate over time is shown in Figure 5.1. Two regions

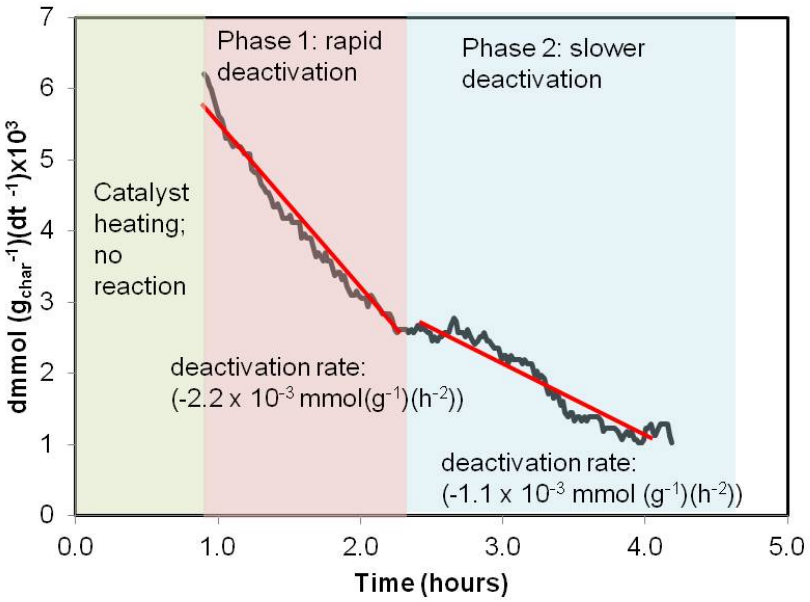

Figure 5.1: Catalyst deactivation for CH_4 cracking reaction.

of deactivation are observed: an initial rapid deactivation followed by a second regime of more gradual deactivation. The reaction rate decreases over time, which reflects catalyst deactivation. Deactivation rate is calculated to be the slope of the line, which is the rate at which the reaction rate is decreasing. The deactivation rate for regimes 1 and 2 were -2.2x10^{-3} mmol g_{char}^{-1} h^{-2} and -1.1x10^{-3}*mmol* g_{char}^{-1} h^{-2}, respectively.

5.1.1 Reactor model

In order to understand how these deactivation rates relate to a gasification process, a system is modeled where all of the char is recycled to be used for tar decomposition. While the actual amounts of tar, char, and synthesis gas will vary depending on the feedstock and reactor conditions, we have used values from a reactor whose experimental performance has been reported in literature by Carpenter et al. [54]. Therefore, using the amount of char and tar generated from this real gasification system, and the reaction kinetics of the char that we have generated we determine if the catalytic performance of the char is high enough to reform all of the tar produced. In the work by Carpenter et al. the char yield was measured to be 22% and the tar yield was 10%. In that process, mixed wood was gasified

with steam at 650^{o}C and a thermal tar cracker downstream was used at 875^{o}C. After the thermal cracker, some tars remain and the catalytic decomposition of these tars is studied here. In this example, a fixed bed of char is placed downstream of the gasifier.

The conversion rates of char were calculated based on the conversion rates that were measured for methane. These kinetics were used because deactivation was observed during the experiments done with methane, so using these kinetics allowed us to account for catalyst deactivation. A paper by Wang et al. measured the kinetics of catalytic steam reforming of methane and toluene and reported the rate of methane reforming to be approximately 1.6 times the rate of toluene reforming [55]. Toluene is a major component of tar, so it is reasonable to assume that toluene reaction rates are similar to that of tar. The kinetics that were measured for methane cracking, as shown in Figure 5.1 were divided by 1.6 in order to achieve reasonable kinetics for toluene decomposition. This calculation gives an initial reaction rate of 3.82x10^{-3} mmol h $^{-1}$ g_{char}^{-1}. The objective is to determine if the amount of char generated will convert all of the tar that is generated, or if the deactivation rate is so rapid that all of the tar cannot be converted with the amount of char produced in the gasification process. In this calculation, a time frame of one day and a flow rate of 1kg h $^{-1}$ of biomass was selected (in other words, the char that is produced in one day is placed in a downstream tar reformer). This system produces 5.28 kg of char per day and a fixed bed reactor with 5.28 kg of char and 0.1 kg h^{-1} of tar is modeled.

The total number of moles of tar that can be converted before the char reaches phase 2 of deactivation was calculated according to Equation 5.1. The result of the calculation outlined in Equation 5.1 shows that during phase 1 deactivation, the amount of char generated by the reactor modeled here can reform 29 kmol of tar. The total amount of tar generated over one day was calculated to be 26 kmol. This indicates that for the char to tar ratios of this reactor, the char will not reach phase 2 deactivation. Therefore, using the char as a catalyst enables the reforming of tar and the activity of the char will not fall below 40% of its initial activity. While the ratios of tar to char will vary based on gasification conditions, this calculation suggests that the reactivity of char is on a reasonable scale for conversion of tar.

$$
\begin{aligned}
n_{phase1} &= \int_0^{t_{phase1}} \frac{dn}{m_{char} \cdot dt} \cdot m_char \cdot \left(\frac{r_{toluene}}{r_{methane}} \right) dt \\
n_{phase1} &= \int_0^{1.2} (1.2.t + 6) \cdot \frac{mol_{CH_4}}{g_{char} \cdot h} \cdot 5280 g_{char} \cdot \left(\frac{1 mol_{toluene}}{1.6 mol_{CH_4}} \right) dt
\end{aligned}
\tag{5.1}
$$

5.2 Energy tradeoff for diverting char from combustion applications

The energy tradeoff for diverting char from possible heat recovery is considered. The energy available by combusting the char is compared to the energy of synthesis gas that would be generated from tar reforming. This is done by comparing the heat of combustion of char to the heating value of the syngas that would be obtained from tar conversion. The two systems considered are shown in Figure 5.2. Both literature data and our own data are used to complete this analysis. Relative char and tar production rates are taken from a paper by Gomez-Barea, where wood waste was pyrolyzed at different temperatures (750-900^{o}C) and the amount of tar, char, and gas was measured [56]. The conversion of tar is obtained from a paper by Abu El Rub et al. where char was used as a catalyst to reform phenol, a model tar compound, and 81.6% conversion was achieved at 700^{o}C in the presence of steam and CO_2 [57]. In our energy balance, energy inputs to the steam reformer should also be accounted for. If the char is placed downstream of the biomass in the gasifier, then the catalytic reformer would not require additional heating, since gasifiers typically operate around 700^{o}C or higher. However, the heat of reaction must be accounted for, therefore the enthalpy for steam reforming of toluene has been included, according to Equation 5.2. Steam reforming is typically used to decompose tars, and, since biomass contains water, the steam will be available in the reactor. The energy recovery from reforming the tar is calculated according to Equation 5.3, where the enthalpy of the reforming reaction is subtracted from the heating value (heat of combustion) of the gasification products.

The heating value of the char was calculated according to Equation 5.4, where the heat of combustion of char was -27.9 kJ kg^{-1} [58]. This value is for char containing approximately

90% carbon. The carbon content of the char generated from gasification experiments was measured to be in this regime, therefore this heating value is appropriate for this system.

The pyrolysis system that is used for this example produces ~20% char, and this value did not vary significantly with temperature. The concentrations of tar were highly dependent on temperature. Gomez-Barea et al. report the percentage of biomass that is in the char, gas, and total condensate, where total condensate includes water. Typically wood contains ~5% water, so 5% of the condensate was considered as water and the remaining condensate was said to be hydrocarbons. The amount of energy that could be recovered from the char and the syngas (from tar conversion) is shown in Figure 5.3. At 750^{o}C, condensate was reported to be ~23% whereas at 900^{o}C, condensate was reported to be only ~10% so significantly less syngas would be produced by reforming tar from high temperature pyrolysis systems. Low temperature systems generate more tars, and therefore more syngas could be recovered from tar reforming. Therefore, at 750^{o}C the energy value of the syngas from tar reforming is higher than that of the char combustion. At higher temperatures, the heat of combustion of char is higher than that of the syngas produced. Although the objective of this study is to develop an understanding of the energy tradeoff for using char as a catalyst for tar decomposition, it does not absolutely determine if the use of char in this application is beneficial. For example, there is an economic benefit to using char in place of metal catalysts, or high temperature thermal conversion systems. This is not reflected in the energy balance.

$$C_7H_{8(g)} + 7H_2O_{(g)} = 7CO_{(g)} + 11H_{2(g)} \qquad \Delta H_{ref} = 869kJ/mol \tag{5.2}$$

$$Q_{syngas} = conversion \cdot n_{tar} \cdot \left(\frac{n_{CO}}{n_{tar}} \cdot HV_{CO} + \frac{n_{H_2}}{n_{tar}} \cdot HV_{H_2} - \Delta H_{ref}\right) \tag{5.3}$$

$$Q_{char} = n_{char} \cdot HV_{char} \tag{5.4}$$

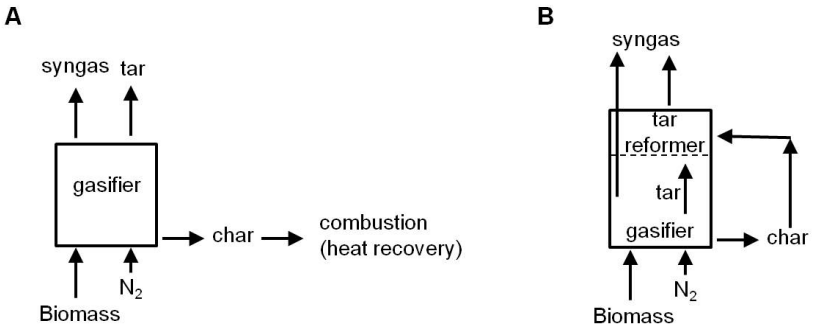

Figure 5.2: Two proposed processes for use of char. A. Char is burned and used for process heat. B. Char is used as a catalyst to reform tars into synthesis gas.

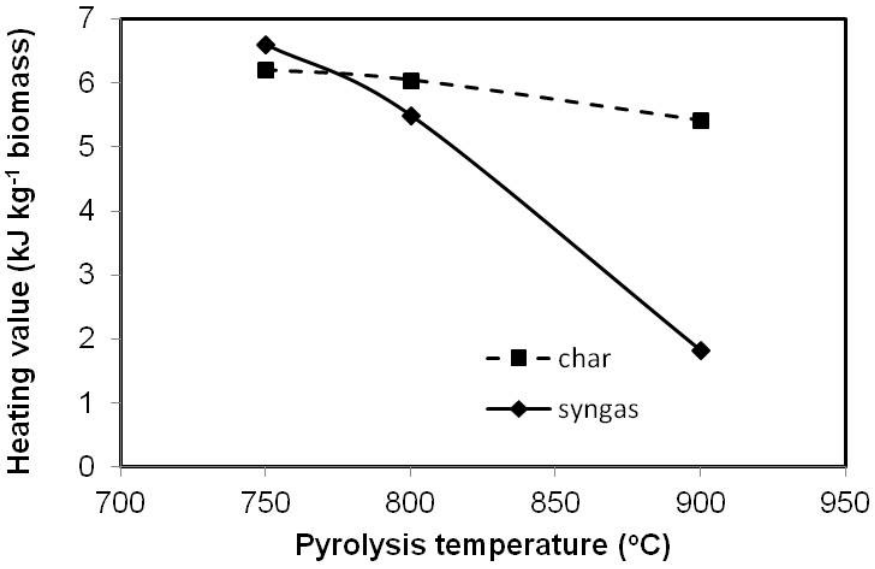

Figure 5.3: Heating value of char compared to heating value of synthesis gas generated from tar reforming with a char catalyst.

5.3 Summary

This section analyzed if the catalytic activity of the char for tar reforming was on an appropriate scale to meet the needs of a real gasification system. In order to make an integrated system, then the amount of char that is produced from a gasifier must be enough to reform all of the tar that would be produced from that system. The deactivation kinetics were measured for the char over 3 hours for methane decomposition. During this time period, the reaction rate decreased to approximately one sixth of the initial rate, therefore it is reasonable to say that the catalyst lifetime would not extend beyond three hours for reactions that produce high amounts of coke, such as cracking reactions. Since the kinetics were measured for CH_4 cracking and the actual reaction would involve toluene decomposition, a factor was used to adjust for the relative rates of the two reactions. Then, a reactor model was used in order to determine if the char produced from a gasifier could reform all of the tar produced. The quantities of tar and char were determined based on a real gasification system that had been reported in the literature [54]. The calculations determined that the catalytic activity of the char and the quantity of char produced is sufficient to reform all of the tar that would be produced from a real gasification system. While the relative quantities of char and tar, as well as the catalytic activity of the char will change with the gasification conditions, this indicates that the activity is on a reasonable scale for the process that is proposed in this thesis. The energy benefit for using the char to catalyze the reforming of tar to syngas was compared to the energy recovered from combusting the char for process heat. At low temperatures, where high quantities of tar are produced, the heating value of the syngas was higher than that of the char combustion whereas at high temperatures ($>770^{o}C$) the heating value of the char combustion was greater than that of the syngas from tar reforming.

Part III

Explanation of catalytic performance

Chapter 6

Surface Area and Porosity

6.1 Influence of surface area and pore size distribution on catalytic performance

Chapter 3 illustrated that the gasification conditions impact the surface area and porosity of the char. This section will explore how these properties influence the catalytic performance of the char. These tests were done for the methane decomposition reaction, using a TGA, according to the procedure described in Chapter 4. The following chars were compared: *CO_2-920-30*, *CO_2-750-30*, *H_2O-750-30*, *H_2O-750-60*. The surface area of each of these char samples is shown in Table 4.2. The mass gain from catalytic methane decomposition for each of the char samples is shown in Figure 6.1. For a given char type (char created in either H_2O or CO_2), higher surface area resulted in higher mass gain, indicating that increased surface area results in higher catalytic activity. However, the activity of the char is not directly proportional to BET surface area. Dufour et. al. showed that the pore size of wood char impacts its catalytic activity when used for methane decomposition [59]. Specifically, they found that in pores with a diameter <1nm, diffusion limitations became significant and therefore activity was not directly proportional to BET surface area when pore size varied. This phenomenon was also observed in the experiments presented here. The mass gain for sample *CO_2-920-30* is lower than for *H_2O-750-60*, even though the surface area of the former is higher. However, a comparison of samples made with CO_2 and steam at

750 ^{o}C showed that char made with CO_2 contained micropores whereas char made with steam did not. So, the lower performance of sample *CO_2-920-30* may be due to diffusion limitations in the micropores of the char. Therefore, when considering which char to use in catalytic applications, it is important to understand the available surface area, which is a function of the specific surface area and the pore size distribution of the char.

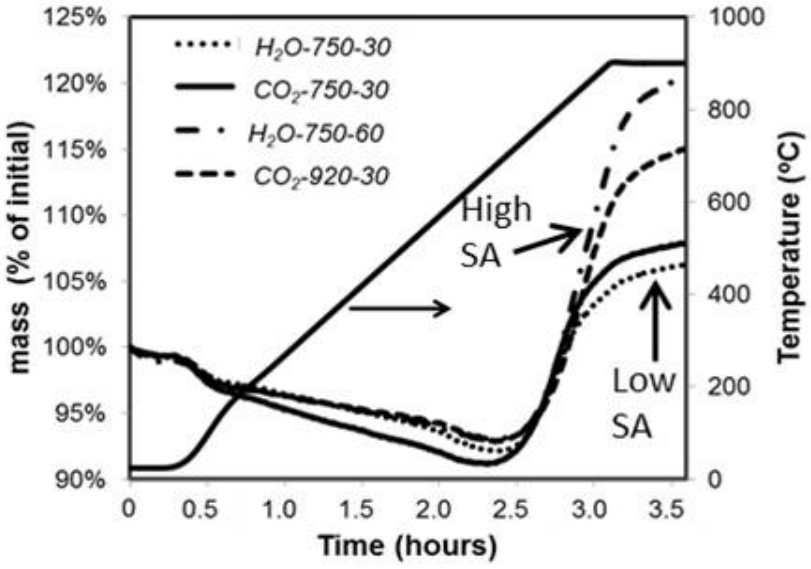

Figure 6.1: Catalytic performance of different char samples for methane cracking

6.2 Catalyst deactivation and pore blocking

The catalyst exhibited clear signs of deactivation, as shown in Figure 6.1, where the slope of the mass gain curve decreases. There are various mechanisms for catalyst deactivation, such as poisoning, sintering, and coking [34]. Coking is known to be a problem with tar reforming reactions, as discussed in Chapter 1. It was therefore important to understand the deactivation mechanism for the char catalyst used in these experiments. Since coke deposition was clearly taking place on the char surface, and we have determined that the char is a porous material, the most likely mechanism for deactivation was pore blocking due to coke formation. In order to verify this, the BET surface area and pore volume were

measured for the char before and after it had been used as a catalyst for CH_4 decomposition at 700^{o}C for 3 hours. After the reaction, the surface area had been reduced to 80% of its original value, and the mesopore volume was reduced by one third. This significant loss in pore volume and surface area confirms that pore blocking takes place, and is most likely the primary mechanism for deactivation. Sintering could also cause loss in surface area and pore volume; however, sintering is much more likely to take place at temperatures which are higher than 700^{o}C.

6.3 Deactivation kinetics

The kinetics of deactivation were tested in a Quantachrome ChemBET instrument. This unit consisted of a flow through packed bed quartz reactor, in a furnace whose temperature was controlled by a built in temperature controller. The sample was heated to 850^{o}C in N_2 and then a mixture of 15% CH_4 (balance N_2) was introduced. The effluent gases were measured with an Inficon 3000 micro gas chromatograph. H_2 production was used to determine conversion, according to Equation 4.1. The temperature of 850^{o}C was chosen because at this temperature significant differences were observed among different char samples, whereas very small differences were observed among different char samples when reactions were done at 700^{o}C, where conversion was very low. This is discussed in more detail in Section 8.4.1. The hydrogen production curves for samples *CO_2- 920-30* and *H_2O-750-60* are shown in Figure 6.2. For sample *H_2O-750-60*, a high production of hydrogen is initially produced, followed by a rapid decline in H_2 concentration. The sample made under CO_2 shows a lower initial activity followed by a more gradual decrease in H_2 production. Figure 6.3 shows the deactivation function plotted versus time for the two samples. The deactivation function, Φ, is defined in Equation 6.1 where r_0 is the initial reaction rate and r_t is the reaction rate at time t (in minutes). The deactivation profiles for other char samples are shown in Appendix A. Because of the different behaviors of samples *CO_2-920-30* and *H_2O-750-60*, these two samples are used to understand the phenomena taking place during catalyst deactivation.

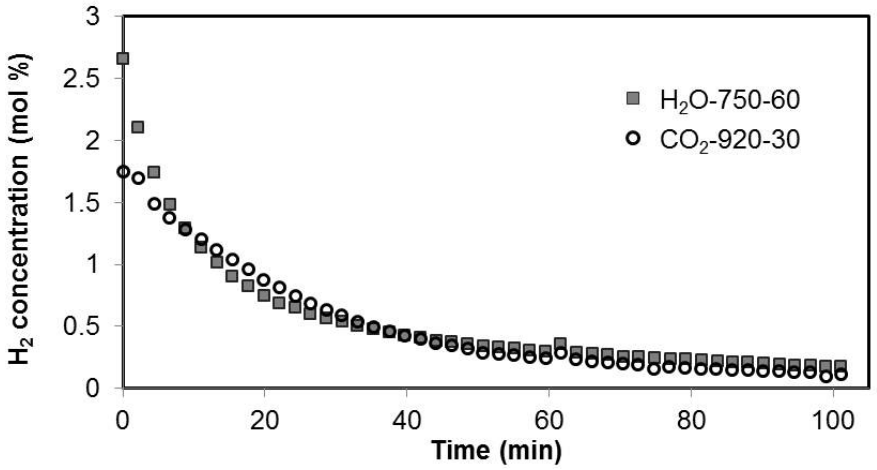

Figure 6.2: H_2 production from CH_4 cracking at 850^{o}C. Error on concentration measurment is 0.03%.

$$\Phi = \frac{r_t}{r_0} \tag{6.1}$$

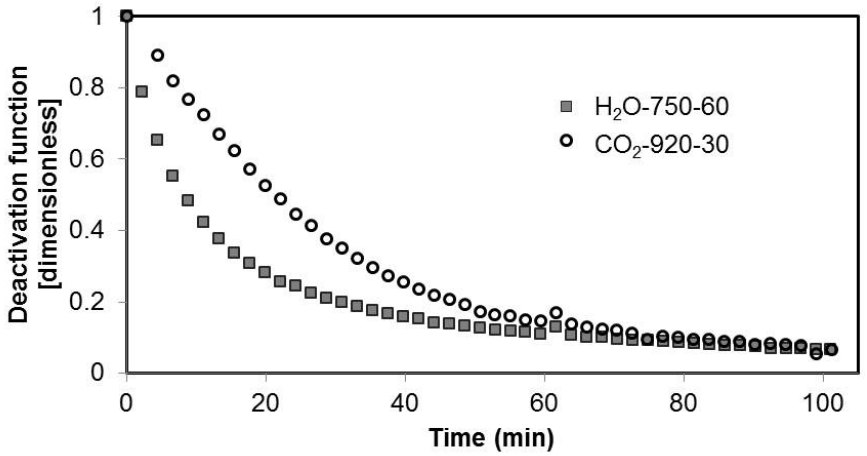

Figure 6.3: Deactivation function for char samples *CO_2-920-30* and *H_2O-750-60* during CH_4 cracking at 850^{o}C.

The deactivation profiles can provide information on the mechanisms of deactivation. As discussed in Section 4.1, deactivation by carbon deposition and pore blocking take place when char is used for methane cracking. Deactivation from carbon deposition has been

extensively studied for many years [60,61]. In porous materials, the catalytic sites may be present in the pores, and the concentration of active sites within the pores may vary. Carbon deposition can eventually block the pores. When this happens, all catalytic sites within the blocked pore will become effectively deactivated, even if these sites themselves do not have carbon deposited on them. Froment and Bischoff have studied catalyst deactivation by carbon deposition extensively, and have determined models for various deactivation conditions [60]. Figure 6.4 shows the deactivation function versus time for catalysts with varying numbers of sites per pore, from Froment and Bischoff [60]. The numbers on the curves represent the number of catalyst sites in a single pore. If the pores are not blocked, and there are no diffusion limitations in the pores, then the deactivation rate will be the same for all of the catalysts used in this example. Therefore, up until one hour of time on stream, these catalysts all have the same deactivation profile. However, once the quantity of coke is high enough that pores become completely blocked, the deactivation profile depends on the number of sites in each pore. For catalysts with a high density of sites per pore, the blocking of a single pore will render many sites deactivated, therefore a sharp decrease in the activity function is observed. For catalysts with fewer sites per pore, the rate of deactivation is still faster than in the first hour, but to a lesser extent.

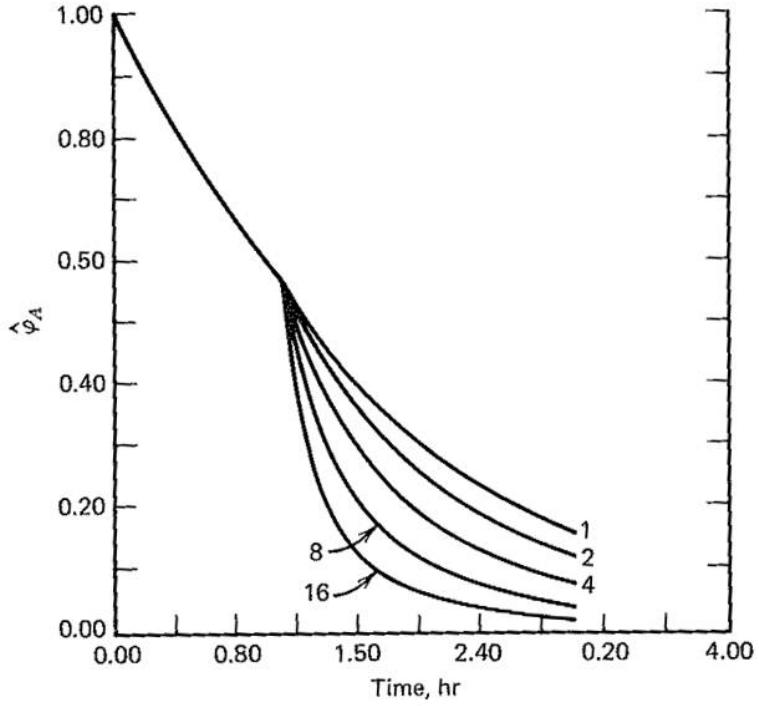

Figure 6.4: Deactivation function versus time for catalysts with different numbers of sites per pore. The y axis shows the deactivation function over time. The numbers on the curves indicate the number of catalyst sites per pore. Pore blocking starts just after one hour, when the different curves diverge. [60]

Figure 6.3 shows the deactivation functions for the two samples tested here. The sample made under CO_2 has a lower slope than that made under H_2O, indicating that char made with CO_2 has fewer sites per pore. This could be due to the difference in porosity, and diffusion limitations in micro pores. The pore network in char often has a fractal nature, where micropores branch off of mesopores. Fu et al. studied the structure of char derived from steam gasification of rice husk and observed that the pore structure of the char had a fractal pattern [62]. Zhang et al. observed a fractal distribution in the porosity of coal and coal char [63]. If the sample has many of its catalytic sites in the micro pores, which are less accessible due to diffusion limitations then one mesopore may contain far fewer active and accessible sites, since many of them will be locked up in the micro pores. A diagram of this

scenario is shown in Figure 6.5, where the catalytic sites contained within the micropores are shaded grey to indicate that they are not accessible due to diffusion limitations. This could explain the slower decrease in the deactivation function for the char made under CO_2.

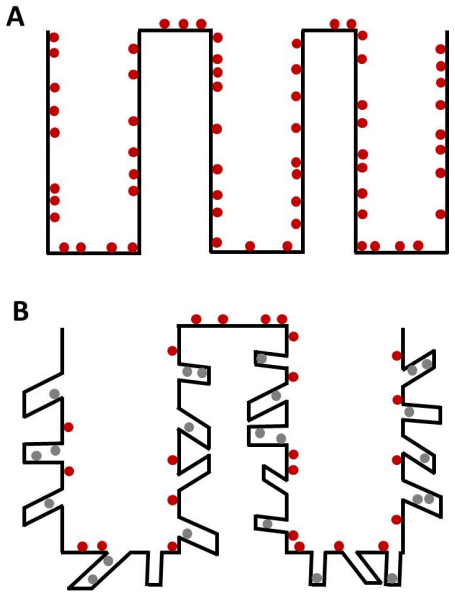

Figure 6.5: Diagram of catalytic sites in mesopores and micropores. Dark red dots represent available catalytic sites and light grey dots represent unavailable sites in micropores. Microporous char has fewer available catalytic sites per mesopore.

6.4 Summary

This chapter studied the influence of porosity and surface area on the catalytic activity of the char. Chars with higher surface areas had higher catalytic activity but diffusion limitations were observed in the micropores of the char. Therefore, chars with higher mesopore surface area will have the best catalytic performance. After being used for catalyzing CH_4 decomposition at 700^{o}C, a 20% reduction in surface area and 33% reduction in mesopore volume were observed, indicating that deactivation takes place via pore blocking. The deactivation function had a steeper decline for mesoporous char that was made in steam compared to microporous char that was made in CO_2. A steeper deactivation function

indicates that there are more catalyst sites per pore, so when one pore becomes blocked, many catalytic sites are lost. Therefore, due to the micropores, high surface area char made in CO_2 has fewer available catalyst sites than high surface area char made in steam.

Chapter 7

Surface Oxygen Functional Groups

It is well known that acid groups play a role in many types of catalytic reactions, such as cracking, isomerization, and polymerization [61]. Therefore, it is of interest to study the acidity of the char catalyst. On carbon surfaces, the acid sites arise from oxygen functionalities on the surface. This chapter investigates the presence of such sites on char, and their influence on its catalytic performance.

7.1 Surface functionalities in carbons

While the porosity of the char clearly plays a role in its catalytic activity, it is well known that the surface functionalities are also important in determining the adsorption of molecules on carbon surfaces. Oxygen sites enhance the adsorption of polar molecules, such as water. Therefore, porosity and surface area are the most important factors in determining the adsorption of non-polar (eg. aromatic) compounds, whereas the surface functional groups influence the adsorption of polar molecules [64]. If the char is used in applications involving polar molecules, for example steam reforming, the surface functionalities should be understood.

Surface functionalities on carbon surfaces have been studied extensively, as they influence the catalytic properties of these materials. Imperfections or defects along the edge of the carbon matrix create highly active sites where other molecules, such as oxygen, nitrogen, hydrogen, or sulfur can adsorb, creating surface functionalities which are active

for catalytic reactions. Oxygen functionalities have been studied most extensively, since they are formed spontaneously and can be increased by oxidative treatments [36]. Surface groups can be acidic (ex. carboxylic acid, lactone, phenol) or basic (ex. pyrone, chromene). Acidic surface groups have been studied extensively and it is understood which types of surface functionalities give rise to surface acidity; however the types of sites that create a basic surface are not as well understood [36, 65]. In general, acidic sites are formed when a surface is heated in an oxidizing environment and basic groups are formed when an oxidized surface is reduced by heating in an inert environment [36]. Some examples of functional groups are shown in Figure 7.1.

Franz et al. studied the effects of surface oxygen groups on the adsorption of various aromatic compounds on carbon [66]. They used ash free activated carbon made from petroleum pitch and tested the adsorption of aromatic compounds such as nitrobenzene, phenol, aniline, and benzoic acid, in aqueous and cyclohexane solution. They found that surface oxygen groups significantly influence the adsorption of aromatic compounds. Specifically, they found that these groups adsorb water which reduces accessibility of the surface sites to aromatic compounds. In the absence of water (in cyclohexane solution), the opposite effect was observed, where oxygen functional groups enhanced the adsorption of aromatic compounds. The competitive adsorption of water molecules and organic compounds on chars was also studied by Bradley et al., who used char to adsorb toxic compounds from humid air streams [67]. They found that adsorption of water on polar sites led to pore blocking, which decreased the adsorption of the target organic compounds. By reducing these sites via thermal desorption, the uptake of organic molecules was improved. Chen et al. used coal-based activated carbons for the conversion of benzene to phenol. They modified the concentration of carboxyl groups on the surface by treating the samples with nitric acid in different concentrations and found that the amount of carboxyl groups on the surface is the most important factor in determining catalytic performance of the activated carbon [68].

Ahumada et al. used activated carbon to catalyze the oxidation of Fe(II) to Fe(III) in aqueous solution. They also found that by increasing the surface oxygen groups (with nitric acid or hydrogen peroxide treatment), conversion increased [69]. Ko et al. used char

generated from MSW or RDF which was activated using a basic (KOH) treatment for NO_x reduction with ammonia. They found that this char, when impregnated with Mn, had better performance than conventional carbon SCR catalysts, and attributed this performance to the high specific surface area, pore volume, and oxygen functional groups [70]. This shows that the role of surface oxygen in char has been extensively studied, and clearly influences the catalytic activity and adsorption properties of carbon surfaces.

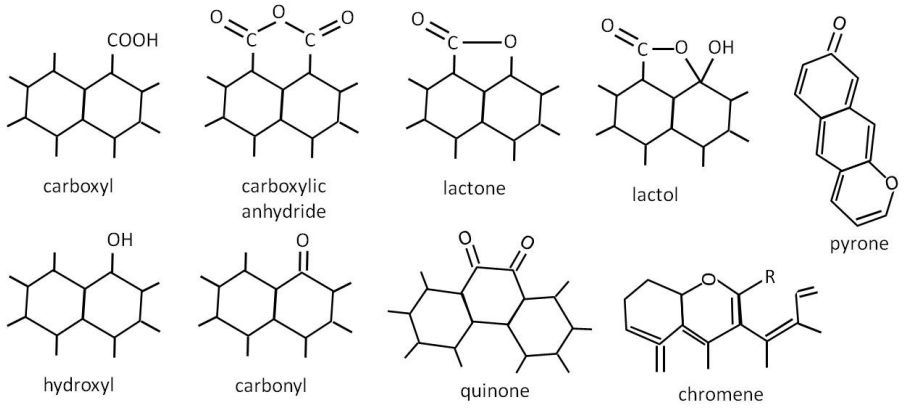

Figure 7.1: Oxygen functional groups on carbon surfaces.

7.2 Identification of functional groups on carbon surfaces

Acid sites on catalysts such as zeolites or other acidic solids are often determined via temperature programmed desorption of a basic gas, such as ammonia. In this method, the catalyst is typically reduced in H_2 and then exposed to ammonia at room temperature. The sample is then heated in an inert environment up to temperatures above 500^oC. In many cases, ammonia peaks desorb at temperatures around 300 or 400^oC [71, 72]. However, for char, some of the acid sites may have desorbed as CO or CO_2 in this temperature range. Therefore ammonia TPD is not an appropriate method to measure acid sites on carbon surfaces, since the surface is likely to have changed at the temperature where these measurements are done.

There have been significant efforts reported in literature to identify the types of functional groups on carbon surfaces [65]. The two methods that are most commonly used for

identification of surface functional groups are temperature programmed desorption (TPD) and Boehm titration, which will be discussed in detail later in this chapter. Some have also used spectroscopic techniques, but this is not nearly as common.

7.2.1 Boehm titration for identification of surface oxygen groups

The Boehm titration method was developed by H. P. Boehm and is described in his publication in 1966 [73]. It has since been used by many and is understood to be one of the most reliable methods for quantifying the different types of acid sites on carbon surfaces [68,74–77]. This method is based on the principle that different types of oxygen groups have different acidities, and can therefore be neutralized by different types of bases. The sample is titrated with bases of different basicities, which allows for the quantification of different types of surface acid sites. The four bases used are sodium bicarbonate ($NaHCO_3$), sodium carbonate (Na_2CO_3), sodium hydroxide (NaOH), and sodium ethoxide (C_2H_5ONa). This process is based on the assumption that sodium bicarbonate neutralizes carboxylic acids, sodium carbonate neutralizes carboxylic acids and lactones, sodium hydroxide neutralizes carboxylic acids, lactones, and phenols, and sodium ethoxide neutralizes all oxygen species. In a practical sense, the sodium ethoxide titration is often excluded due to the assumption that the quantity of very weak acid sites is very small, and therefore essentially all acid sites would be detected with NaOH. Based on these three or four titrations, the number of each type of acid sites can be determined by difference.

There are a number of issues with the Boehm titration method which can lead to inaccurate measurements, and, more importantly, has resulted in inconsistent measurement techniques, making it difficult to compare data acquired by different research groups. One issue with this method is the presence of CO_2, which is easily adsorbed in the micropores of char or activated carbon. The dissolution of CO_2 into the solution will impact the pH, increasing the apparent number of acid sites measured. One way to avoid this is to degas the samples under vacuum at elevated temperatures prior to titration. However, there is a risk of CO_2 adsorption when the sample is transferred, for example, from the degasser to the titration system due to exposure to air.

Dissolved CO_2 in the solution can also impact the measurment, and therefore it is recommended to continuously degas the solution with N_2 or Ar during titration to avoid dissolution of atmospheric CO_2 into the solution [74]. Endpoint determination is another aspect which can vary amongst experimentalists, as it can be done with a variety of different colour indicators, or by measuring the pH. The colour indicators include an element of subjectivity, as the moment when colour change is perceived to have taken place may vary from one individual to the next. In addition, the pH where the colour changes may not be the best pH to determine the acidity of the solution. For strong acid strong base titrations, a pH of 7.0 should be used but most colour indicators do not change colour at this pH. The endpoint can also be determined by the first derivative, where the point with the biggest slope is considered to be the equivalence point.

Another question that has been raised is the length of time required for complete neutralization of the acid sites. In the original publication by Boehm, the mixture was agitated for 16 hours. However, Boehm acknowledged that other authours required up to 10 days for their solutions to equilibrate. Goertzen et al. and Oickle et al. have attempted to standardize the method with their publications in 2010 which identify the main issues and inconsistencies with Boehm titration and propose solutions to these issues [74,75].

7.2.2 Temperature programmed desorption for identification of surface oxygen groups

Temperature programmed desorption (TPD) is commonly used for identification of oxygen groups on carbon surfaces [66, 69, 78, 79]. This method involves heating the carbon at a constant rate in an inert atmosphere, such as nitrogen or helium, and the gases evolved are measured semi-continuously. The gases typically evolved are CO and CO_2 and the temperature at which they desorb indicates the type of oxygen groups on the surface. Szymanski et al. have provided a review of the temperature and gases evolved that are associated with different types of surface groups [79]. However, it is clear from their review of the literature that the temperature range for specific surface functionalities is broad, which can make it difficult to identify the functional groups with this method. There are others who have tried to improve the technique by combining TPD with other

analysis techniques. For example, Brender et al. coupled TPD with mass spectrometry (TPD-MS) and with X-ray photoelectron spectroscopy (TPD-XPS) in order to try to improve the understanding of the change in surface chemistry as the CO and CO_2 groups desorbed from the surface [80].

7.2.3 Identification of surface oxygen groups on char samples

In this thesis, the TPD method has been used for identification of surface oxygen groups. The goal of the tests was to identify the types of functional groups on the surface and to compare samples. In the TPD method, the ambiguity lies primarily in the fact that different authours report different temperatures of desorption for a certain type of surface group. However, this method allows for good comparison of different samples, since the procedure will be the same for all samples. In the Boehm titration method, the error lies in the procedure used for the measurement. Therefore, if we are comparing different samples this error might affect the relative amounts of surface oxygen groups measured on different samples. The samples were heated in a quartz flow through reactor which was coupled to a 3000 Inficon micro gas chromatograph which measured CO and CO_2 evolution.

The TPD profiles for four char samples (*CO_2-750-30*, *CO_2-920-30*, *H_2O-750-30*, *H_2O-750-60*), are shown in Figure 7.2. All char samples show a CO_2 peak around 350^{o}C, which is typically associated with lactones or carboxylic groups [79]. This indicates that the char has acidic sites, which are known to play a role in catalytic reactions, specifically in cracking reactions. A broad peak is also observed at 700^{o}C, which corresponds to carboxylic anhydrides [79]. The CO peak at 1000^{o}C is commonly attributed to basic carbonylic, quinonic, and pyrone structures [79].

Overall, the TPD profiles of all of the the char samples were very similar. The only noticeable difference was that sample *CO_2-920-30* had a slightly larger CO_2 peak at 750^{o}C and a slightly larger CO peak at 1000^{o}C. The TPD profiles confirm the presence of oxygen functional groups on the surface, and show that there are both acidic and basic sites on the char surface, which could play a role in its catalytic performance.

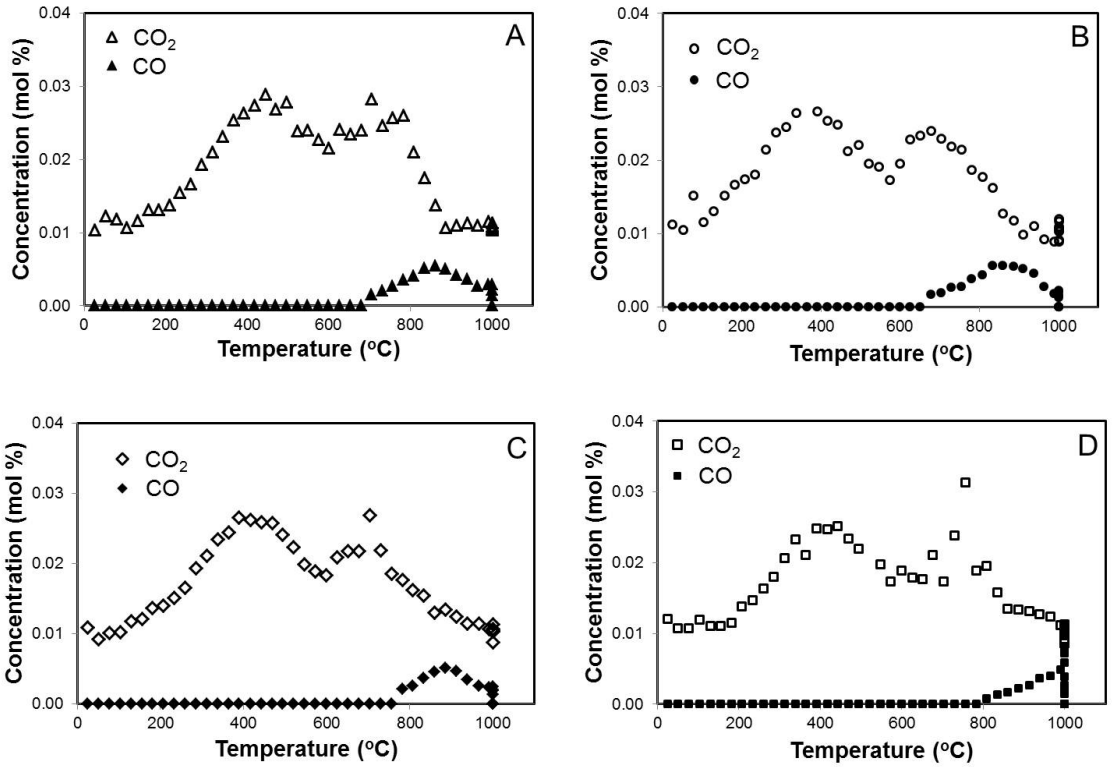

Figure 7.2: TPD profiles of char. A. H_2O-750-30 B. CO_2-750-30 C. H_2O-750-60 D. CO_2-920-30.

7.3 Oxygenation of char surface

As Section 7.1 illustrates, many of the catalytic applications of carbon based materials take place at low temperatures, often in aqueous environments. The catalytic reactions studied here take place at much higher temperatures (above 700^{o}C) and at the gas/solid interface. Therefore, it is reasonable to expect that the role of oxygen groups will be different for the reactions studied here compared to those typically studied and reported in literature.

Since no significant differences in surface oxygen species were observed among the char samples, the char surface was oxygenated in order to understand if surface oxygen groups influence the catalytic performance of char. Oxygenation of carbon surfaces is typically done by immersing the carbon in nitric acid (HNO_3) or hydrogen peroxide (H_2O_2). It is generally accepted that treatment with HNO_3, which is a strong oxidizing acid, oxygenates the surface to a greater extent, so this process was chosen here in order to exaggerate

the effects of surface oxidation [69]. 80 mg of char sample *CO_2-920-30* was immersed in 50mL of 16% nitric acid at 80^{o}C for 2 hours. The sample was then allowed to cool to room temperature and was rinsed multiple times with distilled water. It was dried with a vacuum pump/filter at room temperature.

The BET surface area of the modified char sample was measured to be 385 $m^2\ g^{-1}$, which is significantly lower than raw char, which had a surface area greater than 600 $m^2\ g^{-1}$. The decrease in surface area could not have been due to sintering, since the char was not exposed to temperatures above 120^{o}C, and these temperatures are too low for sintering to take place. It could not be due to pore blocking from acid or water being stuck in the pores, since the sample was evacuated at 120^{o}C before the BET surface area was measured, so the liquids would have been removed from the pores. Therefore, this confirms that the modifications must be due to changes in the surface structure as a result of the oxidation of the surface. In addition, TPD profiles of the oxygenated sample show much larger CO_2 and CO peaks than the non-oxygenated sample, as shown in Figure 7.3.

This decrease in surface area upon oxidation of high surface area carbons has been observed by others [68, 79, 81]. There are various explanations for this decrease in surface area. One reason could be that the bulky COOH groups adsorb at the entrance of the micropores, blocking the access of N_2 or other molecules to the micro pores, which are used to measure the surface area. The loss of surface area has also been attributed to the widening of micropores from the oxidation treatment. Another possible reason that has been discussed by others is that the increased surface oxygen concentrations may attract water molecules which can block the access of other molecules to micropores [68]. If the samples are degassed at high temperature and under vacuum prior to BET measurements, this should not affect the measured surface area, but for samples that are not prepared in this way, the adsorption of water could cause a decrease in measured micropore volume and surface area. Xu et al. oxidized the surface of activated carbons, originating from wood [76]. They found that the oxidative treatments *increased* the surface area of the carbon. The surface areas of the raw material, however, was 570 $m^2\ g^{-1}$, which is much lower than those of the samples whose surface areas were reduced from oxidative treatments, which had surface areas above 850 $m^2\ g^{-1}$ [68,76,79,81]. So perhaps the surface oxygen contributes

to microporosity but only to a certain extent. It may create micropores of a certain size, so for a material with a lower micropore volume to begin with, the oxygen treatment increases the micropore volume. For samples that are already very microporous, the adsorption of oxygen groups may in fact block the micropores, or widen existing micropores.

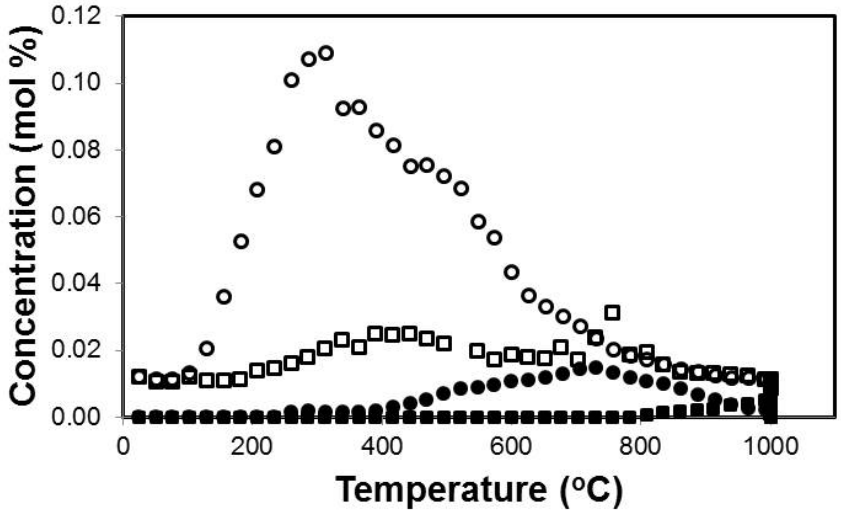

Figure 7.3: CO and CO_2 desorbed during TPD of char and oxidized char. Circles are for oxidized char and squares are for raw char. Empty symbols are CO_2 and filled symbols are CO.

The reaction used to compare the catalytic activity of the oxidized char to the raw char was methane decomposition at 850°C in a quartz flow through reactor. Three samples were compared: *CO_2-920-30* raw, *CO_2-920-30* that was oxidized via nitric acid treatment, and *CO_2-750-30*. Because the surface area decreased with oxidation treatment, the surface area of the oxidized char was more similar to sample *CO_2-750-30*, even though the oxidized char originated from sample *CO_2-920-30*. As the oxidized char sample was heated in nitrogen, the oxygen functional groups desorbed. This is observed in Figure 7.3, which shows the TPD profile of the oxygenated char sample and sample *CO_2-920-30*. A large CO_2 peak is observed at 365°C, which is a result of desorption of oxygen functional groups. Once the temperature reached 850°C, the methane was introduced. Figure 7.4 shows that the hydrogen production was the same for the oxidized sample and the untreated sample *CO_2-*

920-30. The hydrogen production for sample *CO_2-750-30*, whose surface area was much more similar to that of the oxidized char, is distinctly different from the other two samples. It is clear that the catalytic performance of the oxidized char is much more similar to that of the char which was made at 920^{o}C. Therefore, during the heating process the oxygen groups must have desorbed, returning the char to its original form. In addition, the light off temperature was the same for both char samples. This shows that for the methane cracking reaction in a CH_4/N_2 environment, the acidic oxygen functional groups (such as lactones, and carboxylic groups) will not impact the catalytic performance of the char because these functional groups will desorb in the temperature regime where these reactions take place.

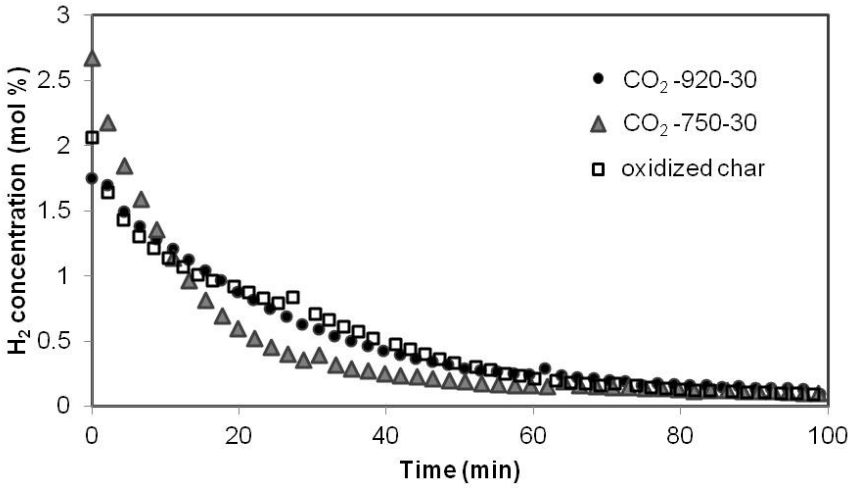

Figure 7.4: Comparison of performance of oxidized char to un-treated char for CH_4 decomposition at 850 ^{o}C

The desorption of oxygen functional groups was observed at temperatures as low as 365^{o}C (this is the temperature of the maximum of the peak; desorption begins at ~200^{o}C), even for chars from gasification processes that took place at temperatures as high as 920^{o}C. The gasification environment contains CO and CO_2; therefore the presence of these gases likely decreases the driving force for the oxygenated surface groups to desorb as CO and CO_2. When the samples are heated in pure nitrogen, thermodynamics are more likely to drive the formation of CO and CO_2, which desorb from the surface. If the char is placed in a secondary reactor directly after the gasifier and the syngas/tar mixture is passed over

the char catalyst then there will be CO and CO_2 in the atmosphere, which will decrease the likelihood of desorption of surface functional groups. It is then possible that the presence of these functional groups can impact the catalytic activity of the char at high temperatures. For example, oxygen groups will enhance the adsorption of polar molecules such was water. This has not yet been reported in the literature since most published research has primarily focused on the use of these types of catalysts at low temperatures (<200^{o}C).

Here, we have demonstrated that even with the acidic functional groups removed, the char has catalytic activity. Heating the char in an environment containing CO_2 prior to using it for catalytic reactions could demonstrate if the retention of these surface groups influences catalytic activity of the char. However, heating of the char in CO_2 could also influence its morphology and composition, since the Boudouard reaction, shown in Equation 7.1, can occur at 700^{o}C. Therefore, there are a variety of factors to be considered if the retention of surface fuctional groups is desired.

$$C + CO_2 = 2CO \tag{7.1}$$

The tests done here were conducted at 850^{o}C. As discussed in Chapter 4, 800^{o}C was the temperature required for catalytic toluene cracking. However, there are other catalytic methods for tar destruction that can be done at lower temperatures. Table 7.1 shows the temperature range for different catalytic tar reforming or oxidation reactions. Therefore, it is possible that the tar could be reformed at lower temperatures via a reforming reaction. This could enable the retention of surface oxygen functional groups, in which case these groups may play a role.

Table 7.1: Temperatures for different catalytic tar destruction reactions

Process	Temperatures reported in literature
Partial oxidation	700-900 [39, 82]
Complete oxidation	500-600^{o}C [83]
CO_2 reforming	550-700^{o}C [51]
Steam reforming	550-900^{o}C [29, 41, 52, 84]

7.4 Summary

This section studied the presence of oxygen functional groups on the char surface and their impact on the catalytic performance of the char. TPD analysis of the char revealed the presence of lactones, carboxylic groups, carbonylic, quinone, and pyrone structures. The char surface was oxygenated via nitric acid treatment at 80^{o}C, and its catalytic activity for methane decomposition at 850^{o}C was compared to the raw char. The acidic oxygen groups desorbed at temperatures below 850^{o}C, and therefore the catalytic activity of the oxygenated char was found to be the same as the raw char. This shows that acidic oxygen functional groups are not necessary in order for the char to have catalytic activity for methane decomposition. While these groups are often considered to be one of the main properties which give carbons their catalytic activity for low temperature reactions, the char can be used at high temperatures, even when many of the oxygen groups have been removed.

Chapter 8

Role of Metals in Catalytic Activity

8.1 Presence of metals and minerals in char

Metals and minerals are present in biomass and it is therefore important to understand their role in the catalytic performance of char. Because of variability in the types of biomass and their growing environments, metal concentrations will vary amongst different biomass species. For example, Dupont et al. characterized the inorganic elements in 21 different types of wood, including spruce, poplar, oak, pine, and beech, and found significant differences [85]. As examples, ash content varied from 0.5-4.3%, calcium varied from 858-15,879 mg kg^{-1} dry biomass, and potassium concentration varied from 112-1784 mg kg^{-1}. While the concentration can vary significantly, the types of metals and minerals tend to be similar amongst different types of biomass, with Ca, Na, K, Si, Mg, P, and Fe being found in most types of biomass [85–88]. In general, the alkali and alkaline earth metallic species (AAEM) compose a greater fraction of the biomass ash than the base metals. Yip et al. characterized the ash of mallee biomass and found that AAEM species make up more than 85% of the ash [87]. They also measured the concentration of AAEM (Ca, Na, K) as a function of biomass conversion and found that there was insignificant loss of these elements during steam gasification at 750^{o}C. However, Kowalski et al. pyrolyzed wood sawdust and observed a release of alkali elements, according to a bimodal spectrum [89]. The first peak was observed at 300^{o}C, and the second, which was attributed to the evaporation of inorganic salts such as KCl, was observed at 600^{o}C. Keown et al. have found that

loss of AAEM species increases with heating rate [90]. However, in spite of the different observations in literature regarding the loss of AAEM species during gasification, it is generally accepted that at least some, if not all, of these species remain in gasification char.

EDS mapping was performed on the char that we produced via poplar wood gasification to understand the distribution of metals in the char. The results for sample *CO_2-920-30* are shown in Figure 8.1. This confirms that these elements are present in the char in clusters, and are also finely dispersed throughout the char. The clusters tend to contain a mixture of metals, and higher concentrations of oxygen are present, indicating that the minerals are in the oxide or carbonate form.

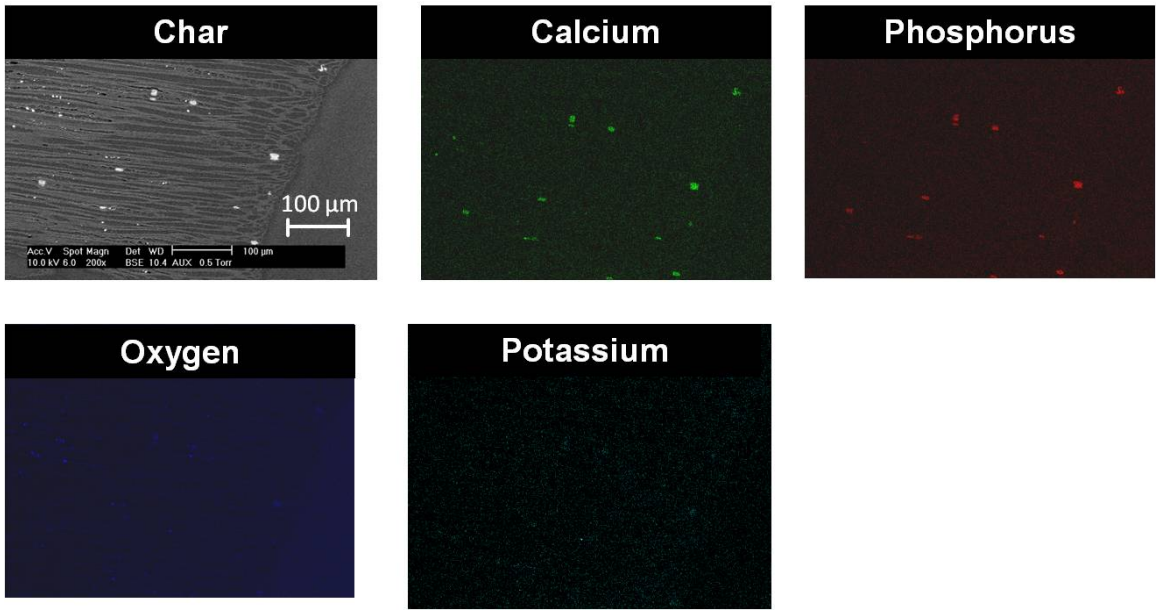

Figure 8.1: EDS image of distribution of Ca, P, K, and O in char sample *CO_2-920-30*. Minerals are generally concentrated in clusters which contain a mix of different elements, and oxygen. The distributions of other elements present in the char (such as Fe, Mn, Mg, etc.) are not visible with this method because concentrations are too low.

8.2 Catalytic activity of inorganic elements in gasification reactions

Some research has shown that the metals and minerals in the biomass play a role in catalyzing gasification reactions. For example, Dupont et al. found that the reaction rate is correlated to the ratio of potassium to silicon, indicating that potassium has a catalytic effect and silicon an inhibitory effect on the gasification reactions [85]. Marquez-Montesinos gasified grapefruit skin char and compared the gasification kinetics of raw char to char that had been washed with H_2SO_4 to remove the metals [91]. They measured a decrease in potassium in the acid washed char and found that the gasification kinetics were slower for the treated char. They also found that the reaction kinetics were higher at higher conversions and attributed this to the higher metal to carbon ratio. While the surface area increases as the reaction proceeds, they calculated a reaction rate per unit surface area (measured with CO_2 adsorption) and found that the reaction rate per unit surface area increased with conversion. Therefore, they concluded that the metals have catalytic activity for gasification reactions. Yip et al. gasified mallee biomass and compared the specific reactivity (defined as the change in amount of carbon per unit time divided by the amount of carbon) for raw biomass and biomass where metals had been removed via acid treatment [87]. For the raw biomass, reactivity increased with conversion; for acid treated biomass, reactivity was much lower and did not change with conversion. As mentioned before, some elements can have an inhibitory effect on the gasification reactions. Habibi et al. found that the potassium can be rendered inactive when potassium aluminosilicate is formed [92]. This was observed during co-gasification of potassium rich switchgrass with high ash sub-bitumous coal.

8.3 Role of metals in catalytic reactions

As discussed above, metals play a role in gasification reactions, which suggests that it is likely that they play a role in catalyzing hydrocarbon decomposition reactions as well. In order to understand the role of metals in catalytic performance of the char, the metals were

removed from the char and the performance of the de-ashed char was compared to that of the raw char.

8.3.1 Experimental method

The metals were removed from the char by treating it in a solution of 16% hydrochloric acid (HCl). It is well known that treating carbon materials in acids will extract the metals, and this process is commonly used to de-ash char [87,91,93]. The char was treated at three conditions:

i Room temperature for 5 hours

ii 50^{o}C for 5 hours

iii Room temperature for 24 hours

After the acid treatment the char was rinsed multiple times with filtered water and then dried at 120^{o}C to ensure that all of the acid had been removed either from the rinsing or evaporated in the furnace.

The removal of metals was confirmed by measuring the metals that were present in the acid solution via inductively coupled plasma (ICP). The acid solution for the two samples that were treated at room temperature (for 5 hours and 24 hours) contained Ca, Na, K, Mg, P, and Si. This shows that treatment in 16% HCl removes the alkali and alkaline earth elements from the char. Since accurate quantification of the concentration of minerals and metals in char is difficult to achieve, the amounts of these elements that remained in the char were not quantified. However, the ICP data confirms that these elements were removed from the char, so the concentration of metals/minerals in the treated char samples would be lower than in the untreated samples. Also, it is likely that treating the char in the acid for 24 hours removed more metals than when it was only treated for 5 hours. The transition metals which have been detected in the char via EDS, such as Fe, Ni, and Mn, were not detected in the acid mixture, so these metals were not removed from the char during the acid treatment at room temperature. In order to extract these metals, the char was treated in the same acid solution at 50^{o}C for 5 hours. The ICP measurements of the

acid mixture from this process showed the presence of Fe, Ni, and Mn, indicating that these metals had been extracted from the char.

The surface areas of the modified char samples were measured in order to understand if the surface structure had been modified by the acid treatments. The surface areas had not changed significantly; the surface areas of each of the modified char samples were within 10% of the raw char sample and were always slightly higher. This procedure is different than the acid treatment described in Chapter 7. In that chapter, nitric acid was used, which added bulky oxygen groups to the surface. Here, hydrochloric acid was used, which did not modify the surface. There was no measurable change in pore volume or pore size distribution from the acid treatments. As shown in Chapter 7, the oxygen groups on the char surface do not influence the catalytic performance of the char for the reactions tested here. So, even if this property was modified during the acid treatment, it would not influence the catalytic performance of the char. Therefore, any changes in catalytic performance of the char will be solely due to the decrease in metals concentration. The catalytic performance of the modified char samples was compared to that of the raw char. The methane cracking reaction was performed in a TGA where the sample was heated in ~30% CH_4 to 900^{o}C at 7^{o}C min^{-1}.

8.3.2 Catalytic performance of de-ashed char

The final mass gain, as a percentage of the dry mass of the char, is shown in Figure 8.2. The treatment at room temperature for 5 hours did not influence the catalytic performance of the char. However, when the char was treated for 24 hours at this condition, the final mass gain was reduced from 16% to 13% , indicating that removing alkali and alkaline elements decreases the catalytic performance of the char. It is well known, and has been reported in literature that these elements play a role in the catalytic performance of the gasification reactions. However, here, we demonstrate that these elements in the char also play a role in the catalyzing cracking reactions. Since hydrocarbon cracking reactions likely take place inside the gasifier, it is possible that the increased production of syngas with biomass that contains metals (compared to de-ashed biomass) is due to the catalytic effects of the metals on cracking of the tars that are produced from gasification. Some of these

elements have been used as catalysts for tar cracking. The most common AAEM based catalysts are mineral oxides or carbonates made from calcium or magnesium [13, 28, 94].

The char that was treated for 5 hours at 50°C also showed a decrease in performance. The final mass gain for this char sample was 14.7%, which is an 8% decrease in activity compared to the raw char sample. The char treated for 5 hours at room temperature displayed no change in activity. Therefore, the loss in activity due to the 5 hour treatment at an elevated temperature is due to the fact that the base metals are also removed, or because a higher concentration of AAEM species has been removed. In order to distinguish the two effects, the concentrations of metals in the char samples would need to be measured. This could be done via ICP if an appropriate dissolution method is used to ensure that the entire char sample is dissolved. This is often a very involved process since the carbon matrix is difficult to decompose and in order to ensure accurate measurements, the entire sample should be dissolved.

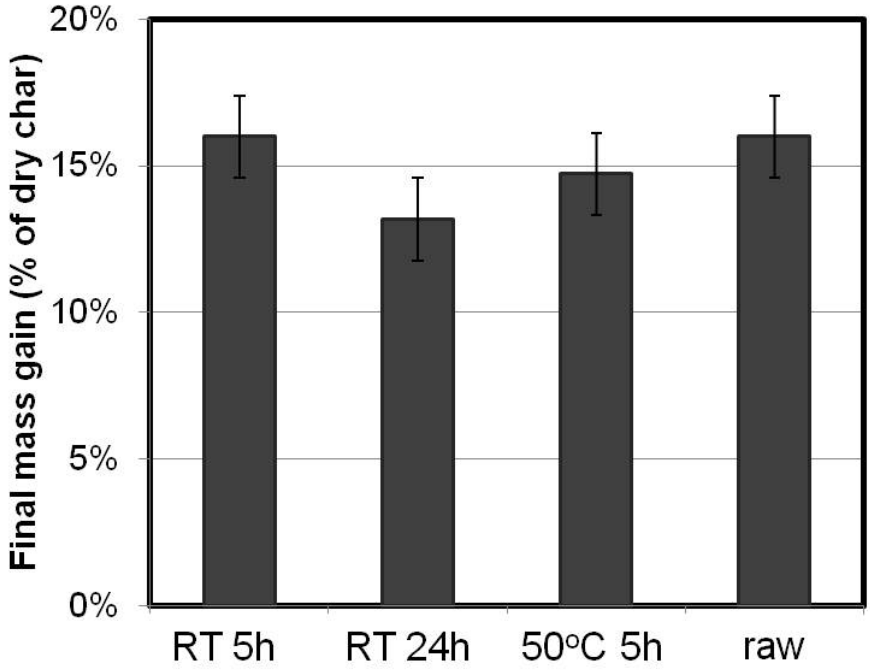

Figure 8.2: Catalytic performance of char and modified char. Removal of metals decreases catalytic performance, indicating that the presence of metals in char impacts its catalytic performance.

8.4 Dispersion of metals in char

It is well known that catalysts must be well dispersed on a surface in order to increase accessibility to the catalyst sites. Therefore both the dispersion and the concentration of the metals and minerals are important.

As discussed in Chapter 3, EDS determined the presence of metals in the char. It was of interest to understand the form of these metals (for example, carbonates, oxides, etc.). For this, we attempted to use X-ray diffraction (XRD), which is a commonly used technique for determining the crystal structure of materials. The XRD spectra showed peaks related to ordered and disordered carbon, as well as one peak that is associated with calcium carbonate (data shown in Appendix C). However, most other metals and minerals were not detected via XRD, which most likely indicates that the particle size is too small to be measured with XRD or it is not crystalline. In a paper by Devi et al., they concluded that the absence of peaks in the XRD spectra of chars indicated that the crystallite size was below ~4nm, which is likely also the case for the chars tested here [95].

However, finely dispersed particles can be mobile under certain conditions, which would change the particle size and dispersion of the element. The mobility of metals on carbon surfaces has been studied. A communication by R. T. K. Baker in the Journal of Catalysis in 1982 discussed the mobility of particles on graphite surfaces [96]. They observed that the particle motion took place at the Tammann temperature, which is defined as 0.51 T_M, where T_M is the melting temperature of the metal. The relationship between the mobility temperature and bulk melting temperature of different elements is shown in Figure 8.3. The temperature where CaO becomes mobile is ~1200^{o}C, which is much higher than most of the metals shown in this diagram. Calcium is one of the elements that is found in the highest concentration in biomass chars, and is in an oxide or carbonate form. The fact that it is less mobile than other elements (because it requires very high temperatures to become mobile) could be beneficial if it participates in catalytic reactions, since it could remain dispersed even if the char/biomass is treated at high temperatures. Iron, on the other hand, can become mobile at temperatures as low as 700^{o}C, so there is much more likelihood of agglomeration of iron particles if the char is heated to high temperatures [96]. This could

explain why iron was only observed in isolated clusters on the char surface whereas calcium was observed throughout the char samples. An understanding of the mobility of inorganic elements on the char or biomass surface is particularly relevant for char catalysts because if the metals are active sites for exothermic reactions then the temperature at the metal sites might be higher which may increase mobility of the metals. In particular, air gasification is exothermic whereas gasification with steam or CO_2 is endothermic, which could result in significant temperature differences at the site where the reaction takes place. The more mobile the particle is, the more likely that it will agglomerate on the surface.

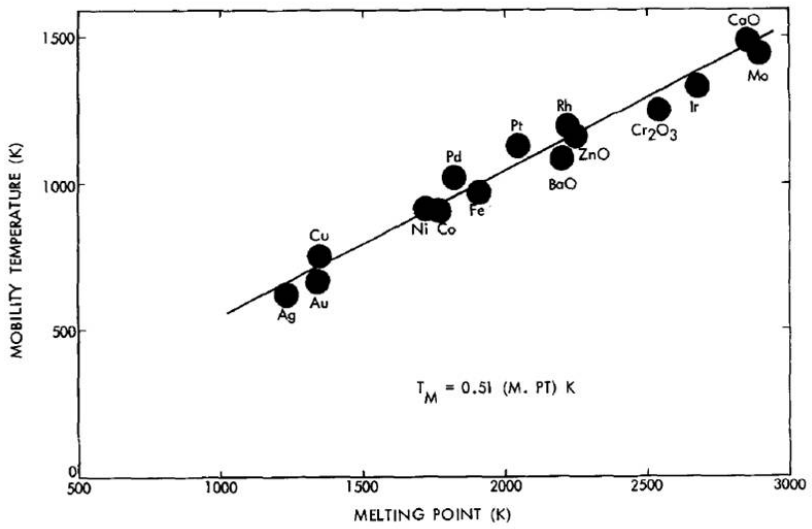

Figure 8.3: Relationship between mobility of particles supported on graphite and their bulk melting temperatures. [96]

The mobility of the metals and minerals on the char surface was studied. This is because catalysts must be well dispersed on a surface in order to increase the number of accessible catalytic sites. It is important to understand the dispersion of metals on the char and if the dispersion will change at elevated temperatures, where the catalytic reactions take place. Therefore both the dispersion and the concentration of the metals and minerals must be considered. The mobility of elements was studied by heating the char to 1000^{o}C in N_2. The concentration of metals and minerals on the surface of the char sample was analyzed quantitatively, using X-ray photoelectron spectroscopy (XPS, Thermo Scientific, Al Kα).

This technique enables the measurement of the composition, with a depth sensitivity on the nanometer scale, giving a true surface measurement. X-rays are used to probe the surface; the incident beam of photons hits the surface, giving rise to secondary electrons whose energies are a function of the binding energy of the atoms making up the solid materials. Therefore, the electron binding energy, which is measured from the secondary electrons, gives information on the types of bonds, and therefore the components that are present on the surface.

The XPS results for three samples are shown in Table 8.1. The first two columns show the measured concentrations for two raw char samples, made in CO_2 at 750 and 920^{o}C. These two samples have similar concentrations of carbon and oxygen (95% and 5%, respectively). The only other elements detected in the samples were calcium and magnesium (Mg was only measured in the sample made at 920^{o}C). The detection limit of the instrument is 0.1at%, so any element that was not detected was either not present in the sample, or was present in concentrations below this limit. The third column shows the concentration of elements measured on sample *CO_2-750-30* that had been heated to 1000^{o}C in N_2. For this sample, P, K, Ca, Na, Mg, Si, and Cl were detected on the surface. In addition, the oxygen to carbon ratio was much higher than the raw char, with oxygen making up 13% and carbon making up 80% of the sample. Therefore, heating the char to 1000^{o}C causes a migration of metals, minerals, and oxygen to the surface of the char. This should not be confused with the oxygen functional groups that desorb at high temperatures, which are discussed in Chapter 7. The oxygen groups which desorb are acidic or basic sites which are made of oxygen and carbon in various configurations. There is also oxygen in the char which is present as part of mineral carbonates or mineral oxides. This oxygen is retained in the char even as it is heated. The presence of inorganic elements and high concentrations of oxygen indicate that there are likely mineral oxides on the surface. There could also be carbonates, but carbonates generally decompose at temperatures below 1000^{o}C, according to Equation 8.1 (shown, as an example, for calcium carbonate). The next section will analyze how the agglomeration of metals and minerals on the surface of the char impacts its catalytic activity.

Table 8.1: Concentration of elements on the char surface measured with XPS (– indicates concentrations were below detection limit of 0.1at%)

Element	*CO_2-750-30*	*CO_2-920-30*	*CO_2-750-30* (heated to 1000^{o}C)
C	94.31	95.33	79.88
O	5.20	4.11	12.82
P	–	–	0.45
K	–	–	3.25
Ca	0.48	0.45	1.37
Na	–	–	0.47
Mg	–	0.10	0.18
Si	–	–	0.57
Cl	–	–	1.00
Fe	–	–	–
Mn	–	–	–

$$CaCO_3 \xrightarrow{750^oC} CaO + CO_2 \tag{8.1}$$

8.4.1 Influence of metal dispersion on catalytic performance of char

The char sample was heated to 1000^{o}C and its activity was compared to an un-treated char sample (made under the same gasification conditions). The catalytic activity was tested in the Quantachrome ChemBET instrument which is a quartz flow-through reactor. The quantity of char catalyst used was 0.02g. For the untreated sample, the char was heated to 700^{o}C in N_2 and then a mix of 23% CH_4 in N_2 was introduced. The reaction proceeded for 3 hours. The effluent gases were measured with an Inficon 3000 micro gas chromatograph. The treated char sample was heated to 1000^{o}C in N_2, held there for 15 min, and then cooled to 700^{o}C at which point the CH_4/ N_2 mixture was introduced. The hydrogen production for the two samples is shown in Figure 8.4. The hydrogen production from the pre-heated char is approximately 60% of the hydrogen produced from the raw char. Therefore, even

though pre-heating the char results in a higher concentration of metals on the surface, the catalytic activity of the char is lower. This is explained by observing the physical changes in the char as it is heated in an ESEM.

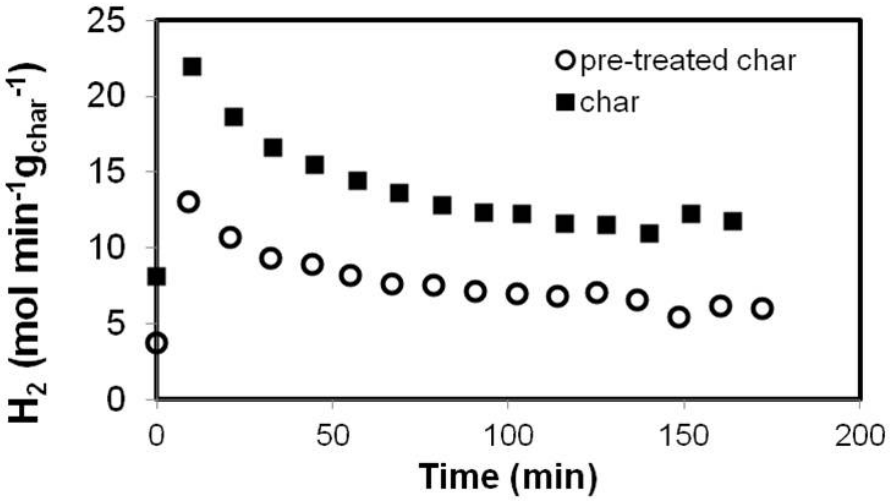

Figure 8.4: H_2 production for catalytic cracking of CH_4. "Pre-treated" char has been heated to 1000^{o}C and "char" has not been pre-treated. Pre-heating char reduced its catalytic activity.

As discussed in Chapter 3, the environmental mode of the ESEM allows for observations of physical changes as the sample is heated. The char was heated in N_2 at 20^{o}C min^{-1} up to 1000^{o}C in the ESEM to observe modifications to the char structure at high temperatures (in the absence of a co-reactant). Figure 8.5 shows sample *H_2O-750-30* at room temperature, 500^{o}C, 700^{o}C, and after being heated to 1000^{o}C. It is clear that as the sample is heated, the metals, minerals, and oxygen (shown as brighter spots) migrate to the surface of the char and eventually form a nearly continuous layer on the surface. Therefore, while the concentration of these elements may be higher on the surface, the agglomeration nevertheless reduces the number of accessible sites. The same experiment was done for a char sample that was made under CO_2 (sample *CO_2-750-30*) and the results are shown in Figure 8.6. For this sample, the metals, minerals, and oxygen migrated to the surface as well but remained in small clusters. In both cases, heating of the char caused migration of metals, minerals, and oxygen to the surface. While the extent of agglomeration was

different for the two samples, in both cases, the agglomeration of metals is a potential cause for the loss in catalytic activity when the char is pre-heated.

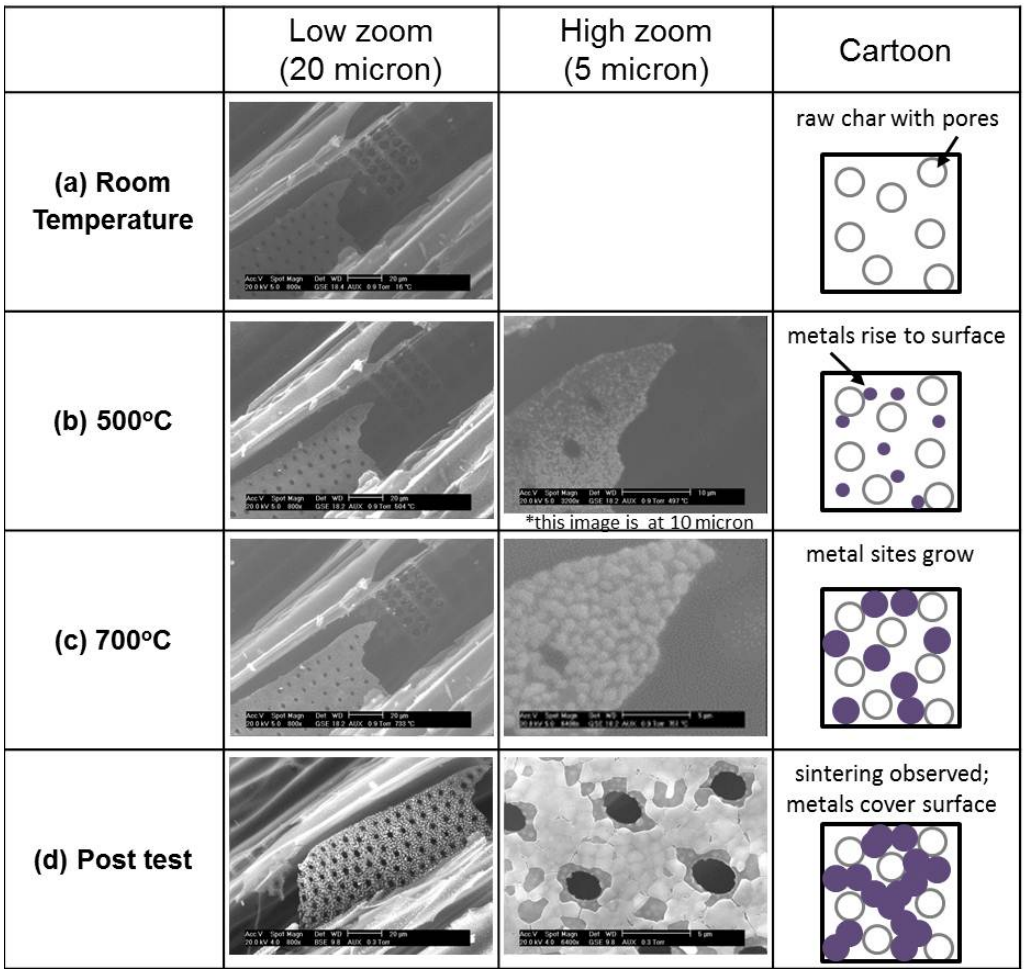

Figure 8.5: Char sample H_2O-750-30 during heating in an ESEM under N_2. As temperature increases, minerals and oxygen, which appear as bright spots on the dark carbon surface, migrate to the surface of the char. At 1000^{o}C metals clusters have agglomerated.

In addition to heating the char in the ESEM, char was heated in a flow through reactor in N_2 to 1000^{o}C, and then observed under the SEM/EDS. While this is a qualitative measurement, some distinct differences were observed when comparing the char that was heated to 1000^{o}C to the char that had not been treated under N_2. On the char that had been heated to 1000^{o}C, we observed clusters of potassium, which were not observed on the char samples that were not pre-treated at high temperatures. An example of this is shown in Figure 8.7,

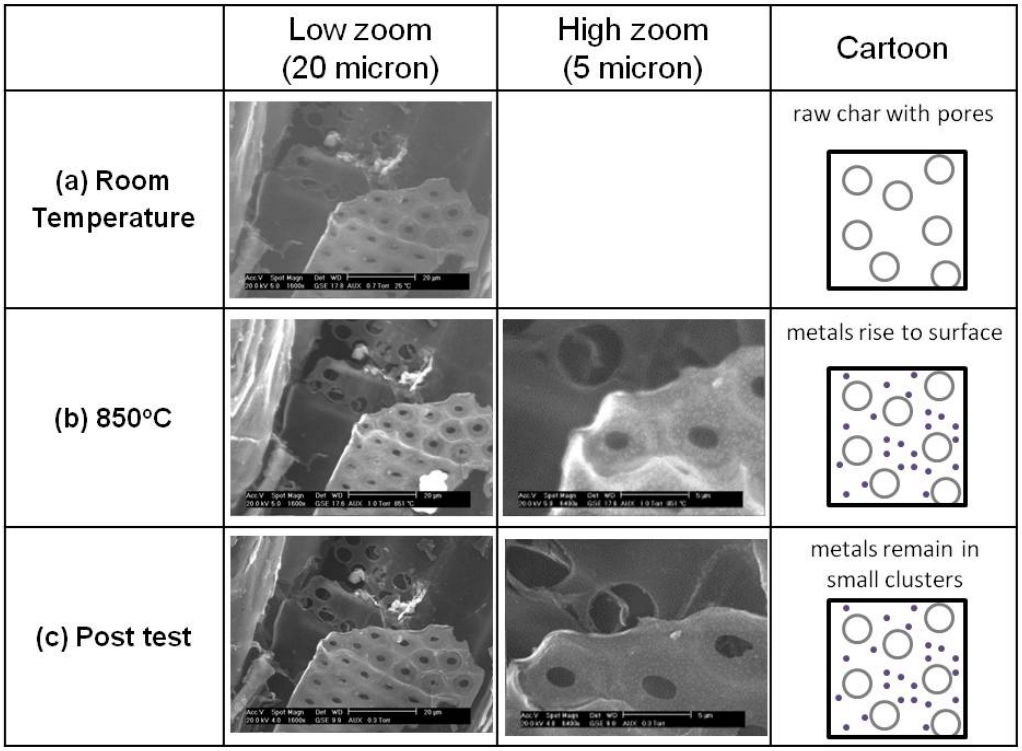

Figure 8.6: Char sample CO_2-750-30 during heating in an ESEM under N_2. As char is heated, oxygen and metals migrate to the surface and remain in isolated clusters.

where the bright spots are clusters of minerals, primarily potassium, as measured with the EDS. The EDS spectra, along with the measured concentrations of elements are found in Appendix B. It is well known that potassium, which is found in biomass, catalyzes the gasification reactions [38,85,87,91,92]. Therefore, it is likely that potassium plays a role in the catalytic decomposition of hydrocarbons as well. The sintering of these minerals thus likely contributes to a decrease in catalytic activity of the char.

Another phenomenon which takes place at high temperatures is sintering of the char, which serves as the catalyst support. In catalysis, sintering of the support is a common cause for catalyst deactivation. When the char is heated to temperatures as high as 1000^{o}C, it is very likely that sintering takes place. Therefore, we must distinguish if the loss in activity for the pre-treated char is due to agglomeration of metals, or sintering of the support. Sample *CO_2-750-30* was heated to 1000^{o}C and the surface area of the heated sample was

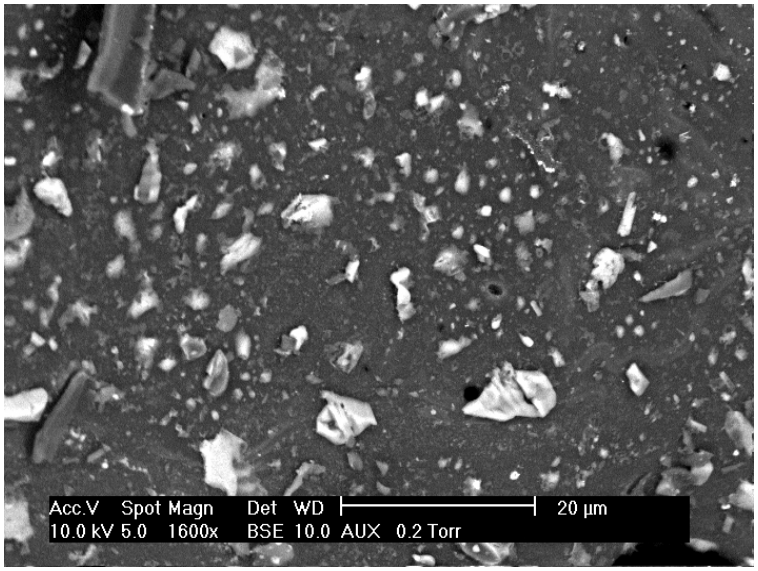

Figure 8.7: Metals agglomerated on the char surface. Potassium, which is known to have catalytic activity in gasification reactions, was observed in clusters on the surface.

measured to decrease by about one third. The hydrogen production for the pre-heated sample was 42% lower than the raw char at the beginning of the test and 33% lower at the end of the test. In order to understand if the difference is primarily due to loss of char surface area, or due to metals agglomeration, we compare the catalytic performance of two char samples that were made at different gasification temperatures in the same gasification environment. These char samples, therefore, have different surface areas, but none have been exposed to 1000^{o}C in N_2, which would cause agglomeration of metals. Similar to the previous tests, this experiment was done in the Quantachrome ChemBET unit using 0.02g of char. The sample was heated to 720^{o}C in N_2 and then the CH_4/N_2 mix was introduced. The surface area of the low surface area char was approximately one third that of the high surface area char. The hydrogen production over one hour is shown in Figure 8.8. It is clear that there is no significant difference in the hydrogen production at this condition, even though the surface areas of the two samples are very different. However, as Figure 8.4 shows, there is a significant difference in performance for the char that was pre-heated, which caused agglomeration of metals. Therefore, dispersion of metals is a key factor which influences catalytic activity of the char. If the char is exposed to conditions where

agglomeration of metals could occur, its catalytic activity will be reduced. It is important to note that this should not be interpreted to mean that surface area does not influence catalytic activity. Chapter 6 showed that surface area has a significant impact on catalytic performance. However, here, the reactions are taking place at low temperatures, which results in very low conversion values. The difference in performance due to surface area is more apparent at higher conversions, which are observed at higher temperatures. The TGA data shown in Figure 6.1 shows that the performance diverges for samples with different surface areas at temperatures that are above 800^{o}C. The experiments discussed in this chapter were done at temperatures of 700 and 720^{o}C.

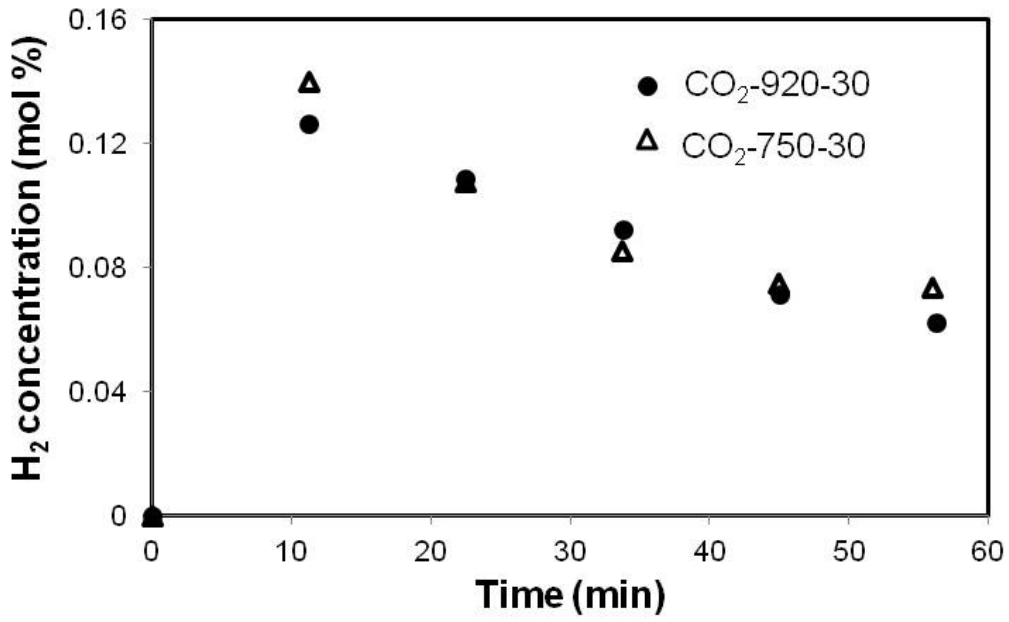

Figure 8.8: Hydrogen produced from catalytic cracking of CH_4 at 720^{o}C. At this temperature, there is no significant difference in performance for chars with different surface areas.

Gasification and pyrolysis can be done at many different conditions. Here we see that gasification in CO_2 or steam at temperatures between 550-920^{o}C creates a char with metals that are highly dispersed on the char. However, for a pyrolysis process that takes place at 1000^{o}C, for example, the char would likely contain agglomerated metals and would have low catalytic activity. Gasification processes with air are also be more likely to contain ag-

glomerated metals, leading to decreased catalytic performance of the char. Sintering of the metals was observed with air gasification in the ESEM, as shown in Chapter 3. In addition, since air gasification is an exothermic reaction, it is more likely that the temperature will be higher at the metal sites where the reactions take place, which could increase the mobility of the elements, causing sintering. So, utilization of char as a catalyst is only possible when appropriate gasification conditions (low temperatures, and CO_2 or steam) are used.

8.4.2 Catalytic activity of metals in steam and CO_2 gasification

As Figures 8.5 and 8.6 show, the mobility of elements is not the same for char samples made from steam gasification versus CO_2 gasification. Significant efforts have been made to compare gasification with steam and CO_2 and to understand the difference in reaction mechanisms and kinetics in these different gasification environments [97–100]. As discussed above, metals play a role in catalyzing gasification reactions, and therefore influence gasification kinetics. Some have stated that the influence of these metals is more significant than the influence of surface area on kinetics [97]. In other cases it has been shown that structural changes in the char during gasification play a larger role in determining the reaction rate [101]. The difference in kinetics for CO_2 and steam gasification is often explained based on the morphology of the char or the different concentrations of products in the gas phase (CO_2 gasification will produce more CO whereas steam gasification will produce more H_2) [97, 99, 100]. However, very little work has been done on comparing the dispersion of metals in the two gasification environments. This presents an area for future work, since metal dispersion may be a relevant parameter which influences reaction kinetics in these different gasification environments.

8.5 Role of carbon in catalytic performance of char

Sections 8.3 and 8.4 have demonstrated the importance of metals in the catalytic activity of char. However, the char is composed of ~85% carbon. This section investigates if the presence (or absence) of carbon influences the catalytic performance of the char. Raw char was used to catalyze the decomposition of methane at 700 ^{o}C. Another sample was

pre-treated by burning off the carbon via exposure to air at 700 ^{o}C for 30 minutes. The hydrogen production from the two samples is shown in Figure 8.9. The activity of the ash is significantly lower than that of the char, which contains ash. Therefore, the presence of carbon improves the catalytic performance of the char by providing a support on which the metals can be dispersed.

In addition to providing a support for the metals, the carbon may also participate in the reactions. This has been shown in research that has been reported in literature. The redox properties of the metal-carbon complexes has been shown to influence the catalytic activity of carbon supported metal catalysts. The ability of the carbon to reduce the metal enables the formation of a metal in a reduced state which is more catalytically active for some reactions. For example, Illán-Gómez et al. used char supported metal catalysts for NO_x reduction and studied the redox properties of the different complexes. They found the activity to be related to the ability of the metal to be oxidized by NO and reduced by carbon [102]. Hsu et al. also used carbon to catalyze the reduction of NO (with NH_3) and found very low activity with metal-free carbon, but when impregnated with iron or copper they achieved high conversions [103]. Similarly, they attribute the activity to the redox properties of the carbon-metal complexes, where the metal was oxidized by NO, and then reduced by carbon.

It is also possible that the carbon itself has catalytic properties. Carbon based catalysts have been used for methane decomposition, and this has been reported in the literature. For example, Serrano et al. used CMK carbons (ordered mesoporous carbons), carbon black, and graphite, which had metal concentrations below 0.005wt% [104]. They were able to successfully crack methane with these catalysts, which demonstrates that the carbon itself has some catalytic activity. Therefore, as demonstrated in this work, the catalytic activity is a result of the catalytic activity of metals, carbon, and the high dispersion of metals which is possible because of the highly porous carbon support.

The amount of carbon in the residue can vary significantly, depending on the reaction conditions. In combustion processes, the amount of carbon remaining is generally very low, in the range of 0.1-1% . In gasification processes, the conversion of carbon will increase as temperature increases. In addition, higher concentrations of oxidant (such as O_2, CO_2,

or H_2O) will decrease the carbon content of the residue. Pyrolysis processes, which use nitrogen as the gasification medium tend to produce high carbon concentrations in the residue, however the char tends to have a lower surface area than chars produced via CO_2 or steam gasification. Therefore, there are a variety of factors to be considered when determining if the char from a particular process will be appropriate to be used in catalytic applications.

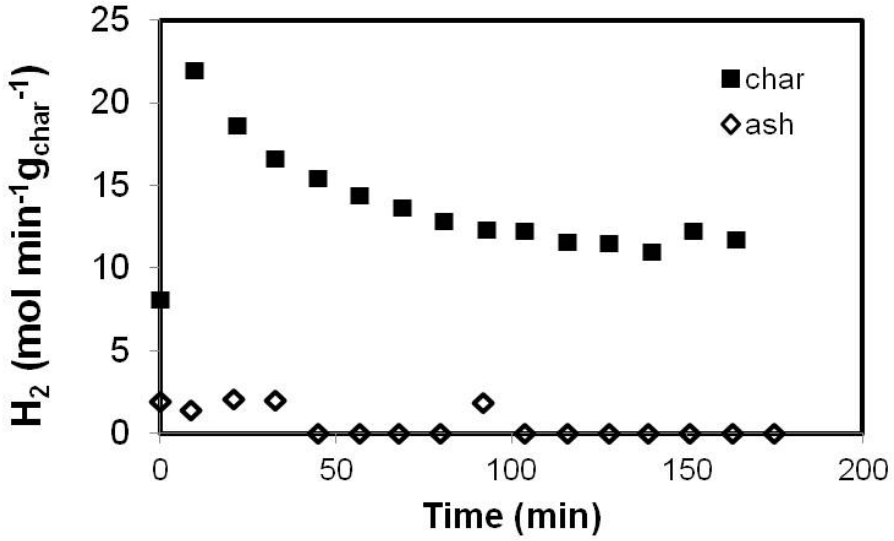

Figure 8.9: Catalytic performance of char compared to ash. The performance of the ash is significantly lower than that of char, which contains ash.

8.6 Summary

This section discussed the role of metals in the catalytic activity of char for hydrocarbon cracking reactions. It is well know that inorganic elements play a role in gasification reactions, however, the role of metals for cracking reactions has not been previously studied. The removal of metals via acid washing of the char resulted in a decrease in catalytic activity for methane cracking, which confirms the contribution of inorganic elements to the catalytic performance of the char. XPS data showed that when the char was heated to 1000^{o}C metals and oxygen migrated to the surface. This resulted in a decrease in the catalytic performance of the char. This was due to the agglomeration of these elements on the surface, which

reduced the number of accessible sites. This was confirmed via observations in the ESEM. Two char samples were heated in N_2 and agglomeration of metals was observed on the surface of the char. Agglomeration was more significant for char samples that were made via gasification with steam, compared to char that was made in CO_2. This may indicate that metals dispersion is relevant when comparing gasification kinetics in steam versus CO_2, but further research needs to be done to confirm this. The catalytic activity of the char that was heated to 1000^oC was lower than the raw char. This shows that metal dispersion is an important factor which influences the catalytic activity of the char.

Part IV

Conclusions

Chapter 9

Conclusions and future work

9.1 Conclusions

This thesis has aimed to address the issue of decomposition of tars and valorization of char from gasification processes. Poplar wood was gasified in a fluidized bed reactor under CO_2 and steam at 550, 750, and 920^{o}C. The char was collected and its properties and catalytic activity were studied, with the goal of utilizing char as a catalyst for tar decomposition. Tar decomposition is often a catalytic process; however, tars often cause catalyst deactivation which can necessitate expensive regeneration or replacement of catalysts. Utilization of char as a catalyst for this process can eliminate the cost of expensive catalysts, and the char can be easily replaced once it is deactivated since it is produced continuously on site.

The catalytic performance of the char was demonstrated for decomposition of methane, propane, and toluene. When compared to a commercial Pt/Al_2O_3 catalyst, the light off temperature of the char catalyst was ~100^{o}C lower than the commercial catalyst for methane decomposition. Catalytic toluene decomposition at 800^{o}C resulted in the formation of H_2, CH_4, benzene, and many methylated aromatic compounds. The decomposition of toluene, which is often used as a surrogate molecule for gasification tar, demonstrated that the char would be a good catalyst for decomposition of gasification tars.

The properties of the char were found to be highly dependent on the gasification conditions. Higher gasification temperatures, or increased residence time resulted in char with higher specific surface area. The BET surface area of the char was measured to be

between 429-687 m^2 g^{-1}. The porosity of the char was also influenced by gasification conditions. Char that was gasified under CO_2 contained micropores whereas char that was made in steam did not. Gasification in an ESEM showed sintering of the metals in the char at 1000^{o}C when steam was used as a co-reactant. Sintering was not observed when gasification was done in a CO_2 environment.

An analysis was done to understand the feasibility of this process from an overall process perspective. It was necessary to understand if the catalytic activity of the char was sufficient to reform all of the tar that would be produced from a gasifier, given that the relative amounts of tar and char would be fixed, based on gasification conditions. Kinetics for the catalytic decomposition of methane with the char catalyst were determined, which accounted for catalyst deactivation. Then, these kinetics were used in a model which took into account real experimental values (reported in literature) for the quantities of tar and char that would be produced from gasification of biomass. It was found that even when catalyst deactivation was accounted for, the activity of the char was high enough to reform all of the tar that would be produced from this model system.

We also considered other uses for the char, such as combustion of the char for process heat. The heating value of the char was compared to the heating value of the syngas that would be produced from tar reforming via utilization of the char as a reforming catalyst. At temperatures below 770^{o}C, when high quantities of tar are produced, the heating value of the products from tar reforming are higher than that of the char, indicating that it is energetically beneficial to utilize the char for reforming, rather than for direct heating. At higher temperatures, the energy recovered from tar reforming is lower, however tars must still be either decomposed or removed in order to prevent problems downstream from deposition or decomposition of tars.

As expected, char properties influenced the catalytic performance of the char. Char with a higher surface area had higher catalytic performance, but there was evidence of diffusion limitations in the micropores of the char. Deactivation was observed over 3 hours of methane decomposition. After the char was used as a catalyst, BET surface area was reduced to 80% of its initial value, and micropore volume was reduced by one third, indicating that deactivation occurs via pore blocking. The deactivation function showed

different profiles for char made in steam versus CO_2. Char made in steam showed a steeper deactivation function compared to char made in CO_2, indicating that there are more catalytic sites per pore in the char made in steam (so deactivation is more rapid because more catalytic sites are lost as a pore becomes blocked). This is explained by the microporosity in the char made in CO_2. Char has a fractal structure therefore the micropores are present as 'branches' off of the mesopores. Since there are diffusion limitations in the micropores, the catalytic sites are not accessible. However, the surface area in the mesopores is reduced by the presence of micropores, therefore microporous char has fewer catalyst sites per mesopore, which is reflected in the deactivation function.

Surface oxygen functionalities are often considered to be one of the main factors which contribute to catalytic activity of carbons. However, most research reported in literature has used carbon materials as a catalyst in low temperature applications (<200^{o}C). The oxygen functional groups on the char surface were identified via temperature programmed desorption (TPD). Acidic groups such as lactones and carboxylic groups and basic groups such as quinones and pyrones were present on all char samples that were analyzed. In order to understand the influence of oxygen functional groups on the catalytic activity, a sample was oxygenated via treatment in nitric acid at 80^{o}C. However, as the sample was heated in N_2 to the reaction temperature, the oxygen functional groups desorbed and the catalytic activity of the treated char was the same as the raw char, indicating that these functional groups are not necessary for catalytic decomposition of CH_4.

The role of metals and minerals in the catalytic performance of char was studied. Metals were removed from the char via treatment in hydrochloric acid and the catalytic activity of the char decreased when the metals were removed. The metals were found to be well dispersed on the char, but heating the char to 1000^{o}C resulted in migration of metals and minerals to the char surface, where agglomeration was observed. This agglomeration reduced the catalytic activity of the char, showing that the presence and dispersion of metals and minerals in the char contribute to its catalytic activity. The catalytic activity of the carbon-free ash was much lower than that of the char, indicating that the carbon structure helps to disperse the metals and minerals.

Overall, this thesis addresses the issue of valorization of the two major by-products from

gasification: tar and char. It has demonstrated that char has catalytic activity and could be used as a catalyst for tar decomposition. Processes that use the char as a catalyst could operate at lower temperatures than those operating with conventional metal catalysts due to the lower light off temperature of the char catalyst. The gasification conditions influence the char properties which impact its catalytic performance. The catalytic performance of the char is attributed to the high surface area and mesopores in the char, as well as the presence of highly dispersed metals and minerals.

9.2 Future work

This thesis has answered some questions relating to the catalytic activity of char, and also opens up areas for future research based on these findings.

This thesis demonstrated that char has catalytic activity for decomposition of toluene, which was used as a surrogate molecule for gasification tars. If it is to be used in this application, further research could be done to understand the mechanism of tar decomposition and tar reforming using this catalyst. In this research, various aromatic compounds were identified from the decomposition of toluene. However, in a real process, the tars should be converted to synthesis gas or other useful liquid compounds. Therefore, a deeper understanding of the mechanism for tar reforming would help to determine what conditions should be used, or what char modifications could be necessary, in order to improve tar conversion to useful products.

This research showed that gasification conditions influence the properties of char. However there are many other gasification conditions that could be tested in order to better understand how to create char with specific properties. For example, the influence of reactant (CO_2 or H_2O) concentration or the effects of mixed atmospheres (CO_2 and H_2O) could be studied. Heating rate may also influence char properties. Future work in this area could enable more specific correlations between gasification conditions and char properties in a wider variety of conditions in order to better understand how specific desired char properties could be obtained.

In this work, the surface oxygen groups desorbed at temperatures that were below the reaction temperature. Other research reported in literature has shown that oxygen groups influence the catalytic properties of carbon materials in low temperature applications. If the char was heated in an environment containing CO or CO_2, or is used at lower temperatures than those tested here, it is more likely to retain the oxygen groups. Therefore, future work could investigate the role of oxygen groups if they are retained on the surface.

This work has shown that the dispersion of metals and minerals in the char is an important factor which influences the catalytic activity of the char. In addition, these inorganic elements are mobile on the char surface in the temperature range where gasification takes place. Other research that has been reported in the literature has looked at the influence of these inorganic elements on gasification kinetics and has found that they enhance the gasification reactions. This work has shown that the gasification environment can influence the dispersion of inorganic elements on the char surface. This may also play a role in gasification kinetics. Where exothermic reactions take place (for example, with air gasification), the temperature would be higher at the reaction site which would increase the mobility of the inorganic elements, leading to agglomeration, which would decrease the catalytic activity of these elements. This work has shown that when gasification is done with CO_2 a high dispersion of inorganic elements is maintained on the surface. The influence of dispersion of inorganics on catalyzing gasification reactions is therefore an area for future work.

This thesis has demonstrated that char has catalytic activity for decomposition of hydrocarbons, and that its catalytic activity is related to its high surface area, mesoporosity, and highly dispersed metals and minerals. This suggests that the char may be a useful catalyst in other applications, such as pollution abatement or fuel conversion. Therefore, future work could investigate other applications for gasification char catalysts or utilization of these chars as a support for other catalysts.

Part V

Bibliography

Bibliography

[1] European-Environment-Agency, "Projected percentage change in renewables consumption by type from 2004 to 2030," *available online at: http://www.eea.europa.eu/data-and-maps/figures/projected-percentage-change-in- renewables-consumption-by-type-from-2004-to-2030*, accessed January 13, 2013 .

[2] M. Z. Jacobson, "Review of solutions to global warming, air pollution, and energy security," *ENERGY & ENVIRONMENTAL SCIENCE*, vol. 2, no. 2, pp. 148–173, 2009.

[3] K. Srirangan, L. Akawi, M. Moo-Young, and C. P. Chou, "Towards sustainable production of clean energy carriers from biomass resources," *APPLIED ENERGY*, vol. 100, pp. 172–186, DEC 2012. 11th International Conference on Clean Energy (ICCE), Fen Chia University, Taichung, TAIWAN, NOV 02-05, 2011.

[4] C. Wells, "Sweden forced to import trash from Norway to create heat and electricity," *NY Daily News*, Oct 2012.

[5] N. Berkowitz, *An introduction to coal technology*. Academic Press, Inc., 1994.

[6] L. D. Smoot and P. J. Smith, eds., *Coal combustion and gasification*. Plenum Press, 1985.

[7] Y. Matsuzaki and I. Yasuda, "Electrochemical oxidation of H-2 and CO in a H-2-H2O-CO-CO2 system at the interface of a Ni-YSZ cermet electrode and YSZ electrolyte," *JOURNAL OF THE ELECTROCHEMICAL SOCIETY*, vol. 147, pp. 1630–1635, MAY 2000.

[8] A. Raje and B. Davis, "Fischer-Tropsch synthesis over iron-based catalysts in a slurry reactor. Reaction rates, selectivities and implications for improving hydrocarbon productivity," *CATALYSIS TODAY*, vol. 36, pp. 335–345, JUN 6 1997.

[9] Entech , *available online at: www.entech-res.com/wtgas*, accessed January 15, 2012.

[10] T.-Y. Mun, J.-O. Kim, J.-W. Kim, and J.-S. Kim, "Influence of operation conditions and additives on the development of producer gas and tar reduction in air gasification of construction woody wastes using a two-stage gasifier," *BIORESOURCE TECHNOLOGY*, vol. 102, pp. 7196–7203, JUL 2011.

[11] M. Granovskii, R. Gerspacher, T. Pugsley, and F. Sanchez, "An effect of tar model compound toluene treatment with high-temperature flames," *FUEL*, vol. 92, pp. 369–372, FEB 2012.

[12] S. Anis and Z. A. Zainal, "Tar reduction in biomass producer gas via mechanical, catalytic and thermal methods: A review," *RENEWABLE & SUSTAINABLE ENERGY REVIEWS*, vol. 15, pp. 2355–2377, JUN 2011.

[13] Z. Abu El-Rub, E. Bramer, and G. Brem, "Review of catalysts for tar elimination in Biomass gasification processes," *INDUSTRIAL & ENGINEERING CHEMISTRY RESEARCH*, vol. 43, pp. 6911–6919, OCT 27 2004.

[14] C. Pfeifer and H. Hofbauer, "Development of catalytic tar decomposition downstream from a dual fluidized bed biomass steam gasifier," *POWDER TECHNOLOGY*, vol. 180, pp. 9–16, JAN 14 2008. 6th International Symposium on Gas Cleaning at High Temperature, Osaka, JAPAN, OCT 20-22, 2005.

[15] T. Furusawa, Y. Miura, Y. Kori, M. Sato, and N. Suzuki, "The cycle usage test of Ni/MgO catalyst for the steam reforming of naphthalene/benzene as model tar compounds of biomass gasification," *CATALYSIS COMMUNICATIONS*, vol. 10, pp. 552–556, JAN 25 2009.

[16] K. Tomishige, T. Miyazawa, M. Asadullah, S. Ito, and K. Kunimori, "Catalyst performance in reforming of tar derived from biomass over noble metal catalysts," *GREEN CHEMISTRY*, vol. 5, no. 4, pp. 399–403, 2003.

[17] G. Ruoppolo, F. Miccio, and R. Chirone, "Fluidized Bed Cogasification of Wood and Coal Adopting Primary Catalytic Method for Tar Abatement," *ENERGY & FUELS*, vol. 24, pp. 2034–2041, MAR 2010.

[18] A. Bridgwater, A. Toft, and J. Brammer, "A techno-economic comparison of power production by biomass fast pyrolysis with gasification and combustion," *RENEWABLE & SUSTAINABLE ENERGY REVIEWS*, vol. 6, pp. 181–248, JUN 2002.

[19] H. Schobert and C. Song, "Chemicals and materials from coal in the 21st century," *FUEL*, vol. 81, pp. 15–32, JAN 2002.

[20] C. Li and K. Suzuki, "Resources, properties and utilization of tar," *RESOURCES CONSERVATION AND RECYCLING*, vol. 54, pp. 905–915, SEP 2010.

[21] A. Ouattara, L. Pibouleau, C. Azzaro-Pantel, S. Domenech, P. Baudet, and B. Yao, "Economic and environmental strategies for process design," *COMPUTERS & CHEMICAL ENGINEERING*, vol. 36, pp. 174–188, JAN 10 2012.

[22] Z. Ab Rahman, N. R. Menon, and K. H. K. Hamid, "AIR GASIFICATION OF PALM BIOMASS FOR PRODUCING TAR-FREE HIGHER HEATING VALUE PRODUCER GAS," *JOURNAL OF OIL PALM RESEARCH*, vol. 23, pp. 1060–1068, AUG 2011.

[23] K. Qin, W. Lin, P. A. Jensen, and A. D. Jensen, "High-temperature entrained flow gasification of biomass," *FUEL*, vol. 93, pp. 589–600, MAR 2012.

[24] X. Meng, W. de Jong, N. Fu, and A. H. M. Verkooijen, "Biomass gasification in a 100 kWth steam-oxygen blown circulating fluidized bed gasifier: Effects of operational conditions on product gas distribution and tar formation," *BIOMASS & BIOENERGY*, vol. 35, pp. 2910–2924, JUL 2011.

[25] M. M. Yung, W. S. Jablonski, and K. A. Magrini-Bair, "Review of Catalytic Conditioning of Biomass-Derived Syngas," *ENERGY & FUELS*, vol. 23, pp. 1874–1887, MAR-APR 2009.

[26] T. YAMAGUCHI, K. YAMASAKI, O. YOSHIDA, Y. KANAI, A. UENO, and Y. KOTERA, "DEACTIVATION AND REGENERATION OF CATALYST FOR STEAM GASIFICATION OF WOOD TO METHANOL SYNTHESIS GAS," *INDUSTRIAL & ENGINEERING CHEMISTRY PRODUCT RESEARCH AND DEVELOPMENT*, vol. 25, pp. 239–243, JUN 1986.

[27] R. Bain, D. Dayton, D. Carpenter, S. Czernik, C. Feik, R. French, K. Magrini-Bair, and S. Phillips, "Evaluation of catalyst deactivation during catalytic steam reforming of biomass-derived syngas," *INDUSTRIAL & ENGINEERING CHEMISTRY RESEARCH*, vol. 44, pp. 7945–7956, OCT 12 2005.

[28] L. Di Felice, C. Courson, D. Niznansky, P. U. Foscolo, and A. Kiennemann, "Biomass Gasification with Catalytic Tar Reforming: A Model Study into Activity Enhancement of Calcium- and Magnesium-Oxide-Based Catalytic Materials by Incorporation of Iron," *ENERGY & FUELS*, vol. 24, pp. 4034–4045, JUL 2010.

[29] D. Swierczynski, C. Courson, and A. Kiennemann, "Study of steam reforming of toluene used as model compound of tar produced by biomass gasification," *CHEMICAL ENGINEERING AND PROCESSING*, vol. 47, pp. 508–513, MAR 2008. 10th Congress of the French-Chemical-Engineering-Society, Lab Genie Chim, Toulouse, FRANCE, JUN 20-22, 2005.

[30] C. Fernandez-Pereira, J. A. de la Casa, A. Gomez-Barea, F. Arroyo, C. Leiva, and Y. Luna, "Application of biomass gasification fly ash for brick manufacturing," *FUEL*, vol. 90, pp. 220–232, JAN 2011.

[31] S. Meyer, B. Glaser, and P. Quicker, "Technical, Economical, and Climate-Related Aspects of Biochar Production Technologies: A Literature Review," *ENVIRONMENTAL SCIENCE & TECHNOLOGY*, vol. 45, pp. 9473–9483, NOV 15 2011.

[32] M. Carrier, A. G. Hardie, U. Uras, J. Goergens, and J. H. Knoetze, "Production of char from vacuum pyrolysis of South-African sugar cane bagasse and its characterization as activated carbon and biochar," *JOURNAL OF ANALYTICAL AND APPLIED PYROLYSIS*, vol. 96, pp. 24–32, JUL 2012.

[33] N. B. Klinghoffer, M. J. Castaldi, and A. Nzihou, "Catalyst Properties and Catalytic Performance of Char from Biomass Gasification," *INDUSTRIAL & ENGINEERING CHEMISTRY RESEARCH*, vol. 51, pp. 13113–13122, OCT 10 2012.

[34] R. M. Heck and R. J. Farrauto, *Catalytic air pollution control*. Wiley Interscience, 2002.

[35] S. Turn, C. Kinoshita, D. Ishimura, and J. Zhou, "The fate of inorganic constituents of biomass in fluidized bed gasification," *FUEL*, vol. 77, pp. 135–146, FEB 1998.

[36] P. Serp and J. L. Figueiredo, eds., *Carbon Materials for Catalysis*. Wiley, 2009.

[37] J. S. Prasad, V. Dhand, V. Himabindu, and Y. Anjaneyulu, "Production of hydrogen and carbon nanofibers through the decomposition of methane over activated carbon supported Ni catalysts," *INTERNATIONAL JOURNAL OF HYDROGEN ENERGY*, vol. 36, pp. 11702–11711, SEP 2011.

[38] T. Sueyasu, T. Oike, A. Mori, S. Kudo, K. Norinaga, and J.-i. Hayashi, "Simultaneous Steam Reforming of Tar and Steam Gasification of Char from the Pyrolysis of Potassium-Loaded Woody Biomass," *ENERGY & FUELS*, vol. 26, pp. 199–208, JAN 2012.

[39] N. Striugas, K. Zakarauskas, G. Stravinskas, and V. Grigaitiene, "Comparison of steam reforming and partial oxidation of biomass pyrolysis tars over activated carbon derived from waste tire," *CATALYSIS TODAY*, vol. 196, pp. 67–74, NOV 30 2012.

[40] D. Wang, W. Yuan, and W. Ji, "Char and char-supported nickel catalysts for secondary syngas cleanup and conditioning," *APPLIED ENERGY*, vol. 88, pp. 1656–1663, MAY 2011.

[41] Z. A. El-Rub, E. A. Bramer, and G. Brem, "Experimental comparison of biomass chars with other catalysts for tar reduction," *FUEL*, vol. 87, pp. 2243–2252, AUG 2008.

[42] Z. Min, P. Yimsiri, M. Asadullah, S. Zhang, and C.-Z. Li, "Catalytic reforming of tar during gasification. Part II. Char as a catalyst or as a catalyst support for tar reforming," *FUEL*, vol. 90, pp. 2545–2552, JUL 2011.

[43] W. Chaiwat, I. Hasegawa, and K. Mae, "Alternative Reforming Methods of Primary Tar Released from Gas Treatment of Biomass at Low Temperature for Development of Pyrolysis/Gasification Process," *INDUSTRIAL & ENGINEERING CHEMISTRY RESEARCH*, vol. 49, pp. 3577–3584, APR 21 2010.

[44] P. Sannigrahi, A. J. Ragauskas, and G. A. Tuskan, "Poplar as a feedstock for biofuels: A review of compositional characteristics," *BIOFUELS BIOPRODUCTS & BIOREFINING-BIOFPR*, vol. 4, pp. 209–226, MAR-APR 2010.

[45] R. M. GERMAN, "Surface area reduction kinetics during intermediate stage sintering," *Journal of the American Ceramic Society*, vol. 61, no. 5-6, pp. 272–274, 1978.

[46] J. White and G. Kuczynski, "Sintering and related phenomena," *Ed. GC Kuczynski, Gordon and Breech*, p. 245, 1967.

[47] R. German and Z. Munir, "Surface area reduction during isothermal sintering," *Journal of the American Ceramic Society*, vol. 59, no. 9-10, pp. 379–383, 1976.

[48] D. R. Lide, ed., *CRC Handbook of Chemistry and Physics, 88th ed.* CRC Press, 2008.

[49] P. Girods, A. Dufour, V. Fierro, Y. Rogaume, C. Rogaume, A. Zoulalian, and A. Celzard, "Activated carbons prepared from wood particleboard wastes: Characterisation and phenol adsorption capacities," *JOURNAL OF HAZARDOUS MATERIALS*, vol. 166, pp. 491–501, JUL 15 2009.

[50] M. A. Uddin, H. Tsuda, S. Wu, and E. Sasaoka, "Catalytic decomposition of biomass tars with iron oxide catalysts," *FUEL*, vol. 87, pp. 451–459, APR 2008. 9th China-Japan Symposium on Coal and C (1) Chemistry, Chengdu, PEOPLES R CHINA, OCT 22-28, 2006.

[51] M. Kong, Q. Yang, J. Fei, and X. Zheng, "Experimental study of Ni/MgO catalyst in carbon dioxide reforming of toluene, a model compound of tar from biomass gasifi-

cation," *INTERNATIONAL JOURNAL OF HYDROGEN ENERGY*, vol. 37, pp. 13355–13364, SEP 2012.

[52] L. Wang, Y. Hisada, M. Koike, D. Li, H. Watanabe, Y. Nakagawa, and K. Tomishige, "Catalyst property of Co-Fe alloy particles in the steam reforming of biomass tar and toluene," *APPLIED CATALYSIS B-ENVIRONMENTAL*, vol. 121, pp. 95–104, JUN 13 2012.

[53] G. V. Reklaitis, *Introduction to material and energy balances*. Wiley, 1983.

[54] D. L. Carpenter, R. L. Bain, R. E. Davis, A. Dutta, C. J. Feik, K. R. Gaston, W. Jablonski, S. D. Phillips, and M. R. Nimlos, "Pilot-Scale Gasification of Corn Stover, Switchgrass, Wheat Straw, and Wood: 1. Parametric Study and Comparison with Literature," *INDUSTRIAL & ENGINEERING CHEMISTRY RESEARCH*, vol. 49, pp. 1859–1871, FEB 17 2010.

[55] X. Wang and R. Gorte, "A study of steam reforming of hydrocarbon fuels on Pd/ceria," *APPLIED CATALYSIS A-GENERAL*, vol. 224, pp. 209–218, JAN 25 2002.

[56] A. Gomez-Barea, S. Nilsson, F. Vidal Barrero, and M. Campoy, "Devolatilization of wood and wastes in fluidized bed," *FUEL PROCESSING TECHNOLOGY*, vol. 91, pp. 1624–1633, NOV 2010.

[57] Z. Abu El-Rub, E. A. Bramer, and G. Brem, "Experimental comparison of biomass chars with other catalysts for tar reduction," *FUEL*, vol. 87, pp. 2243–2252, AUG 2008.

[58] R. H. Perry and D. W. Green, eds., *Perry's Chemical Engineers' Handbook*. McGraw Hill, 1997.

[59] A. Dufour, A. Celzard, B. Ouartassi, F. Broust, V. Fierro, and A. Zoulaljan, "Effect of micropores diffusion on kinetics of CH4 decomposition over a wood-derived carbon catalyst," *APPLIED CATALYSIS A-GENERAL*, vol. 360, pp. 120–125, JUN 1 2009.

[60] G. F. Froment and K. B. Bischoff, *Chemical reactor analysis and design*. Wiley, Second ed., 1990.

[61] C. H. Bartholomew and R. J. Farrauto, *Fundamentals of industrial catalytic processes*. Wiley-Interscience, 2006.

[62] P. Fu, S. Hu, J. Xiang, W. Yi, X. Bai, L. Sun, and S. Su, "Evolution of char structure during steam gasification of the chars produced from rapid pyrolysis of rice husk," *Bioresource Technology*, vol. 114, no. 0, pp. 691 – 697, 2012.

[63] B. ZHANG and S. LI, "DETERMINATION OF THE SURFACE FRACTAL DIMENSION FOR POROUS-MEDIA BY MERCURY POROSIMETRY," *INDUSTRIAL & ENGINEERING CHEMISTRY RESEARCH*, vol. 34, pp. 1383–1386, APR 1995.

[64] F. Rodriguez-Reinoso, "The role of carbon materials in heterogeneous catalysis," *CARBON*, vol. 36, no. 3, pp. 159–175, 1998. 23rd Biennial Conference on Carbon (Carbon 97), PENN STATE UNIV, UNIVERSITY PK, PA, JUL 13-18, 1997.

[65] H. BOEHM, "SOME ASPECTS OF THE SURFACE-CHEMISTRY OF CARBON-BLACKS AND OTHER CARBONS," *CARBON*, vol. 32, no. 5, pp. 759–769, 1994.

[66] M. Franz, H. Arafat, and N. Pinto, "Effect of chemical surface heterogeneity on the adsorption mechanism of dissolved aromatics on activated carbon," *CARBON*, vol. 38, no. 13, pp. 1807–1819, 2000.

[67] R. H. Bradley, M. W. Smith, A. Andreu, and M. Falco, "Surface studies of novel hydrophobic active carbons," *APPLIED SURFACE SCIENCE*, vol. 257, pp. 2912–2919, JAN 15 2011.

[68] C.-h. Chen, J.-q. Xu, M.-m. Jin, G.-y. Li, and C.-w. Hu, "Direct Synthesis of Phenol from Benzene on an Activated Carbon Catalyst Treated with Nitric Acid," *CHINESE JOURNAL OF CHEMICAL PHYSICS*, vol. 24, pp. 358–364, JUN 2011.

[69] E. Ahumada, H. Lizama, F. Orellana, C. Suarez, A. Huidobro, A. Sepulveda-Escribano, and F. Rodriguez-Reinoso, "Catalytic oxidation of Fe(II) by activated carbon in the presence of oxygen. Effect of the surface oxidation degree on the catalytic activity," *CARBON*, vol. 40, no. 15, pp. 2827–2834, 2002.

[70] J. H. Ko, Y.-H. Kwak, K.-S. Yoo, J.-K. Jeon, S. H. Park, and Y.-K. Park, "Selective catalytic reduction of NOx using RDF char and municipal solid waste char based catalyst," *JOURNAL OF MATERIAL CYCLES AND WASTE MANAGEMENT*, vol. 13, pp. 173–179, OCT 2011.

[71] R. V. Sharma, K. K. Soni, and A. K. Dalai, "Preparation, characterization and application of sulfated Ti-SBA-15 catalyst for oxidation of benzyl alcohol to benzaldehyde," *CATALYSIS COMMUNICATIONS*, vol. 29, pp. 87–91, DEC 5 2012.

[72] B. Li, G.-S. Hu, L.-Y. Jin, X. Hong, J.-Q. Lu, and M.-F. Luo, "Characterizations of Ru/ZnO catalysts with different Ru contents for selective hydrogenation of crotonaldehyde," *JOURNAL OF INDUSTRIAL AND ENGINEERING CHEMISTRY*, vol. 19, pp. 250–255, JAN 25 2013.

[73] H. P. Boehm, "Chemical identification of surface groups," vol. 16, pp. 179 – 274, 1966.

[74] S. L. Goertzen, K. D. Theriault, A. M. Oickle, A. C. Tarasuk, and H. A. Andreas, "Standardization of the Boehm titration. Part I. CO2 expulsion and endpoint determination," *CARBON*, vol. 48, pp. 1252–1261, APR 2010.

[75] A. M. Oickle, S. L. Goertzen, K. R. Hopper, Y. O. Abdalla, and H. A. Andreas, "Standardization of the Boehm titration: Part II. Method of agitation, effect of filtering and dilute titrant," *CARBON*, vol. 48, pp. 3313–3322, OCT 2010.

[76] X. Jiaquan, L. Huihui, Y. Ruiguang, L. Guiying, and H. Changwei, "Hydroxylation of Benzene by Activated Carbon Catalyst," *CHINESE JOURNAL OF CATALYSIS*, vol. 33, pp. 1622–1630, OCT 2012.

[77] G. Szymanski and G. RYCHLICKI, "IMPORTANCE OF OXYGEN-SURFACE GROUPS IN CATALYTIC DEHYDRATION AND DEHYDROGENATION OF BUTAN-2-OL PROMOTED BY CARBON CATALYSTS," *CARBON*, vol. 29, no. 4-5, pp. 489–498, 1991.

[78] H. Teng, Y. Tu, Y. Lai, and C. Lin, "Reduction of NO with NH3 over carbon catalysts - The effects of treating carbon with H2SO4 and HNO3," *CARBON*, vol. 39, no. 4, pp. 575–582, 2001.

[79] G. Szymanski, Z. Karpinski, S. Biniak, and A. Swiatkowski, "The effect of the gradual thermal decomposition of surface oxygen species on the chemical and catalytic properties of oxidized activated carbon," *CARBON*, vol. 40, no. 14, pp. 2627–2639, 2002.

[80] P. Brender, R. Gadiou, J.-C. Rietsch, P. Fioux, J. Dentzer, A. Ponche, and C. Vix-Guterl, "Characterization of Carbon Surface Chemistry by Combined Temperature Programmed Desorption with in Situ X-ray Photoelectron Spectrometry and Temperature Programmed Desorption with Mass Spectrometry Analysis," *ANALYTICAL CHEMISTRY*, vol. 84, pp. 2147–2153, MAR 6 2012.

[81] B. Pradhan and N. Sandle, "Effect of different oxidizing agent treatments on the surface properties of activated carbons," *CARBON*, vol. 37, no. 8, pp. 1323–1332, 1999.

[82] Y. Richardson, J. Blin, and A. Julbe, "A short overview on purification and conditioning of syngas produced by biomass gasification: Catalytic strategies, process intensification and new concepts," *PROGRESS IN ENERGY AND COMBUSTION SCIENCE*, vol. 38, pp. 765–781, DEC 2012.

[83] U. Menon, H. Poelman, V. Bliznuk, V. V. Galvita, D. Poelman, and G. B. Marin, "Nature of the active sites for the total oxidation of toluene by CuO-CeO2/Al2O3," *JOURNAL OF CATALYSIS*, vol. 295, pp. 91–103, NOV 2012.

[84] A. Sarioglan, "Tar removal on dolomite and steam reforming catalyst: Benzene, toluene and xylene reforming," *INTERNATIONAL JOURNAL OF HYDROGEN ENERGY*, vol. 37, pp. 8133–8142, MAY 2012.

[85] C. Dupont, T. Nocquet, J. A. Da Costa, Jr., and C. Verne-Tournon, "Kinetic modelling of steam gasification of various woody biomass chars: Influence of inorganic elements," *BIORESOURCE TECHNOLOGY*, vol. 102, pp. 9743–9748, OCT 2011.

[86] M. Mozaffari, C. Rosen, M. Russelle, and E. Nater, "Chemical characterization of ash from gasification of alfalfa stems: Implications for ash management," *JOURNAL OF ENVIRONMENTAL QUALITY*, vol. 29, pp. 963–972, MAY-JUN 2000.

[87] K. Yip, F. Tian, J.-i. Hayashi, and H. Wu, "Effect of Alkali and Alkaline Earth Metallic Species on Biochar Reactivity and Syngas Compositions during Steam Gasification," *ENERGY & FUELS*, vol. 24, pp. 173–181, JAN 2010. Sino/Australian Symposium on Advanced Coal and Biomass Utilisation Technologies, Wuhan, PEOPLES R CHINA, DEC 09-11, 2009.

[88] S. V. Vassilev, D. Baxter, L. K. Andersen, C. G. Vassileva, and T. J. Morgan, "An overview of the organic and inorganic phase composition of biomass," *FUEL*, vol. 94, pp. 1–33, APR 2012.

[89] T. Kowalski, C. Ludwig, and A. Wokaun, "Qualitative evaluation of alkali release during the pyrolysis of biomass," *ENERGY & FUELS*, vol. 21, pp. 3017–3022, SEP-OCT 2007.

[90] D. Keown, G. Favas, J. Hayashi, and C. Li, "Volatilisation of alkali and alkaline earth metallic species during the pyrolysis of biomass: differences between sugar cane bagasse and cane trash," *BIORESOURCE TECHNOLOGY*, vol. 96, pp. 1570–1577, SEP 2005.

[91] F. Marquez-Montesinos, T. Cordero, J. Rodriguez-Mirasol, and J. Rodriguez, "CO2 and steam gasification of a grapefruit skin char," *FUEL*, vol. 81, pp. 423–429, MAR 2002.

[92] R. Habibi, J. Kopyscinski, M. S. Masnadi, J. Lam, J. R. Grace, C. A. Mims, and J. M. Hill, "Co-gasification of biomass and non-biomass feedstocks: Synergistic and inhibition effects of switchgrass mixed with sub-bituminous coal and fluid coke during co2 gasification," *Energy & Fuels*, 2013.

[93] T. L. Eberhardt and H. Pan, "Elemental analyses of chars isolated from a biomass gasifier fly ash," *FUEL*, vol. 96, pp. 600–603, JUN 2012.

[94] L. Devi, K. Ptasinski, and F. Janssen, "A review of the primary measures for tar elimination in biomass gasification processes," *BIOMASS & BIOENERGY*, vol. 24, no. 2, pp. 125–140, 2003.

[95] T. G. Devi, M. P. Kannan, and V. P. Abduraheem, "Jump in the air gasification rate of potassium-doped cellulosic chars," *FUEL PROCESSING TECHNOLOGY*, vol. 91, pp. 1826–1831, DEC 2010.

[96] R. BAKER, "The relationship between particle motion on a graphite surface and Tammann temperature," *JOURNAL OF CATALYSIS*, vol. 78, no. 2, pp. 473–476, 1982.

[97] C. Di Blasi, "Combustion and gasification rates of lignocellulosic chars," *PROGRESS IN ENERGY AND COMBUSTION SCIENCE*, vol. 35, pp. 121–140, APR 2009.

[98] I. I. Ahmed and A. K. Gupta, "Kinetics of woodchips char gasification with steam and carbon dioxide," *APPLIED ENERGY*, vol. 88, pp. 1613–1619, MAY 2011.

[99] H. C. Butterman and M. J. Castaldi, "Biomass to Fuels: Impact of Reaction Medium and Heating Rate," *ENVIRONMENTAL ENGINEERING SCIENCE*, vol. 27, pp. 539–555, JUL 2010. International Conference on Themal Treatment Technologies and Hazard Waste Combustors, Cincinnati, OH, MAY 12-22, 2009.

[100] C. Botero, R. P. Field, H. J. Herzog, and A. F. Ghoniem, "Impact of finite-rate kinetics on carbon conversion in a high-pressure, single-stage entrained flow gasifier with coal–co¡ sub¿ 2¡/sub¿ slurry feed," *Applied Energy*, vol. 104, pp. 408–417, 2013.

[101] D. M. Keown, J.-I. Hayashi, and C.-Z. Li, "Drastic changes in biomass char structure and reactivity upon contact with steam," *FUEL*, vol. 87, pp. 1127–1132, JUN 2008.

[102] M. Illan-Gomez, E. Raymundo-Pinero, A. Garcia-Garcia, A. Linares-Solano, and C. de Lecea, "Catalytic NOx reduction by carbon supporting metals," *APPLIED CATALYSIS B-ENVIRONMENTAL*, vol. 20, pp. 267–275, APR 5 1999.

[103] L. Hsu and H. Teng, "Catalytic NO reduction with NH3 over carbons modified by acid oxidation and by metal impregnation and its kinetic studies," *APPLIED CATALYSIS B-ENVIRONMENTAL*, vol. 35, pp. 21–30, DEC 10 2001.

[104] D. P. Serrano, J. A. Botas, J. L. G. Fierro, R. Guil-Lopez, P. Pizarro, and G. Gomez, "Hydrogen production by methane decomposition: Origin of the catalytic activity of carbon materials," *FUEL*, vol. 89, pp. 1241–1248, JUN 2010. Symposium on Advanced Fossil Energy Utilization, Tampa, FL, APR 26-30, 2009.

[105] M. Guerrero, M. P. Ruiz, A. Millera, M. U. Alzueta, and R. Bilbao, "Characterization of biomass chars formed under different devolatilization conditions: Differences between rice husk and eucalyptus," *ENERGY & FUELS*, vol. 22, pp. 1275–1284, MAR-APR 2008.

Part VI

Appendices

Appendix A

Kinetics of methane cracking

This section shows the kinetic tests for the char samples that were not discussed in Chapter 6. These samples showed primarily very similar trends, therefore it was not particularly relevant to discuss them in the main body of the text. The H_2 production is shown in Figure A.1 and the deactivation function is shown in Figure A.2. We see very similar trends to the data from the TGA, shown in Chapter 4. The char made at 550^{o}C has significantly lower activity than the other char samples, and a much lower deactivation coefficient. The two samples that were made at 750^{o}C for 30 min had very similar catalytic activities.

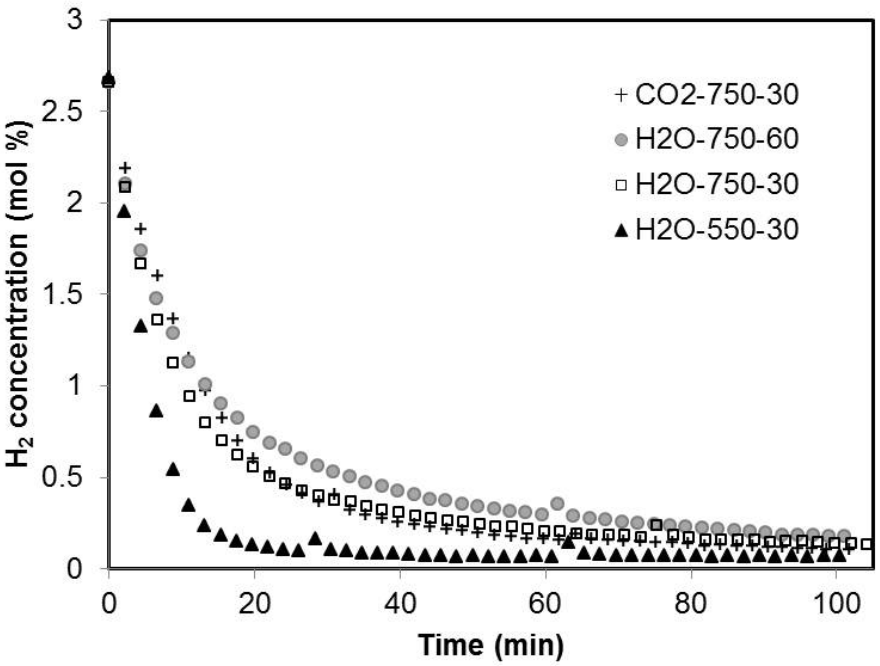

Figure A.1: H_2 production for various char samples during catalytic cracking of CH_4 at 850^{o}C.

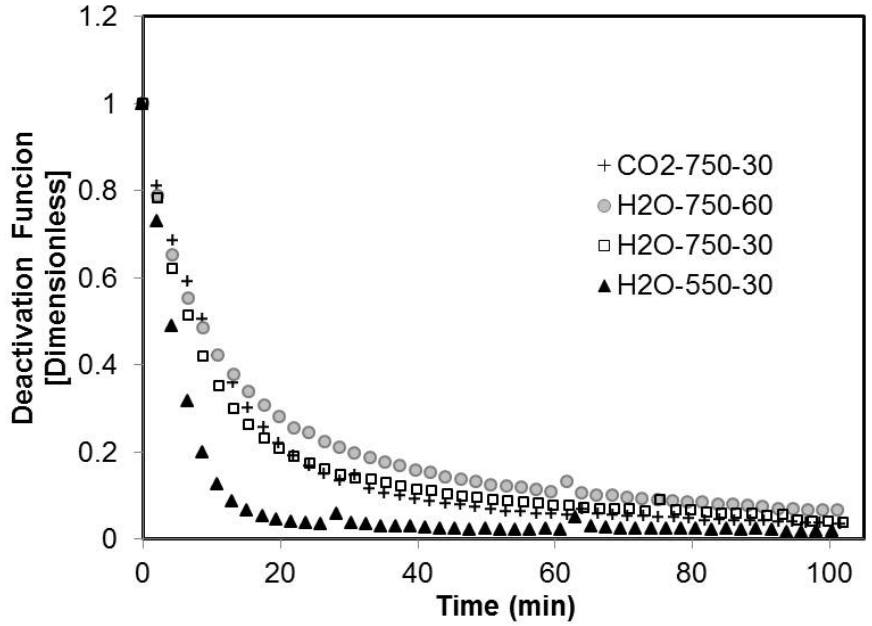

Figure A.2: Deactivation function for various char samples during catalytic cracking of CH_4 at 850^{o}C.

Appendix B

EDS Spectra

This section shows the EDS spectra for a char sample that was produced under steam at 750^{o}C for 30 min. This sample was heated to 1000^{o}C prior to being used for catalytic cracking of methane at 700^{o}C. Figure B.1 shows an image of the char where individual points are identified as a, b, c, d. Elemental analysis was done on each of these four points, and the EDS spectra, along with the quantification of the composition at these locations is shown in Figures B.2, B.3, B.4, and B.5, respectively.

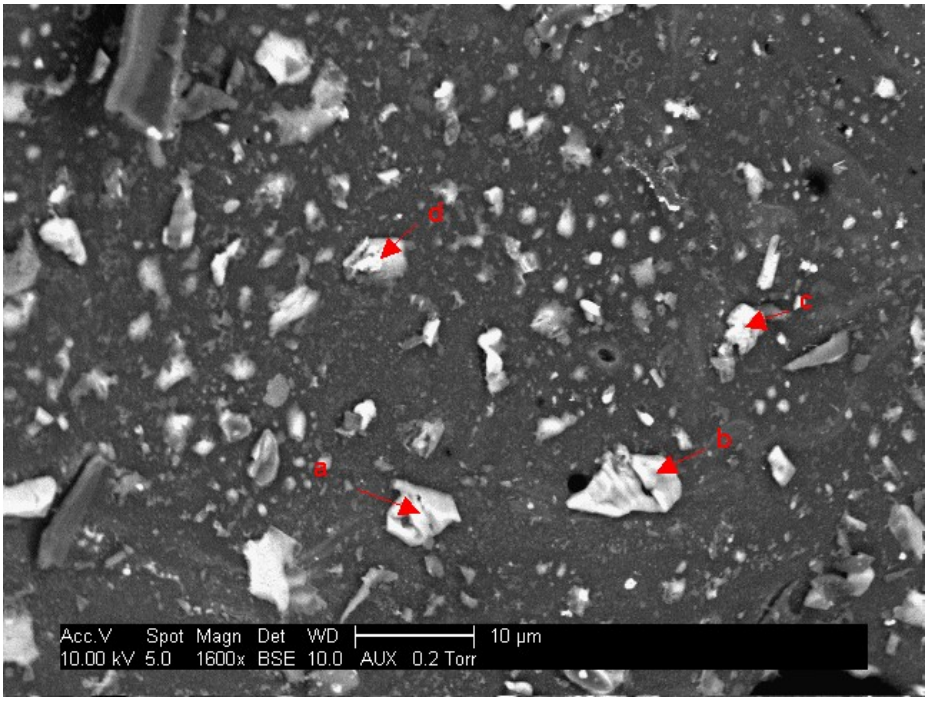

Figure B.1: SEM image of char showing locations of EDS analysis.

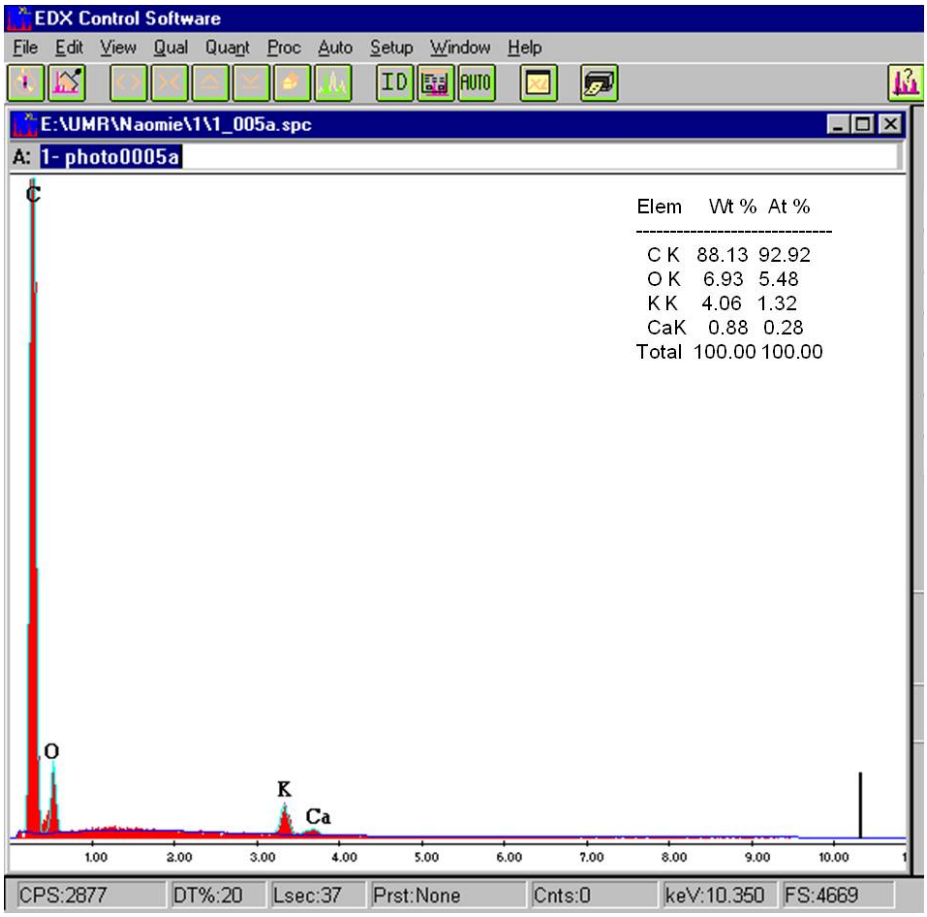

Figure B.2: EDS spectrum for point a from Figure B.1

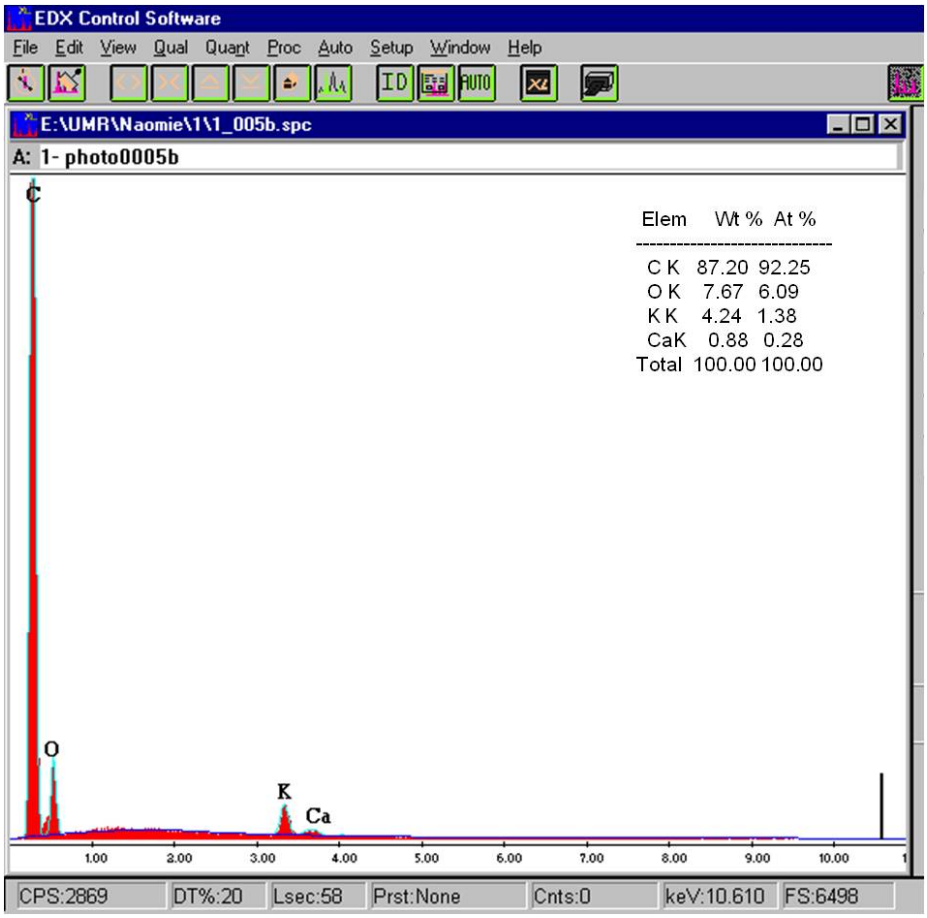

Figure B.3: EDS spectrum for point b from Figure B.1

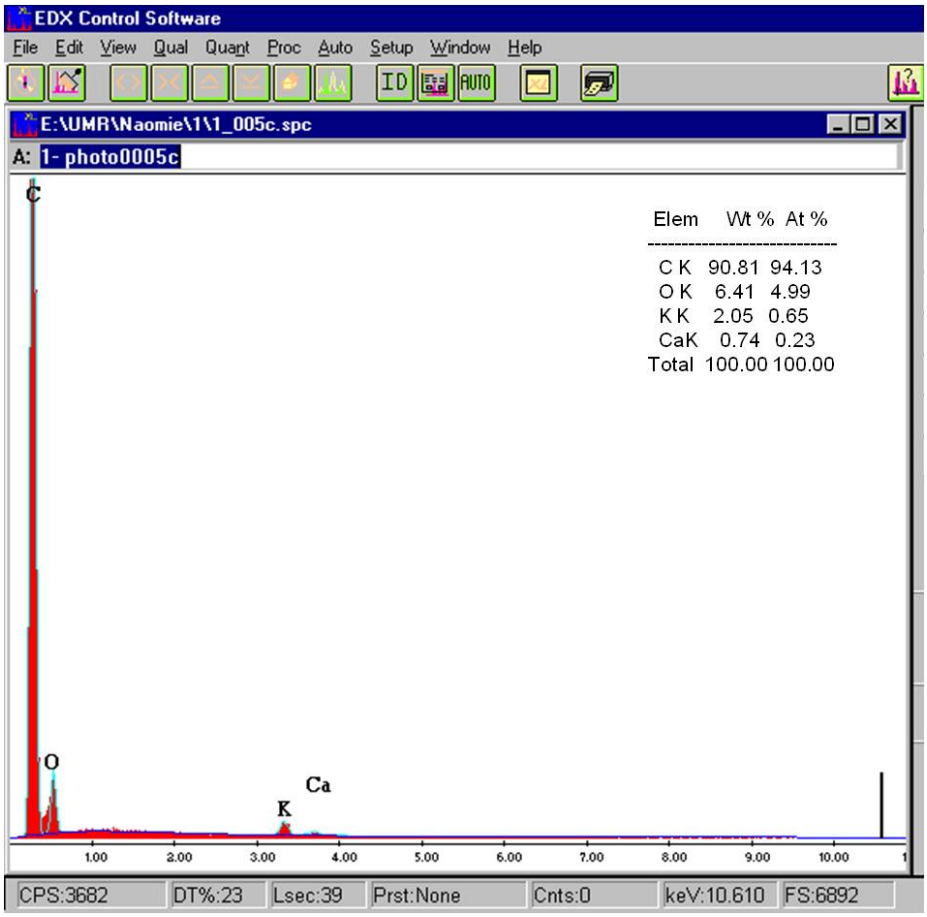

Figure B.4: EDS spectrum for point c from Figure B.1

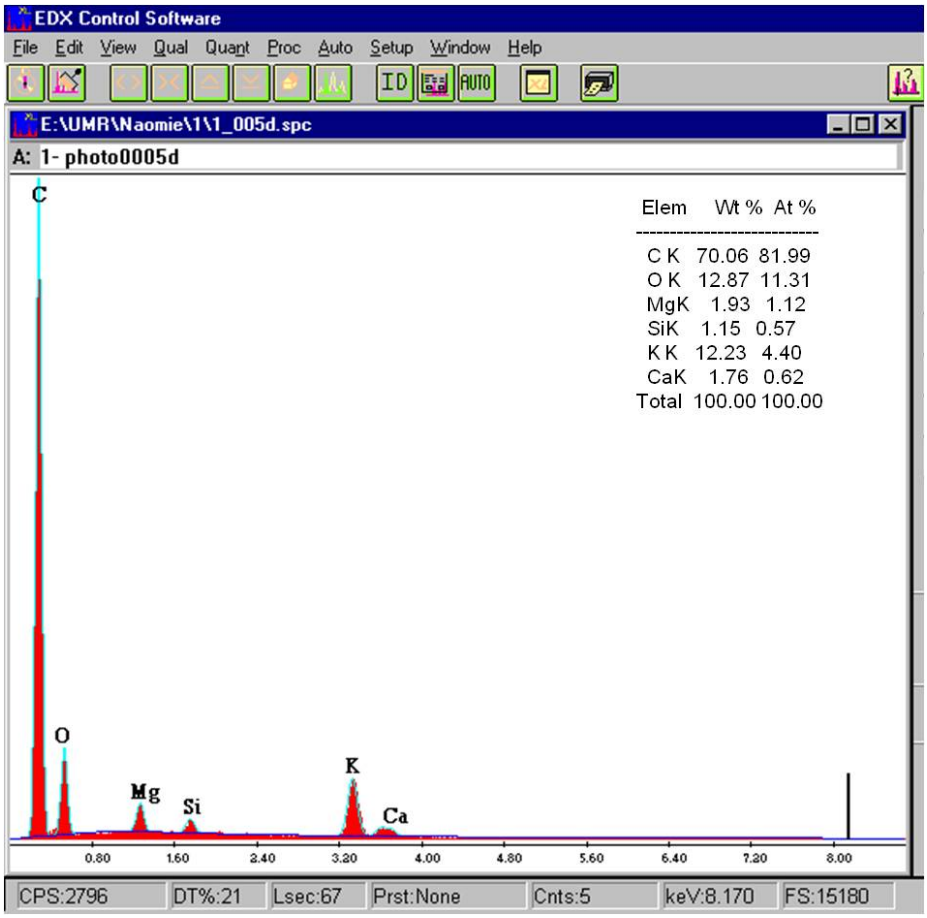

Figure B.5: EDS spectrum for point d from Figure B.1

Appendix C

XRD Results

This section shows the X-ray diffraction patterns of the char samples. Figures C.1 and C.2 show the results for the chars made in H_2O and CO_2, respectively. The broad band at 2θ values of 23^o has been attributed to a highly disordered structure, while the band at 2θ values of 44 represents ordered graphitic carbon [105]. The peak at 2θ values of 29^o has been attributed to calcite ($CaCO_3$) [105]. While some peaks are observed in the XRD spectrum, the EDS data shows the presence of many other elements, including Fe, Ni, Al, Mn, Mg, etc. which are not easily detectable with XRD measurements.

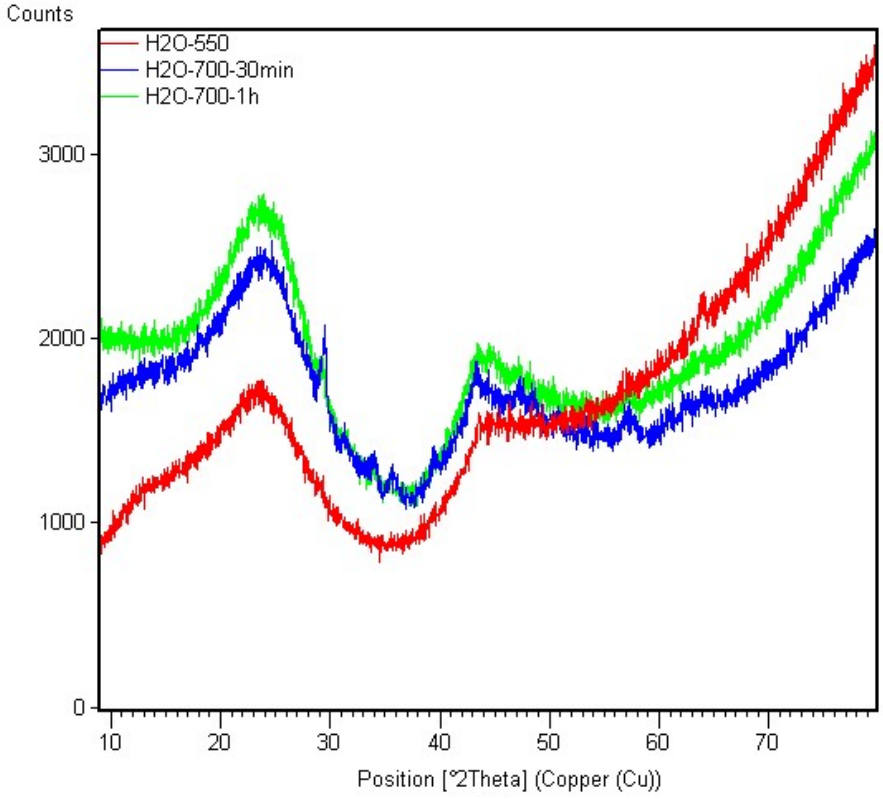

Figure C.1: X-ray diffraction pattern for char samples made in H_2O.

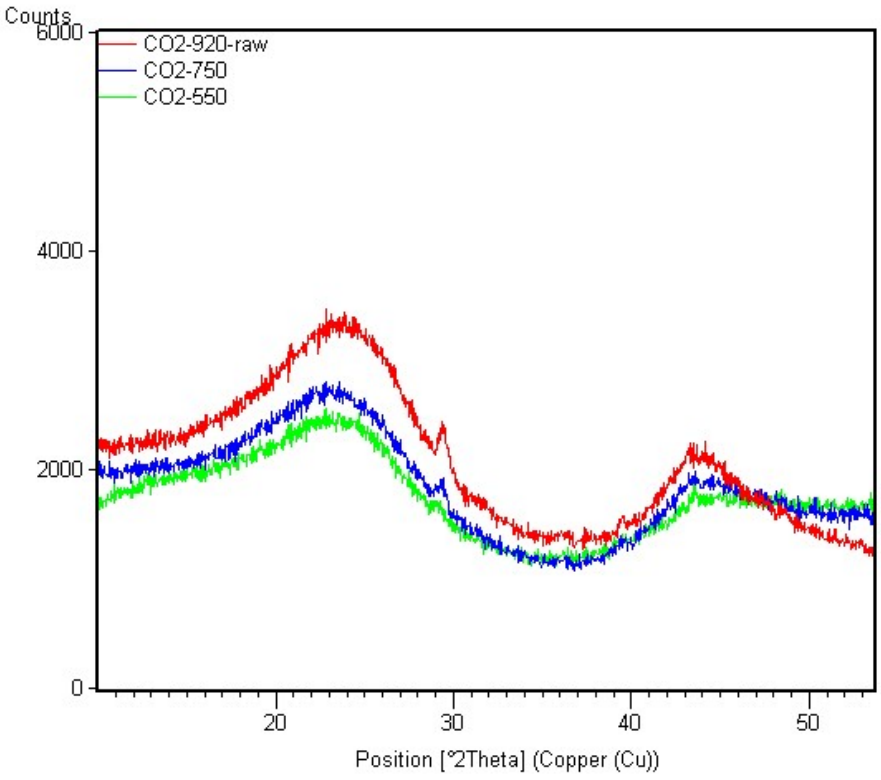

Figure C.2: X-ray diffraction pattern for char samples made in CO_2.

Appendix D

ESEM images of char

D.1 ESEM-EDS principle

An environmental scanning electron microscope (ESEM) was used in many parts of this research and this section discusses the principle of operation of this instrument, since its method of use was very relevant to many aspects of the research presented here. The Environmental SEM differs from a conventional SEM in that it includes a diaphragm (diameter of 300 microns) between the sample chamber and the column containing the electron gun, which produces a pressure drop, enabling higher pressures (up to 10 Torr) to be achieved in the sample chamber. Observing samples under higher pressures with a low accelerating voltage enables the observation of non-conductive samples without having to coat them in a conductive material. Observing non-conductive samples using a high voltage will lead to an accumulation of charge on the surface, which reduces the quality of the image.

The ESEM detects back scattered electrons (BSE), secondary electrons (SE), and gaseous secondary electrons (GSE), which are secondary electrons that are detected when the instrument is in the environmental (higher pressure) mode. The back scattered electrons are generated within the sample, to a depth of 10-100nm, enabling the detection of chemical contrasts. With the SE (or GSE) detector the electron diffusion region penetrates to a depth of a few nm, giving a more detailed image of the surface morphology.

The type of detection can be used to help understand the samples being observed in the ESEM. One of the main issues with using this instrument to observe the char is that the metals are minerals are finely dispersed in a very thin layer on the surface, making it difficult to measure them with the EDS. The EDS uses X-rays to measure the elements present which penetrate below the surface, and measure molecules that are present within a sphere with a diameter of ~1 micron. Therefore, very thin layers on the surface, or very small particles will be difficult to measure with EDS, even though they can be observed with the SEM. Using the two detectors can help to differentiate if the observed differences are morphological, compositional or both. This is made easier with the Environmental SEM, which operates in a low vacuum mode, eliminating the need to coat the sample with a conductive metal prior to analysis. Figure D.1 shows an image that was taken with the GSE detector and the BSE detector. Figure D.1A shows a distinct chemical contrast, indicating that the composition of the particles that are on the surface are of a different composition than the base. In this case, the particles are big enough that EDS could measure that these particles contain potassium and calcium. However, in other cases, where the particles were too fine, or the layer too thin to obtain any reasonable measurements with EDS, comparing the images obtained with the two detectors enabled an understanding of whether different elements were present on the surface.

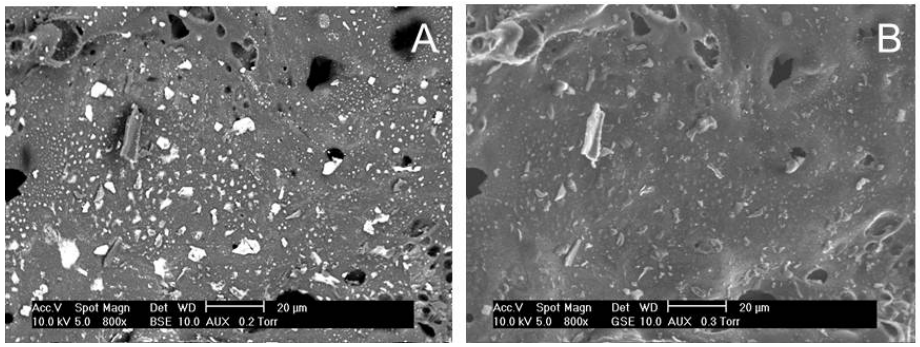

Figure D.1: Comparison of images taken with (a) BSE and (b) GSE detectors. This enables an understanding of whether changes are morphological or chemical, when they are too small to be measured with EDS.

EDS mapping is a technique where the instrument measures the concentration of various elements over a specified area by creating a grid over the area and measuring the concentrations at each spot on the grid. The program then produces an image in color for each element selected, where the intensity of the color corresponds to the concentration of that element. This technique requires that the sample be very flat. This is because the EDS detector is positioned at an angle relative to the sample and therefore 'bumps' in the surface can interfere with the detection. The sample was therefore treated by immersing it in an epoxy resin which hardened to produce a solid transparent polymer with the char particles within it. The resin block was then sanded down on a board that was sprayed with a liquid containing successively smaller particles of diamonds (9 microns, 6 microns, 3 microns, 1 micron) in order to produce a smooth surface. One problem arising from the use of the epoxy resin is related to the porosity of the char samples. Because they are very porous, a large portion of each image taken is the resin. The resin is non-conductive, which results in the accumulation of electrons on the surface. The charged sample will then interfere with the signal, creating an image that is of poor quality. However, for some char samples high quality images were obtained where the porosity of the char was lower.

D.2 ESEM images of used char catalyst

This section shows ESEM images of char sample *CO_2-750-30* that was treated in different conditions, and observed in the ESEM in order to understand the morphological changes to the char. Figure D.2 shows a char sample which was heated to 700^{o}C in N_2 and then used to catalyze CH_4 decomposition. Small, isolated bumps, which are $\sim 1\mu m$ in diameter are visible on the surface. This is either carbon deposition on the surface from the decomposition of CH_4 or morphological changes in the char itself which are formed as a result of thermal treatment of the char. Figure D.3 shows char which was heated to 1000^{o}C in N_2 and then cooled to 700^{o}C, at which point CH_4 was introduced. This sample shows a distinctly different surface structure than the char which was not heated to 1000^{o}C, since the surface is almost completely covered in the bumps, which are slightly larger than those on the un-treated char.

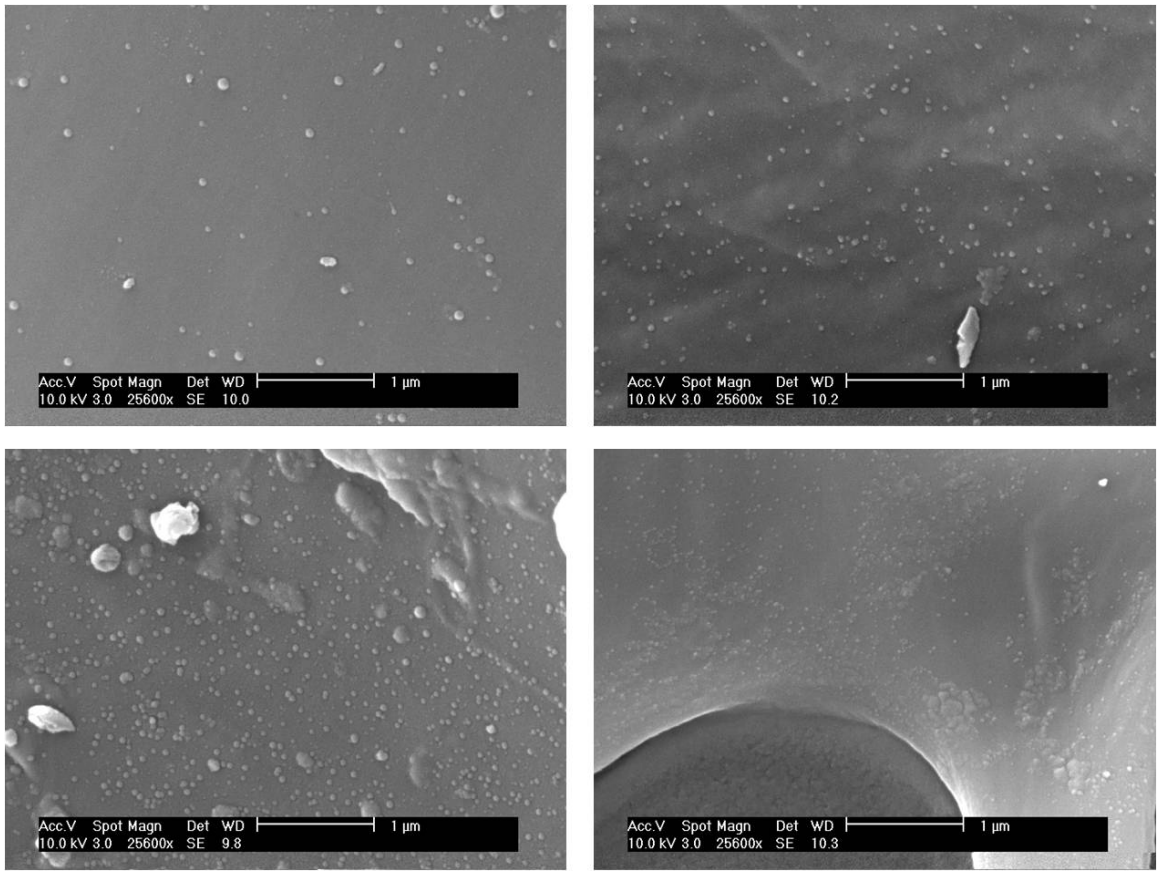

Figure D.2: ESEM image of char surface after being used to catalyze CH_4 decomposition at 700^{o}C. Char sample was *CO_2-750-30*. Four images show different locations on the surface. Magnification bar is 1 micron.

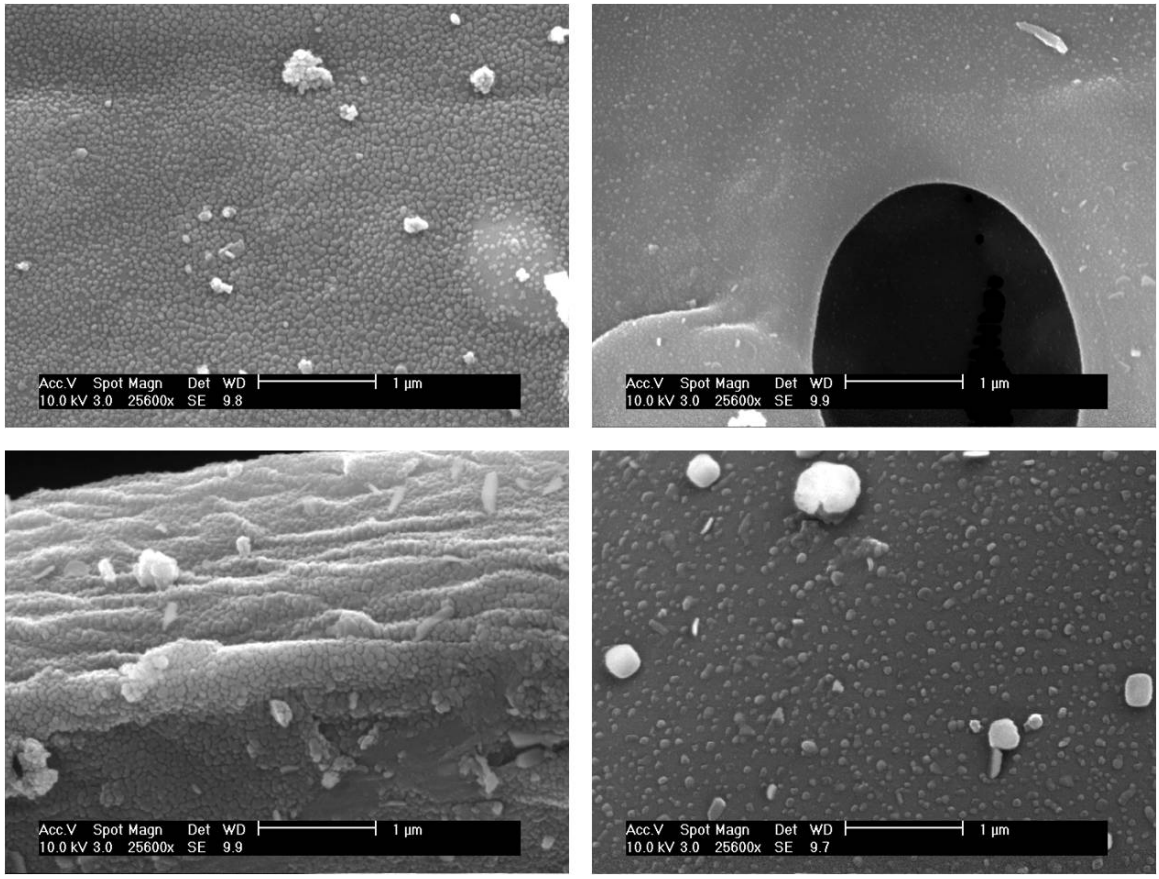

Figure D.3: ESEM image of char surface after being used to catalyze CH_4 decomposition at 700^{o}C. Char sample was *CO_2-750-30* and was heated to 1000^{o}C in N_2 prior to CH_4 reaction. Four images show different locations on the surface. Magnification bar is 1 micron.

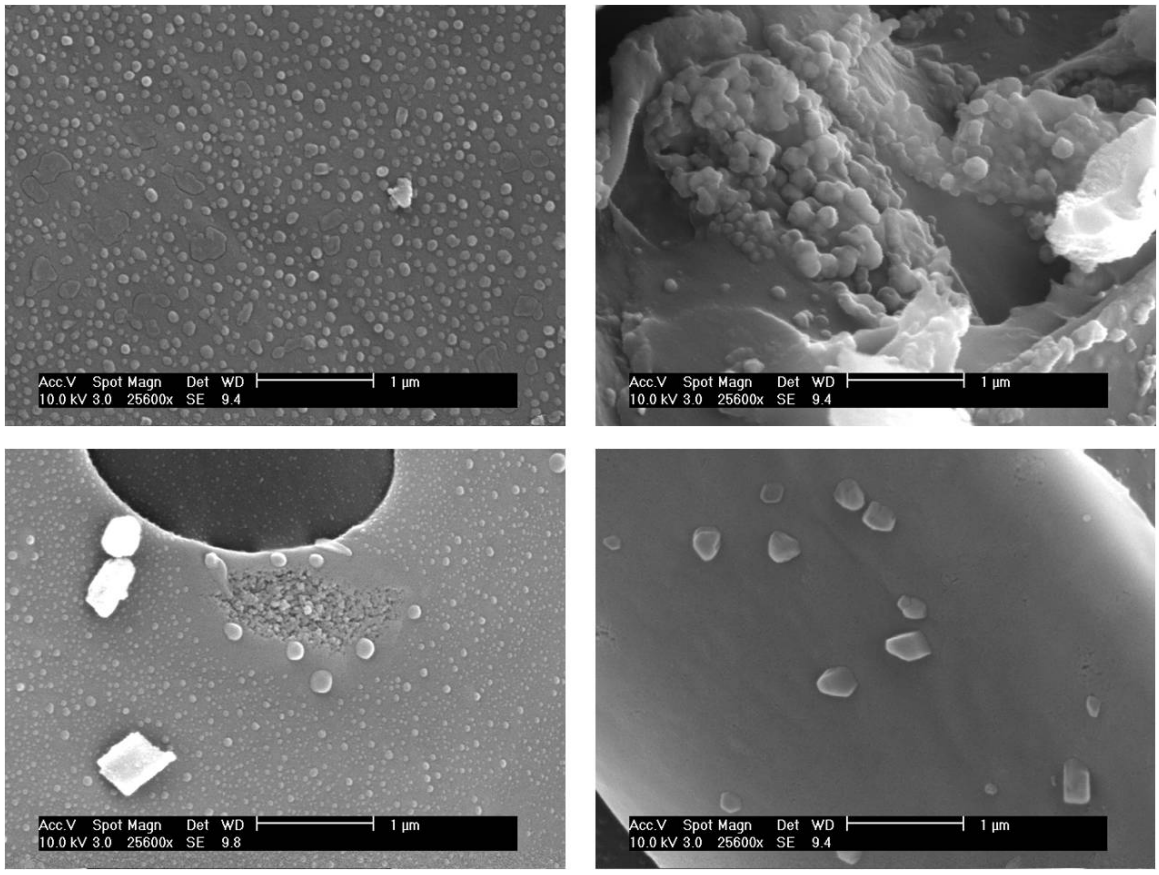

Figure D.4: ESEM image of char surface after being heated to 1000^{o}C. Char sample was *CO_2-750-30*. Four images show different locations on the surface. Magnification bar is 1 micron.

Appendix E

ICP Results

Table E.1: Concentration of inorganic elements in char samples (units are ppm unless otherwise indicated).

Element	Raw wood	CO_2 *920-30*	CO_2 *750-30*	CO_2 *550-30*	H_2O- *750-60*	H_2O- *750-30*	H_2O- *550-30*
Fe	<50	<50	<50	<50	0.30%	278	603
Ca	0.52%	0.83%	1.09%	0.78%	1.64%	1.54%	0.63%
Na	<50	66	64	67	148	104	92
P	113.5	571	1050	0.70%	1210	705	608
K	0.12%	0.79%	0.72%	–	1.25%	1.54%	1.08%
Si	<50	70	63	<50	952	95	70
Mg	340.5	0.12%	0.12%	985	0.21%	0.16%	941
Ni	<50	<50	<50	<50	321.5	<50	<50
Mn	<50	<50	<50	<50	76.5	<50	<50
Al	<50	<50	<50	<50	864	55	<50